EVALUATION OF NETWORK RTK

IN SOUTHERN ONTARIO

AMIR SAEIDI

A THESIS SUBMITTED TO THE FACULTY OF GRADUATE STUDIES

IN PARTIAL FULFILLMENT OF THE REQUIREMENTS FOR THE DEGREE OF

MASTER OF SCIENCE

GRADUATE PROGRAM IN EARTH AND SPACE SCIENCE

YORK UNIVERSITY

TORONTO, ONTARIO

AUGUST 2012

EVALUATION OF NETWORK RTK IN SOUTHERN ONTARIO

by **Amir Saeidi**

A thesis submitted to the Faculty of Graduate Studies of York University in partial fulfilment of the requirements for the degree of

MASTER OF SCIENCE

EVALUATION OF NETWORK RTK IN SOUTHERN ONTARIO

by **Amir Saeidi**

By virtue of submitting this document electronically, the author certifies that this is a true electronic equivalent of the copy of the thesis approved by York University for the award of the degree. No alteration of the content has occurred and if there are any minor variations in formatting, they are as a result of the conversion to Adobe Acrobat format (or similar software application).

Supervisor: Sunil Bisnath

Examination Committee Members:

1. Jian-Guo Wang (Chair)
2. Costas Armenakis (Member)
3. Robert Allison (Outside member)

This page is intentionally left blank.

Abstract

Network Real-Time Kinematic (RTK) has become popular in the past decade as an efficient method of precise, real-time positioning. Its relatively low cost and ease-of-use makes it a good candidate to replace static relative Global Positioning System (GPS) in, e.g., land surveying. A lack of previous studies aroused the interest of the Ministry of Transportation of Ontario (MTO) to request York University to complete a comprehensive study of the performance of network RTK in southern Ontario and whether it is a suitable method for MTO control surveying. Extensive fieldwork campaigns in the winter of 2010 and summer of 2011 were carried out and ~300 hours of static and ~50 hours of kinematic network RTK data were collected from three different service providers. A set of metrics were defined to characterize the performance of network RTK: availability, time-to-first-fix, precision, accuracy, solution integrity and moving average filtering. The data were used to characterize the horizontal performance of network RTK services and the results along with a set of guidelines and specifications were provided (Saeidi et al., 2011; Bisnath et al., 2012). This thesis presents the horizontal network RTK performance evaluation, as well as the vertical and kinematic performance. The aforementioned metrics are used to evaluate the quality of network RTK in southern Ontario, and to compare to similar services available in other locations. The result have revealed expected ~2-3 cm (95%) precision for the horizontal and vertical components; however, large horizontal and vertical biases were observed, which can be as high as 4 cm. The solution integrity has shown that typically, 3σ solution uncertainties

are larger than the actual errors, unless large biases exist. Moving average filtering has confirmed that due to large outliers and spikes in the solutions, 1 second observation periods are not sufficient to provide a precise solution; larger observation windows should be used, e.g., 5 minutes, to reduce the magnitude of maximum errors. The kinematic analysis has revealed issues with synchronization and timing between different data sets. Also, low solution availability while using the network RTK in kinematic mode is seen throughout the results. Overall, network RTK service performance in southern Ontario is slightly lower than the norm reported from similar services in other places.

Acknowledgements

I would like thank my supervisor, Dr. Sunil Bisnath, for giving me the opportunity to work on this research study. He has helped and encouraged me throughout the program. I would also like to thank my parents for their endless support and motivation to continue my studies. I would like to express my gratitude to MTO and NSERC for financial support and making this study possible. Special thanks go to Cansel Survey Equipment Inc., Leica Geosystems and Sokkia Canada for providing the research equipment and technical support. Finally, I want to dedicate this thesis to my wife, who has always given me endless moral support and encouragement.

TABLE OF CONTENTS

Abstract .... **iv**

Acknowledgements .... **vi**

Table of Contents .... **vii**

List of Figures .... **xi**

List of Tables .... **xv**

List of Acronyms .... **xvi**

List of Symbols .... **xviii**

1. Introduction **1**

1.1 Overview of GPS and GNSS 1

1.2 Thesis Objectives and Novelty of Research 6

1.3 Thesis Outline 7

2. Aspects of Network RTK **10**

2.1 Relative Positioning 10

2.2 Baseline RTK 14

2.3 Network RTK 16

2.3.1 Correction Generation 18

2.3.1.1 Error Sources 18

2.3.1.2 Network Initialization 19

2.3.1.3 Common Ambiguity Level 22

2.3.1.4 VRS Correction Generation Algorithm 23

2.3.1.5 MAC Correction Generation Algorithm 24

2.3.1.6 FKP Correction Generation Algorithm 26

2.3.2 Interpolation to Rover Location 28

2.3.2.1 Interpolation in FKP 32

2.3.2.2 Interpolation in VRS 34
2.3.2.3 Interpolation in MAC 35
2.3.3 Correction Transmission 37
2.3.3.1 RTCM SC-104 Protocols 38
2.3.3.2 One-Way (Broadcast) Communication 40
2.3.3.3 Two-Way (Bi-linear) Communication 43
2.4 Summary 43
3. Methodology for Static and Kinematic Evaluations 44
3.1 Similar Network RTK Evaluation Studies 44
3.2 Static Methodology and Fieldwork 48
3.2.1 Test Configuration 50
3.2.2 Equipment 51
3.2.3 Site locations 52
3.2.4 Reference Coordinates of Test Locations 54
3.3 Kinematic Methodology and Fieldwork 56
3.3.1 Equipment Set-up 56
3.3.2 Test Locations 58
3.4 Performance Analyses Metrics 61
3.4.1 Availability 62
3.4.2 Time-To-First-Fix 62
3.4.3 Precision 62
3.4.4 Accuracy 62
3.4.5 Solution Integrity 63
3.4.6 Moving Average Filtering 63
4. Static Network RTK Evaluations 64
4.1 Solution Quality 64
4.2 Availability 69
4.2.1 Winter Campaign 70
4.2.2 Summer Campaign 73

4.2.3 Data Gap Analysis ... 75
4.3 Time-To-First-Fix ... 78
4.4 Horizontal Precision ... 80
4.4.1 Winter Campaign ... 81
4.4.2 Precision Repeatability ... 84
4.4.3 Overall Horizontal Precision ... 87
4.5 Vertical Precision ... 90
4.5.1 Winter Campaign ... 91
4.5.2 Precision Repeatability ... 93
4.6 Horizontal Accuracy ... 97
4.6.1 Winter Campaign ... 97
4.6.2 Repeatability: Summer versus Winter ... 105
4.7 Vertical Accuracy ... 109
4.7.1 Repeatability: Summer versus Winter ... 115
4.8 Horizontal Solution Integrity ... 118
4.9 Vertical Solution Integrity ... 124
4.10 Horizontal Moving Average Filtering ... 127
4.10.1 Precision ... 128
4.10.2 Maximum Error ... 131
4.11 Vertical Moving Average Filtering ... 134
4.11.1 Precision ... 135
4.11.2 Maximum Error ... 137
4.12 Summary ... 140

5. Kinematic Network RTK Evaluation ... 142
5.1 Analysis Methodology ... 142
5.2 Availability ... 147
5.3 Solution Quality ... 150
5.4 Precision ... 153
5.5 Baseline Accuracy ... 155

5.6 Solution Integrity 158
5.7 Summary 161

6. Conclusions, Recommendations and Future Studies 162

6.1 Conclusions 163
6.2 Recommendations 166
6.2.1 Network Geometry 166
6.2.2 Datum 167
6.2.3 Quality Control 167
6.2.4 Window of Observation 168
6.2.5 Visibility 169
6.2.6 Raw GPS Observations 169
6.2.7 Sectioning 169
6.2.8 Solution Calibration 170
6.2.9 Network RTK Solution Quality 171
6.2.10 Fieldwork: Traversing 171
6.3 Future Studies 172

7. References 174

A. Company 'A' Results and Analysis .... Error! Bookmark not defined.
B. Company 'B' Results and Analysis .... Error! Bookmark not defined.
C. Company 'C' Results and Analysis .... Error! Bookmark not defined.
D. Kinematic Results and Analysis .... Error! Bookmark not defined.

LIST OF FIGURES

Figure 2.1: Network RTK reference station configuration (Bisnath, 2011) 16
Figure 2.2: Linear FKP planes for four reference stations (Wubbena et al., 2001).......... 27
Figure 2.3. Methods of communication for network RTK 41
Figure 3.1: Test set up used by Edwards et al. (2008) 46
Figure 3.2: Test set up used at each test site 51
Figure 3.3: Network RTK reference stations in southern Ontario - late 2010 53
Figure 3.4: Network RTK test locations used in southern Ontario 53
Figure 3.5: Control survey data collection procedure for coordinate determination 56
Figure 3.6: Kinematic test antenna arrangement 57
Figure 3.7: St. Catharines to Kitchener test run 59
Figure 3.8: Kitchener to Windsor test run 59
Figure 3.9: Windsor to London test run 60
Figure 3.10: Toronto to Jarvis test run 60
Figure 3.11: Barrie to Toronto test run 61
Figure 4.1: Example of “Good” quality network RTK solution 65
Figure 4.2: Example of “Not so good” quality network RTK solution 66
Figure 4.3: Biases in network RTK solution 67
Figure 4.4: Sinusoidal behaviour in network RTK solution 68
Figure 4.5: Availability percentage in winter campaign for Company ‘A’ 71
Figure 4.6: Availability percentage in winter campaign for Company ‘B’ 72
Figure 4.7: Availability percentage in winter campaign for Company ‘C’ 73
Figure 4.8: Availability percentage in summer campaign for Company ‘A’ 74
Figure 4.9: Availability percentage in summer campaign for Company ‘B’ 74
Figure 4.10: Availability percentage in summer campaign for Company ‘C’ 75
Figure 4.11: TTFF in winter campaign for Company ‘A’ 79
Figure 4.12: TTFF in winter campaign for Company ‘B’ 79
Figure 4.13: TTFF in winter campaign for Company ‘C’ 80

Figure 4.14: Horizontal precision (95%) in winter campaign for Company ‘A’............. 82
Figure 4.15: Horizontal precision (95%) in winter campaign for Company ‘B’............. 82
Figure 4.16: Horizontal precision (95%) in winter campaign for Company ‘C’............. 83
Figure 4.17: Comparison of winter and summer campaign precision for Company ‘A’ . 85
Figure 4.18: Comparison of winter and summer campaign precision for Company ‘B’ . 85
Figure 4.19: Comparison of winter and summer campaign precision for Company ‘C’ . 86
Figure 4.20: Overall precision of all data points collected in winter campaign 88
Figure 4.21: Winter horizontal precision histogram showing 95% confidence interval .. 88
Figure 4.22: Overall precision of all data points collected in summer campaign............ 89
Figure 4.23: Summer horizontal precision histogram showing 95% confidence interval 90
Figure 4.24: Vertical precision (95%) in winter campaign for Company ‘A’................. 91
Figure 4.25: Vertical precision (95%) in winter campaign for Company ‘B’................. 92
Figure 4.26: Vertical precision (95%) in winter campaign for Company ‘C’................. 93
Figure 4.27: Comparison of winter and summer campaign vertical precision for Company ‘A’ 94
Figure 4.28: Comparison of winter and summer campaign vertical precision for Company ‘B’........ 94
Figure 4.29: Comparison of winter and summer campaign vertical precision for Company ‘C’........ 95
Figure 4.30: Ionosphere activity on site 'bel' test dates in winter (left) and in summer (right) at 12:00 pm 96
Figure 4.31: Mean error in winter campaign for Company ‘A’ 98
Figure 4.32: Horizontal biases in winter campaign for Company ‘A’ 99
Figure 4.33: Mean error in winter campaign for Company ‘B’.................................... 100
Figure 4.34: Horizontal biases in winter campaign for Company ‘B’........................... 101
Figure 4.35: Mean error in winter campaign for Company ‘C’.................................... 102
Figure 4.36: Horizontal biases in winter campaign for company ‘C’............................ 102
Figure 4.37: Horizontal rms in winter campaign for Company ‘A’ 103

Figure 4.38: Horizontal rms in winter campaign for Company ‘B’ 104
Figure 4.39: Horizontal rms in winter campaign for Company ‘C’ 104
Figure 4.40: Long-term repeatability for Company ‘A’ 106
Figure 4.41: Long-term repeatability for Company ‘B’ 106
Figure 4.42: Long-term repeatability for Company ‘C’ 107
Figure 4.43: Mean vertical error in winter campaign for Company ‘A’ 110
Figure 4.44: Vertical biases in winter campaign for Company ‘A’............................... 110
Figure 4.45: Mean vertical error in winter campaign for Company 'B'.......................... 111
Figure 4.46: Vertical biases in winter campaign for Company ‘B’ 112
Figure 4.47: Mean vertical error in winter campaign for Company 'C'.......................... 112
Figure 4.48: Vertical biases in winter campaign for Company ‘C’ 113
Figure 4.49: Vertical rms in winter campaign for Company 'A'.................................... 114
Figure 4.50: Vertical rms in winter campaign for Company 'B'.................................... 115
Figure 4.51: Vertical rms in winter campaign for Company 'C'.................................... 115
Figure 4.52: Long-term vertical repeatability for Company 'A' 116
Figure 4.53: Long-term vertical repeatability for Company 'B'..................................... 117
Figure 4.54: Long-term vertical repeatability for Company 'C'..................................... 117
Figure 4.55: Company ‘C’ network RTK errors versus 1, 2 and 3 σ for ‘lon’ 120
Figure 4.56: Solution integrity for Company ‘C’ at ‘kit’... 121
Figure 4.57: Solution integrity for Company ‘B’ at ‘win’... 122
Figure 4.58: Solution integrity for Company ‘A’ at ‘kin’ 123
Figure 4.59: Company ‘C’ vertical error versus 1, 2 and 3σ for ‘pet’ 125
Figure 4.60: Solution integrity for Company ‘C’ at ‘bel’.. 126
Figure 4.61: Solution integrity for Company ‘B’ at ‘bel’.. 127
Figure 4.62: Moving average filtering vs. precision for Company ‘A’ 129
Figure 4.63: Moving average filtering vs. precision for Company ‘B’ 129
Figure 4.64: Moving average filtering vs. precision for Company ‘C’ 130
Figure 4.65: Moving average filtering vs. maximum error for Company ‘A’................ 132
Figure 4.66: Moving average filtering vs. maximum error for Company ‘B’................ 132

Figure 4.67: Moving average filtering vs. maximum error for Company ‘C’ 133
Figure 4.68: Moving average filtering vs. vertical precision for Company ‘A’ 135
Figure 4.69: Moving average filtering vs. vertical precision for Company ‘B’ 136
Figure 4.70: Moving average filtering vs. vertical precision for Company ‘C’ 137
Figure 4.71: Moving average filtering vs. maximum error for Company ‘A’ 138
Figure 4.72: Moving average filtering vs. maximum error for Company ‘B’ 139
Figure 4.73: Moving average filtering vs. maximum error for Company ‘C’ 139
Figure 5.1: Linear time-tag discrepancy for Company 'C' vs. Company 'B' 144
Figure 5.2: Correlation between baseline error and vehicle speed for Company 'A' vs. Company 'B' 145
Figure 5.3: Solution discrepancy due to time-tags being fraction of a second ahead or behind actual GPS observation time for Company 'A' 146
Figure 5.4: Fixed solution lost due to bridge 149
Figure 5.5: Solution recovery time after encountering obstacles 150
Figure 5.6: Kinematic baseline error between three pairs of antennas (Kitchener → Windsor) 152
Figure 5.7: Kinematic baseline error between three pairs of antennas (Jarvis → Toronto) 153
Figure 5.8: Kinematic 3D 1σ precision for each set of comparison in each kinematic run 154
Figure 5.9: Mean baseline errors for each set of comparison in each kinematic run 156
Figure 5.10: Baseline rms for each set of comparison in each kinematic run 157
Figure 5.11: Baseline error vs. scaled 1σ, 2σ and 3σ internal equipment uncertainties . 159
Figure 5.12: Correlation between 95% equipment uncertainty and the actual baseline error 160
Figure 6.1: Forward and backward traversing for control survey set-up using network RTK 172

LIST OF TABLES

Table 2.1: Summary of interpolation methods of network RTK 32
Table 2.2: RTCM 3.0 message components 38
Table 2.3: Summary of commonly used techniques of network RTK 40
Table 3.1: Data types collected during the field campaigns 50
Table 3.2: Models of equipment used for the fieldwork.. 52
Table 3.3: Information on the static test site monuments 54
Table 3.4: CACS sites used in processing and proximity to test sites.............................. 55
Table 3.5: Kinematic test details.. 58
Table 4.1: Data gaps in winter campaign for Company ‘A’ (1 Hz data rate)................... 76
Table 4.2: Data gaps in winter campaign for Company ‘B’ (1 Hz data rate)................... 77
Table 4.3: Data gaps in winter campaign for Company ‘C’ (1 Hz data rate)................... 78
Table 4.4: Statistical test for repeatability of horizontal precision 87
Table 4.5: Statistical test for repeatability of vertical precision 96
Table 4.6: Statistical test of repeatability for mean error.. 108
Table 4.7: Statistical test of repeatability for vertical mean error.................................. 118
Table 4.8: Statistics for improvement of precision with various time bin sizes 131
Table 4.9: Statistics for improvement of maximum error with various time bin sizes... 134
Table 4.10: Statistics for improvement of vertical precision with various time bin sizes 137
Table 4.11: Statistics for improvement of maximum error with various time bin sizes. 140
Table 5.1: Kinematic run total solution availabilities for each kinematic run............... 148

LIST OF ACRONYMS

AIUB	Astronomical Institute, University of Bern
ARP	Antenna Reference Point
CACS	Canadian Active Control Points
CBN	Canadian Base Network
CDMA	Code Division Multiple Access
COMPASS	Chinese satellite navigation system
CORS	Continuously Operating Reference Stations
COSINE	Control Survey Information Exchange
CQ	Coordinate Quality
CSRS	Canadian Spatial Reference System
DGPS	Differential Global Positioning System
DOP	Dilution of Precision
FARA	Fast Ambiguity Resolution Approach
FDMA	Frequency Division Multiple Access
FKP	Flächenkorrekturparameter (Area Correction Parameters)
GALILEO	European satellite navigation system
GDOP	Geometric Dilution of Precision
GLONASS	Russian satellite navigation system
GNSS	Global Navigation Satellite System
GPS	Global Positioning System
GSD	Geodetic Survey Division
ICD	Interface Control Document
IGS	International GNSS Service
ITRF	International Terrestrial Reference Frame
LAMBDA	Least-squares Ambiguity Decorrelation Adjustment
MAC	Master Auxiliary Concept
MNR	Ministry of Natural Resources

MTO	Ministry of Transportation of Ontario
NEU	North, East and Up
NOAA	National Oceanic and Atmospheric Administration
NRCAN	Natural Resources Canada
NRTK	Network Real-Time Kinematic
NTRIP	Network Transport of RTCM via Internet Protocol
OTF	On-The-Fly
PPP	Precise Point Positioning
PPP-RTK	Precise Point Positioning and Real-Time Kinematic Integration
QC	Quality Control
rms	Root Mean Squared
RTCM	The Radio Technical Commission for Maritime Services
RTK	Real-Time Kinematic
SPP	Single Point Positioning
SSR	State Space Representation
TEC	Total Electron Content
TGO	Trimble Geomatics Office
TRS	Temporary Reference Station
TTFF	Time-To-First-Fix
UHF	Ultra High Frequency
VCV	Variance-Covariance Matrix
VHF	Very High Frequency
VRS	Virtual Reference Station
WADGPS	Wide Area Differential Global Positioning System

LIST OF SYMBOLS

Δ	single-difference
$\nabla\Delta$	double-difference
A	design matrix
c	speed of light in a vacuum
$\delta t_A, \delta T^j$	receiver and satellite clock offsets
D_X, D_Y, D_Z	datum translation vector component
F	F-test ratio
f	signal frequency
I_A^j	ionospheric error
λ	carrier signal wavelength
M_A^j	multipath error
N_A^j	carrier-phase ambiguity
P	weight matrix
P_A^j	pseudorange observation
$\emptyset_A^j$	carrier-phase observation
φ_u, λ_u, H	geodetic user coordinates
Q_x	cofactor matrix
ρ_A^j	range between receiver and satellite
T_A^j	tropospheric error
V	differenced residual error
$\Delta X_{u,m}, \Delta Y_{u,m}, \Delta Z_{u,m}$	baseline components between user and master station

1. INTRODUCTION

Over the past two decades, the Global Positioning System (GPS) has become ubiquitous in outdoor positioning and navigation. Other Global Navigation Satellite Systems (GNSS), such as Russian satellite navigation system (GLONASS), European satellite navigation system (GALILEO) and Chinese satellite navigation system (COMPASS), can also provide similar positioning and navigation services. GPS has been steadily augmented to improve performance using such techniques as Differential Global Positioning System (DGPS), relative GPS, RTK and network RTK. This thesis focuses on the performance of one of these augmentations, network RTK, in the southern Ontario region.

1.1 Overview of GPS and GNSS

The Global Positioning System constellation consists of (nominally) 32 satellites, each orbiting the Earth at an altitude of 20,200 km and completing one revolution in 12 sidereal hours. GPS became fully operational in 1994 with 24 satellites placed in orbit. The satellites are placed in 6 different orbital planes with inclinations of $\sim 55^{o}$ with at least 4 satellites in each orbital plane to maximize availability (Hoffman-Wellenhof et al., 2001). This orbital structure means that at higher latitudes the satellites rise to lower elevation angles, though ensuring that signals from at least 4 satellites are transmitted to Earth's surface at anytime, in any location and practically under any weather condition.

Onboard each GPS satellite are atomic clocks, which generate pure sine waves at a 10.23 MHz frequency. Using integer multipliers, this fundamental frequency is used to produce two carrier waves L1 and L2, which are used by the satellites to send timing signals to users. The L1 and L2 frequencies are 1575.42 MHz and 1227.60 MHz, respectively (Tekmon, 2012). Also, the L5 frequency is being introduced in newly launched satellites, which operates at 1176.45 MHz. GPS satellites use Code Division Multiple Access (CDMA) signals to relay information about their identity, signal time-tag, clock corrections and position. Two types of codes are generated by each satellite: the Coarse/Acquisition (C/A)-code and the Precision (P)-code. The C/A-code is broadcast at a rate of 1 Mbps, which is repeated every 1 ms. The P-code is broadcast at a rate of 10 Mbps, is 266 days in length, and is reset every week. The wavelengths of the L1 and L2 carrier waves are 19.05 cm and 24.45 cm, respectively.

On the user side, the receiver obtains the time-tagged signals to determine the range between the user and the satellite. Since the position of the satellites are known, 3 or more range observations from different satellites should allow for 3D user position determination (Hoffman-Wellenhof et al., 2001; Leick, 2004). However, a problem arises due to the lack of synchronization between the satellite and receiver clocks requiring the estimation of an additional receiver clock offset term, and therefore at least 4 satellites must be simultaneously observed. This is the reason why the measured range between a satellite and receiver is known as a "pseudorange".

The underlying carrier wave (also referred to as "carrier-phase") can also be used for positioning, by counting the number of oscillations taken by the carrier wave to arrive at the receiver to determine the range. These ranges are measured more accurately, as the respective carrier-phase wavelengths are very short (~19 cm and ~24 cm), which enables the receiver to position itself more accurately than by simply using the code signals. However, this mode introduces a problem of determining the departure phase of the carrier wave, since the raw carrier-phase signal does not contain any time-of-transmission information. This is known as the "ambiguity" of the carrier-phase measurements. Determining the carrier-phase ambiguity of a GPS signal is the key to centimetre-level positioning due to the short wavelengths of the carrier wave (Tekmon, 2012). Relative positioning using GPS is a popular technique. Simultaneous measurements from multiple receivers can be used to remove or reduce common errors in the GPS signal, such as receiver and satellite clock errors. RTK and network RTK are methods using the relative positioning principal and are explained in more detail in Chapter 2.

The development of GPS has been a rather rapid process. From the mid-1980s up to now there have been many different augmentations and advances in the utilization of GPS as a reliable method for outdoor positioning. Even before GPS reached its full operational capability in 1995, there had been many new discoveries and steps towards the realization of real-time, centimetre-level positioning for civil applications. The development and testing of the first Macrometer receiver in 1982 that verified relative-positioning surveying accuracy of 1-2 parts per million (ppm) and the construction of a thirty-station, first-order network densification in the Eifel region in Germany using GPS observations in 1983 (Leick, 2004). Also, the development of the TI-4100 dual-frequency, P-code receiver from Texas Instruments and relative accuracy performance of 1 ppm using only 15 minutes of observations rapidly brought GPS relative positioning closer to becoming a real-time, precise positioning technology (Remondi, 1985; Leick, 2004).

Remondi (1985) developed an algorithm for centimetre-level relative positioning of a moving antenna using the carrier-phase observations in seconds. Another major step was the creation of the On-The-Fly (OTF) ambiguity resolution methodology (Seeber and Wubbena, 1989), which removed the requirement for a static antenna initialization for ambiguity resolution. This technique could be used in both post-processing and real-time applications. Noting these advances in relative positioning, the navigation community began to take advantage of relative positioning in attempts to eliminate errors common to co-observing receivers. The main objective was to extend the baselines lengths in relative positioning. This gave way to the development of Wide Area Differential GPS (WADGPS), as well as many other efforts for the standardization of real-time differential GPS. Despite all of these developments, universal real-time positioning using carrier-phase observations was not efficiently possible until the introduction of fast and reliable ambiguity resolution techniques, such as the Least-square Ambiguity Decorrelation Adjustment (LAMBDA) approach by Teunissen (1993) and Fast Ambiguity Resolution Approach (FARA) by Frei and Beutler (1990). The result is what is termed real-time kinematic (RTK), which can provide centimetre-level positioning in seconds. However, baseline RTK has its limitations, such as degradation of performance with longer baseline distances (>10-15 km), so network RTK was developed in the early-2000s to reduce some of these limitations.

Aside from GPS, there are a number of other GNSS. GLONASS is the Russian navigation satellite system, which is currently approaching full operational capability. GLONASS, as of July 2012, has 24 satellites in orbit, comprising a full constellation. The satellite broadcast signals on different L1 and L2 frequencies. Much like GPS, GLONASS broadcasts HP (high precision code, equivalent to P-code) on both L1 and L2 and SP (standard precision code, equivalent to C/A) code on L2 frequency (GLONASS ICD, 2002). The major difference between GPS and GLONASS is the use of the Frequency Division Multiple Access (FDMA) methodology by GLONASS, as opposed to CDMA used by GPS. The 24 satellites in the complete GLONASS constellation use 12 different frequency channels. Each frequency channel is used by a pair of satellite on the same orbital plane that are 180º apart, allowing for two satellites using the same channel to never be observed at the same time (Tekmon, 2012).

GALILEO is another global navigation satellite system, which is being built by the European Union and European Space Agency. In terms of constellation structure, GALILEO is very similar to GPS. The full constellation will consist of 30 satellites operating in 3 orbital planes. Two GIOVE (GALILEO in-orbit validation element) test satellites have been launched in 2005 and 2006, GIOVE A and B, which have been used to test the operational capability and orbit determination algorithms of GALILEO (Tekmon, 2012). Two IOV (in-orbit validation) satellites were launched in 2011, which are test bed satellites and are very close to the final GALILEO design, and two more IOV satellites are scheduled to be launched in September of 2012. GALILEO is designed and constructed to be compatible and interoperable with GPS.

COMPASS is another planned global navigation satellite system. COMPASS is an extension of the BeiDou navigation system experiment, which provides navigation and positioning services in China. The full COMPASS constellation will include 30 MEO (medium Earth orbit) and 5 GEO (geostationary Earth orbit satellites). Ten satellites have been launched so far and 25 more satellites are planned to be launched to complete the constellation. COMPASS satellites operate in 4 different L-band frequencies B1, B1-2, B2 and B3 (Tekmon, 2012). Much like GPS, COMPASS uses the CDMA technique for signalling.

1.2 Thesis Objectives and Novelty of Research

The general objective of this thesis is to evaluate the performance of network RTK services in southern Ontario. This study involves testing all available services currently operating in Ontario provided by Cansel Survey Equipment Inc., Sokkia Canada, and Leica Geosystems. The first portion of the study contains a thorough evaluation of the static horizontal performance of network RTK, which was a feasibility study commissioned by MTO. An extensive report was put together outlining the results of the study which included the quality of horizontal static surveying using network RTK in southern Ontario, as well as detailed guidelines for the use of network RTK in control surveying to meet MTO's survey specifications (Saeidi et al., 2011; Bisnath et al., 2012).

My role in this project was to collect, process and analyze the data as well as to synthesize the final report. The second portion of this thesis extends the evaluation of the vertical static performance, as well as the performance of network RTK in kinematic mode in southern Ontario.

One of the novel aspects of this study is the amount of data collected for both the static and kinematic analyses, which helps identify systematic issues and characteristics. The static fieldwork involves collection of 8 hours of continuous network RTK solutions, from three different service providers, at 9 test sites, totalling over 350 hours of network RTK data in an area of over 65,000 km^2. The collected kinematic data include many tens of hours of network RTK solutions while travelling throughout southern Ontario. Another novel aspect of this study is the extensive use of predefined performance metrics to evaluate the performance of network RTK. Typically, evaluation studies focus on solution availability, accuracy and precision (Jonsson et al., 2002; Al Marzooqi et al., 2006; Edwards et al., 2008; Aponte et al., 2009; Delcev et al., 2009; Rubinov et al., 2011). However, this study adds the use of moving average filtering and solution integrity and examines the impact of each metric on the end user. Finally, no published study of this magnitude has been done for the evaluation of network RTK services anywhere in the world and specifically in southern Ontario.

1.3 Thesis Outline

Chapter 2 provides detailed information on various aspects and development of relative positioning using GPS. Concepts such as double-differencing and ambiguity resolution are discussed. The various components, advantages and shortcomings of baseline RTK are outlined and described briefly. Various methods of network RTK are described and the major steps involved in the design and realization of network RTK are given.

Chapter 3 provides details on the methodology used for both the static and kinematic network RTK testing. The test locations and trajectories (for kinematic tests) are illustrated. The equipment used and the amount of data collected to perform the analysis are also described. Also, recent researches published on this topic are reviewed and their results briefly discussed.

Chapter 4 provides an in-depth analysis of the static network RTK results. The sections are categorized by predefined performance metrics used to qualify the performance of network RTK. Also, the horizontal and vertical results are shown separately in their respective sub-sections. Various issues and results seen from all three service providers are shown and discussed. Statistical testing is used, where applicable, to test the long-term repeatability of the network RTK solutions.

Chapter 5 provides the results of the kinematic analysis. Issues encountered during the course of the kinematic analysis are provided and strategies to overcome these problems are presented. The results of the analysis are also compared to similar studies performed on the quality of kinematic network RTK.

Finally, Chapter 6 summarizes the findings of the overall evaluation of network RTK in southern Ontario. Some of the guidelines and specifications submitted to the MTO are shown and discussed. And suggestions for future work beyond this study are presented.

2. ASPECTS OF NETWORK RTK

The objective of this chapter is to outline the process of development of relative precise positioning, which leads to the development of baseline RTK and its expansion to network RTK. Some of the developments of various methods and technologies considered important steps toward real-time precise positioning. The basic concepts of relative positioning are covered, such as the double-differencing technique, ambiguity resolution methodologies, as well as detailed information on baseline RTK and network RTK.

2.1 Relative Positioning

In relative positioning, unlike single point positioning which only requires one set of observations, the baseline vectors between two or more stations (or receivers) are determined utilizing simultaneous measurements. Using double-differenced observations (to be discussed), the relative baseline vector between each pair of receivers can be determined (Hoffman-Wellenhof et al., 2001; Leick, 2004). Typically, in relative positioning, one receiver is held fixed with known coordinates and the other receiver's coordinates are determined relative to the fixed position of the static receiver (Hoffman-Wellenhof et al., 2001).

Double-differencing eliminates the satellite and receiver clock errors in the observation model (Hoffman-Wellenhof et al., 2001). Double-differencing can also significantly reduce the error contributed by atmospheric refraction. This method can be performed on pseudorange and carrier-phase observables, though only the use of latter can provide centimetre-level positioning accuracy, which is the focus of this section. The model for carrier-phase measurements is:

$$\emptyset_A^j(t_A) = \rho_A^j + cdt_A + cdT^j + T_A^j - I_A^j + \lambda N_A^j + M + \varepsilon \tag{1}$$

where at epoch t_p, $\emptyset_A^j$ is the phase measurement (in metres), $\rho_A^j$is the range between satellite j and observer A (in metres), $c\delta t_A$is the receiver clock error (in metres), cdT^j is the satellite clock error (in metres), T_A^j is the tropospheric delay (in metres), I_A^j is the ionospheric delay (in metres), N_A^j is the carrier phase ambiguity term between satellite j and observer A (in cycles), M is the signal multipath (in metres) and ε is the measurement noise (in metres). The single-differenced model can be obtained by subtracting the carrier-phase observables for two pairs of receivers with respect to a common satellite. The carrier-phase single-differenced measurement between points A and B with respect to satellite j is given by:

$$\Delta\emptyset_{AB}^j = \left(\emptyset_A^j - \emptyset_B^j\right) \tag{2}$$

Utilizing the carrier-phase model, the single-differenced carrier-phase measurement model can be obtained:

$$\Delta\emptyset_{AB}^j = \Delta\rho_{AB}^j + c\Delta dt_{AB} + \Delta T_{AB}^j - \Delta I_{AB}^j + \lambda\Delta N_{AB}^j + \Delta M_{AB}^j + \Delta\varepsilon_{AB}^j \tag{3}$$

with ΔN_{AB}^j as the single-difference ambiguity term. Though, the advantage of eliminating the satellite clock offset dT^j is readily seen (Hoffman-Wellenhof et al., 2001; Leick, 2004). A Double-differenced carrier-phase measurement is the subtraction of two single-difference observables, but with respect to two satellites instead of one. The carrier-phase double-difference observable shown below is between points A and B and satellites j and i.

$$\nabla\Delta\emptyset_{AB}^{ji} = \Delta\emptyset_{AB}^{j} - \Delta\emptyset_{AB}^{i} = \left(\emptyset_{A}^{j} - \emptyset_{B}^{j}\right) - \left(\emptyset_{A}^{i} - \emptyset_{B}^{i}\right) \tag{4}$$

By substituting (1) in (4), the double-differenced carrier-phase model becomes:

$$\nabla\Delta\emptyset_{AB}^{ji} = \nabla\Delta\rho_{AB}^{ji} + \nabla\Delta T_{AB}^{ji} - \nabla\Delta I_{AB}^{ji} + \lambda\nabla\Delta N_{AB}^{ji} + \nabla\Delta M_{AB}^{ji} + \nabla\Delta\varepsilon_{AB}^{ji} \tag{5}$$

Over short baselines (< 10 km), the residual tropospheric and ionospheric errors can be ignored. however, for longer baselines, sufficient modelling of the atmospheric parameters is required in order to obtained centimetre-level accuracy (Hoffman-Wellenhof et al., 2001; Leick, 2004).

One of the challenges of using carrier-phase double-differenced measurement in relative positioning is the determination of the ambiguity term, $\nabla\Delta N_{AB}^{ji}$. Estimated real-valued ambiguities can be used to obtain a positioning solution. However, these ambiguities are inherently integers and constraining them to "fixed" integers in the estimation process, as opposed to real-valued "float" numbers, allows for centimetre-level positioning accuracy.

The objective is to constrain the estimated ambiguities of the float solution using the covariance information from estimates of the double-differenced ambiguities. The change in the square of the residuals by fixing float ambiguities to integers must be minimized and this criterion is used to select the best integer candidates. Statistical testing, such as the F-test for variances, is then used to validate the best integer candidates.

In the early days of GPS surveying, test sets of integer ambiguities were obtained by simply rounding the float ambiguities to the nearest integer (Leick, 2004). This method works well with long periods of observation where the float solution has had sufficient observations from the movements of satellites and change in geometry to estimate ambiguities close to their actual values. However, when attempting to shorten the period of observation to a few epochs, the estimated float ambiguities will not necessarily be close to their integer values. This is where an efficient algorithm for fixing ambiguities is required (Leick, 2004). With an algorithm that can fix ambiguities within a few epochs of the first observation, cycle slips (which are errors in the counted number of carrier-phase cycles typically cause by loss of lock or satellite blockage) become harmless, as the ambiguities could be fixed almost immediately after an occurrence. Also, with a sufficiently rapid ambiguity resolution algorithm, the distinction between static and kinematic relative positioning become less relevant.

There have been many efforts since the mid-1980s to fix ambiguities and most have been described as OTF methods. Some include: the ambiguity mapping function technique (Remondi, 1985) and the same refined for kinematic data (Mader, 1990; 1992); the least-squares ambiguity searching approach (Hatch, 1989; 1990); and integrated on-the-fly ambiguity resolution (Abidin, 1993). The methods mentioned are steps taken towards the realization of real-time kinematic relative positioning. Some of the more popular methods of ambiguity resolution that are currently employed in real-time kinematic approaches are LAMBDA (Teunissen, 1993) and FARA (Frei and Beutler, 1990). Teunissen (1993) introduced the LAMBDA method, which is an integer least-squares estimator and has a very high probability of correct integer estimation. The probabilistic justification of this method, as well as its speed, has made the technique widely popular and generally accepted as the most efficient method of carrier-phase ambiguity resolution (Leick, 2004). The efficiency of this method lies in its ability to decorrelate the integer ambiguity search space, which greatly speeds up the process of finding eligible integer candidates.

2.2 Baseline RTK

Baseline real-time kinematic (RTK) was proposed in the early-1990s as a method of using a static base and transmitting carrier-phase observations to a mobile receiver to fix ambiguities and therefore determine position at the centimetre-level with respect to the reference station, in real-time. Baseline RTK is generally known to perform very well over short distances (<15 km) (NRCan, 2012), i.e., an accuracy of about 1 cm + 1 ppm. However, with longer baselines, the spatial decorrelation of ionospheric and tropospheric induced errors causes performance to rapidly degrade until the rover is no longer able to resolve ambiguities or even keep a continuous communications connection to its base. This being said, baseline RTK is still one of the most popular techniques of relative positioning and used for land surveying, construction and outdoor engineering work due to its cost-effectiveness and ease of use.

The common approach is to compute the corrections at the base and send them via radio link to the rover (Leick, 2004). Transmitting corrections requires less data load than transmitting raw observations due to the small size of the corrections. The float ambiguities are first estimated at the base station using pseudorange measurements. A phase discrepancy is computed by subtracting the range (between the base station and each satellite) from carrier-phase measurement and estimated ambiguity, which forms the carrier-phase correction that is sent to the rover.

One of the major disadvantages of baseline RTK is that two sets of RTK-enabled receivers are required, each costing many thousands of dollars. A base is needed to generate the corrections for the rover in order to be able to use baseline RTK and obtain carrier-phase ambiguity fixed solutions (Vollath et al., 2002). Another shortcoming of baseline RTK is the time needed to setup and monitor the reference station which adds to the cost of using the technology. There are commercial companies that offer baseline RTK services in clusters of reference stations and can broadcast corrections to their clients via a radio link or even the Internet. However, these services cannot escape the major disadvantage of using baseline RTK, which is performance degradation due to the increase of distance of the rover from the base with baselines longer than ~15 km (Vollath et al, 2002; NRCan, 2012). Part of the issue is due to the rover requirement to maintain a line-of-sight to the base in order to receive the corrections via the radio connection. However, this issue can be potentially mitigated by using a signal repeater or an Internet connection.

2.3 Network RTK

Network Real-Time Kinematic (RTK) is a concept that is based on single-baseline RTK, which was developed in the late-1980s / early-1990s and is still being used today. The initial idea for the network approach was to use an array of reference stations, as opposed to just one reference station in baseline RTK, to better model the behaviour of distance dependant errors. In this manner, the major issue of spatial decorrelation of some error sources over distance from a reference station can be overcome, extending the coverage of the single baseline RTK system. Also, since network data are available for interpolation the reference stations can be 10s of kilometres (40 - 70 km) apart (Janssen, 2009). Figure 2.1 shows the approximate spacing between the reference stations for baseline RTK and network RTK. With network RTK (on the right) only 5 reference can provide coverage for an area of 10,000 km^2; while the same area would need over 25 reference stations with baseline RTK (on the left) technology.

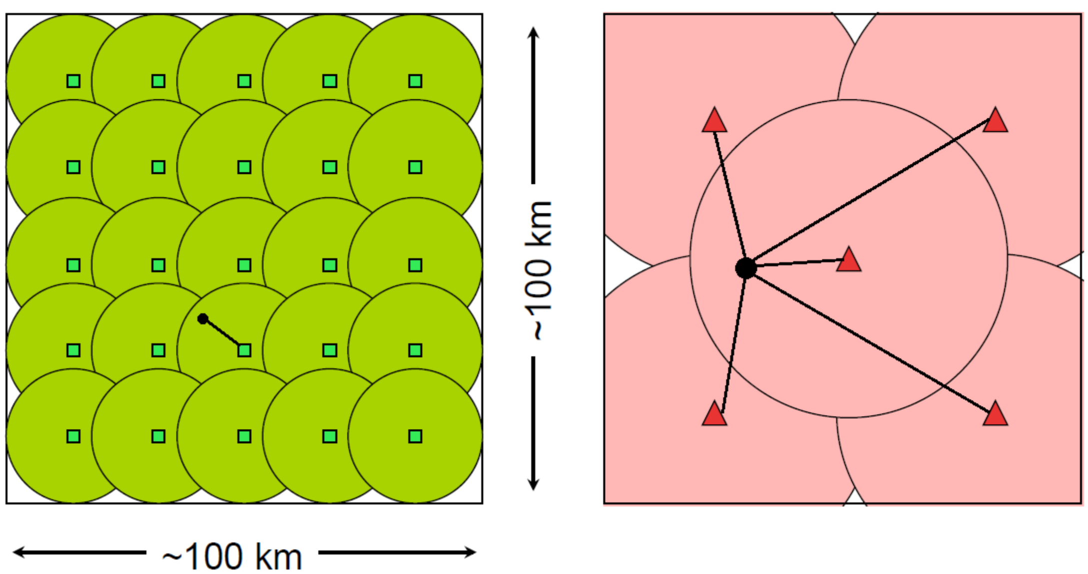

Figure 2.1: Network RTK reference station configuration (Bisnath, 2011)

The motivation for providing this background information is to aid in the performance evaluation of network RTK in southern Ontario, as each of the systems operating use different methods and network architecture, which need to be taken into consideration in the evaluation process. Several competing techniques are available today, including Virtual Reference Station (VRS), Master Auxiliary Concept (MAC) and Area Correction Parameters (in German Flächenkorrekturparameter or FKP). These methods share some common aspects in their design; however, the techniques of communicating and providing corrections to users differ significantly. Some of the proprietary variations of these methods are Trimble's VRS (VRSNow) and Leica's MAX and i-MAX, which will be explained further.

In VRS, the rover sends its approximate position to the central processing facility where corrections are interpolated and the "virtual" observations are generated. These observations are then sent back to the rover and using double-differencing, the position of the rover is determined relative to the virtual reference station. In MAC, however, all of the corrections are generated and sent to the rover where it is interpolated and applied to the carrier-phase observables. Two-way communication is not required for the MAC technique. In FKP, each reference station uses observations from surrounding reference stations to generate correction coefficients. These coefficients as well as reference station coordinates are broadcast and received by the rover where they are applied to carrier-phase observables.

Though commercially utilized network RTK techniques differ in some aspects, all possess four major steps, in some form, in order to provide their users with the corrections needed for centimetre-level, real-time positioning: correction generation, interpolation to rover location, correction transmission and correction application (Lachapelle and Alves, 2002). The correction application process is typically infused with correction interpolation. Details of each step will be described in more detail for the three popular commercial network RTK techniques: VRS, FKP and MAC.

2.3.1 Correction Generation

In order to further define this step of the network RTK process, the errors involved need to be described. In correction generation, the major goal is to resolve the ambiguities between the permanent reference stations and compute the network corrections.

2.3.1.1 Error Sources

There are three error sources that need to be mitigated in order to enable centimetre-level positioning accuracy at a rover's location: ionospheric, tropospheric and orbit (Euler et al., 2001). The ionosphere is a dispersive medium, meaning that the attenuation of signals is proportional to the inverse of the signal frequency squared. Currently GPS satellite broadcast at two different frequencies (L1 and L2) and is being expanded to include a third frequency for civil applications (L5). One strength of obtaining observations from both frequencies is the use of linear combinations of observables to efficiently remove the ionospheric error. In the case of network RTK, linear combinations are used at the reference stations to determine the magnitude of dispersive errors (Euler et al., 2001; Wei et al., 2006).

Tropospheric delay is a non-dispersive error source, which can elongate the runtime of GPS signal by refraction (Leick, 2004). This is mainly due to differing amounts of vapour content in the troposphere, caused by different weather conditions. There are general models which can reduce the effect of this error source, though it cannot be completely eliminated in the single point positioning sense. In relative positioning this error can be reduced significantly using double-differencing.

Orbit error is the error in computation of the "true" position of each satellite. GPS satellite ephemeris are broadcast using the navigation message in the GPS signal; however, these positions are only accurate to within a few metres (Leick, 2004). To reduce the magnitude of the orbit errors, various sources of high-precision orbits exist, such as the International GNSS Service (IGS). The IGS UltraRapid orbits can provide predicted decimetre-level satellite orbits for real-time use. In network RTK, the orbit errors are generally considered as part of the non-dispersive residuals, which includes the tropospheric error as well.

2.3.1.2 Network Initialization

In order to successfully determine integer ambiguities for a network of reference stations, the coordinates of each reference station must be known precisely. At least 24 hours of 30 seconds dual-frequency observations are required to coordinate each reference station (IGS, 2012; Stone, 2002). Reference stations are typically located where there is maximum visibility (3^{o} - 5^{o} above horizon) with minimum sources of multipath. Also, since network RTK is used at the local level, the reference station coordinates should be tied into the local datum using multiple high precision monuments.

Knowing accurately the positions of the reference stations and taking advantage of fixed baselines, the double-differenced ambiguity between each reference station is easily computed. The double-difference ambiguities between each pair of reference stations can be determined by first determining the integer ambiguity of the widelane linear combination (Sun et al., 1999):

$$\emptyset_{WL} = \emptyset_{L1} - \emptyset_{L2} \tag{6}$$

where $\emptyset_{WL}$ is the widelane carrier phase observable and $\emptyset_{L1}$ / $\emptyset_{L2}$ are the L1 and L2 carrier-phase observables, respectively. Using the double-differencing model, the double-differenced ambiguities will be:

$$\Delta\nabla N_{ab,WL}^{12} = \Delta\nabla N_{ab,L1}^{12} - \Delta\nabla N_{ab,L2}^{12} \tag{7}$$

where $\Delta\nabla$ is the double-differencing symbol and $N_{ab,WL}^{12}$ is the double-differenced ambiguity between reference stations *a* and *b* and satellites 1 and 2 using the widelane linear combination. The widelane ambiguities are easily fixed as the wavelength of the combination is 86.4 cm, as opposed to 24 cm and 19 cm for L1 and L2, respectively. The longer wavelength allows for fast double-differenced ambiguity resolution over long baselines (up to a few 100 km). Chen and Lachapelle (1995) describes a detailed method of ambiguity search method which can be utilized in determination of the widelane ambiguities. After the widelane ambiguities are determined, the measurements derived from the iono-free linear combination are used to determine the L1 ambiguities as follows (Sun et al., 1999):

$$\Delta\nabla N_{ab,IF}^{12} = \Delta\nabla N_{ab,L1}^{12} - \frac{f_2}{f_1}\Delta\nabla N_{ab,L2}^{12} \tag{8}$$

where $\Delta\nabla N_{ab,IF}^{12}$ is the double-differenced iono-free linear combination ambiguity and f_1/ f_2 are the L1 and L2 frequencies, respectively. Using the L2 ambiguity term, equation (8) can be solved to the form:

$$\Delta\nabla N_{ab,L1}^{12} = \frac{\Delta\nabla N_{ab,IF}^{12} - \frac{f_2}{f_1}\Delta\nabla N_{ab,WL}^{12}}{1 - \frac{f_2}{f_1}} \tag{9}$$

which allows for the determination of the L1 double-differenced ambiguity derived from the iono-free linear observations. The L2 ambiguity can then be determined using equation (7). The L1 and L2 ambiguity constraints can be imposed to check the quality of the integer ambiguities, as well as to reduce the size of the ambiguity search space effectively speeding up the process. The constraints are based on the property that ensures the double-differenced ambiguities in a closed-loop add up to zero (Leick, 2004):

$$\Delta\nabla N_{AB} + \Delta\nabla N_{BC} + \Delta\nabla N_{AC} = 0 \tag{10}$$

where $\Delta\nabla N_{AB}$/ $\Delta\nabla N_{BC}$/$\Delta\nabla N_{AC}$ are double-differenced ambiguities between stations A/B, B/C and A/C. After the successful completion of the ambiguity resolution step (which should satisfy all the conditions set by the constraint equations), the validation process can take place. Residuals from the double-differenced measurements are the major indicator used to validate the integer ambiguities as the relative baselines are fixed. All errors (such as orbit, atmosphere, noise and multipath) would be present in the residuals (Sun et al., 1999). The F-ratio test is used to validate the integer ambiguities using the quadratic forms of double-differenced residuals for smallest and second smallest ambiguity combinations (Wang et al., 2000):

$$F = \frac{\Omega_2}{\Omega_1} \tag{11}$$

where Ω_1 is the quadratic form for the smallest residuals and Ω_2 is the quadratic form for the second smallest residuals. Typically, the ratio is set an arbitrary value of 2 (Wang et al., 2000). A value of 2 ensures that the quadratic form of the second smallest residuals is at least 2 times larger than the quadratic form of the smallest residuals.

2.3.1.3 Common Ambiguity Level

Maintaining a common ambiguity level is one of the keys of network RTK (Euler et al., 2001, Tekmon, 2012). When a network is operating at common ambiguity, level all double-difference ambiguities are fixed relative to the same reference satellite. One of the main issues with common ambiguity levels in a network is availability of common view satellites. Satellites can go out of view or a reference station can lose lock on a satellite, which forces the network to reassess its reference satellite, causing a switch in reference satellite. Typically, when a loss of lock to a reference satellite occurs the network switches to the next satellite that will be visible for the longest period of time. This process can be quickly completed without the need to reinitialize network ambiguities using linear transformations (Tekmon, 2012), e.g.:

$$\Delta\nabla N_{AB}^{ij} \rightarrow \Delta\nabla N_{AB}^{kj} = \Delta\nabla N_{AB}^{ij} - \Delta\nabla N_{AB}^{ik} = \Delta\nabla N_{AB}^{kj} \tag{12}$$

As can be seen from equation (12), for a switch from reference satellite i to k, linear combinations of double-differenced integer ambiguities with respect to reference satellite i can be used to derive the integer ambiguities with respect to a new reference satellite j (Euler et al., 2001). The maintenance of a common ambiguity level over a network guarantees the linear property of double-differenced integer ambiguities. This property can be used to reduce the ambiguity search space, as well as to validate the obtained integer ambiguities across a network. Sub-networks and overlapping areas are formed in order to make this process simpler.

2.3.1.4 VRS Correction Generation Algorithm

After the double-differenced ambiguities are resolved between reference stations, the main focus of the network RTK software is to generate corrections, which will be later interpolated for the location of the rover. First, a look at the double-difference model is required (Wei et al., 2006):

$$\lambda\left(\Delta\nabla N_{AB}^{ij} + \Delta\nabla\emptyset_{AB}^{ij}\right) = \left(\Delta\nabla\rho_{AB}^{ij} - \Delta\nabla I_{AB}^{ij} + \Delta\nabla T_{AB}^{ij}\right) \tag{13}$$

The $\Delta\nabla N_{AB}^{ij}$ is obtained in the previous step, $\Delta\nabla\emptyset_{AB}^{ij}$ is known through the double-differencing of the carrier-phase observations and $\Delta\nabla\rho_{AB}^{ij}$ is obtained using the fixed coordinates of the reference stations and the position of the satellites. Hence, the troposphere and ionosphere errors can be determined.

For VRS corrections, the errors provided above in equation (13) can be further separated into dispersive and non-dispersive components. The dispersive term is the ionosphere error. Due to the distance between the reference stations (10s of kilometres apart), the ionospheric delay will have the most dominant influence on the solution (Wei et al., 2006). The dispersive and non-dispersive errors can easily be detached using:

$$V = V^{disp} + V^{non-disp} \tag{14}$$

$$V = \Delta\nabla T_{AB}^{ij} - \Delta\nabla I_{AB}^{ij} = \lambda\left(\Delta\nabla N_{AB}^{ij} + \Delta\nabla\emptyset_{AB}^{ij}\right) - \Delta\nabla\rho_{AB}^{ij} \tag{15}$$

The iono-free principal is used to determine the dispersive term (ionospheric error) using the following dual-frequency, linear combinations:

$$\begin{aligned}\Delta\nabla I_{AB}^{ij} = \frac{{f_2}^2}{{f_1}^2 - {f_2}^2}\Big[\big(\Delta\nabla\emptyset_{AB,L1}^{ij}\lambda_1 - \Delta\nabla\emptyset_{AB,L2}^{ij}\lambda_2\big) + (\Delta\nabla N_{AB,L1}^{ij}\lambda_1 \\ - \Delta\nabla N_{AB,L2}^{ij}\lambda_2)\Big]\end{aligned} \tag{16}$$

And using equation (14) the non-dispersive can be determined as follows:

$$V^{non-disp} = V - V^{disp} = V + \Delta\nabla I_{AB}^{ij} \tag{17}$$

2.3.1.5 MAC Correction Generation Algorithm

MAC correction generation process is very similar to VRS in the sense that the corrections are still decomposed into their dispersive and non-dispersive components. However, single-differences from the master station to the auxiliary reference stations (secondary reference stations that are farther from the user than the master station) are used to generate corrections for the rover (Euler et al., 2001). Using VRS, double-differences are required to interpolate and generate observations at the virtual reference station. However, since MAC does not require observation generation for a virtual reference station and the interpolation process is performed entirely by the receiver, the single-differenced observations suffice for the interpolation and correction generation process. Also, utilizing single-differences allow for the estimation of the receiver clock terms, which is one step closer to the State Space Representation (SSR) approach to network RTK. The SSR approach helps model each individual error source separately using undifferenced observables, as opposed to observation space representation (OSR) that is currently used in network RTK (Wubbena et al., 2005).

The number of auxiliary stations used depend on their proximity to the master station. In MAC, all relevant single-differences between the auxiliary and master reference stations are considered to compute the corrections differences using (Euler et al. 2001):

$$V_{AB}^{i} = \Delta\rho_{AB}^{i} - \lambda\Delta\emptyset_{AB}^{i} + c.dt_{AB}^{i} - \Delta I_{AB}^{i} + \Delta T_{AB}^{i} + \lambda\Delta N_{AB}^{i} \tag{18}$$

The satellite to reference station $\Delta\rho_{AB}^{i}$ range can be obtained using the known coordinates for the stations, as well as the GPS ephemeris. The single-differenced receiver clock dt_{AB}^{i} is estimated by each reference stations using pseudorange observations. The single-differenced ambiguity term has integer properties, as with the original and the double-differenced carrier phase observation model. ΔN_{AB}^{i} is determined using the double-differenced ambiguity that is initially resolved between reference stations with respect to the same reference satellite. The following relationship between the double- and single-ambiguity sets is used to determine ΔN_{AB}^{i} (Euler et al., 2001):

$$\Delta\nabla N_{AB}^{i1} = \Delta N_{AB}^{i} - \Delta N_{AB}^{1} \rightarrow \Delta N_{AB}^{i} = \Delta\nabla N_{AB}^{i1} + \Delta N_{AB}^{1} \tag{19}$$

The ambiguity term is estimated by adding ΔN_{AB}^{1} to the double-differenced resolved ambiguities. ΔN_{AB}^{1} is typically arbitrarily chosen, however, it is eliminated later by the baseline processing at the rover or it can be estimated as a modified clock term (Tekmon, 2012). Now that all the necessary terms have been determined, the errors V can be detached into dispersive and non-dispersive components (Euler et al., 2001).

$$V_{AB,L1}^{i,disp} = \frac{{f_2}^2}{{f_2}^2 - {f_1}^2} V_{AB,L1}^{i} - \frac{{f_2}^2}{{f_2}^2 - {f_1}^2} V_{AB,L2}^{i} \tag{20}$$

$$V_{AB}^{i,nondisp} = \frac{{f_1}^2}{{f_1}^2 - {f_2}^2} V_{AB,L1}^{i} - \frac{{f_2}^2}{{f_1}^2 - {f_2}^2} V_{AB,L2}^{i} \tag{21}$$

2.3.1.6 FKP Correction Generation Algorithm

The FKP corrections are generated in a similar manner as MAC and VRS. Double-differences between the reference stations are used to generate dispersive/non-dispersive correction pairs. Also, since traditional FKP uses the non-centralize approach and each reference station broadcasts a set of correction parameters, it differs from VRS in that sense. Though, in terms of correction generation, it is almost identical to VRS. The derivation of the corrections uses the double-differenced model; however, the grouping of the variables are slightly different than previously shown:

$$V_{AB}^{1i} = \Delta\nabla\rho_{AB}^{1j} - \lambda\Delta\nabla\emptyset_{AB}^{1j} - \Delta\nabla I_{AB}^{1j} + \Delta\nabla T_{AB}^{1j} + \lambda\Delta\nabla N_{AB}^{1j} \tag{22}$$

All parameters are known except for the ionospheric and tropospheric delays ($\Delta\nabla I_{AB}^{1j}, \Delta\nabla T_{AB}^{1j}$). Satellite *1* is used here as the indication for cluster reference satellite with respect to which all the in-between reference stations ambiguities are resolved. A residual orbit error parameter can also be added to this model, though in either case the residual effects will be part of the non-dispersive error component. The double-differenced corrections used in FKP are as shown below (Wubbena et al., 1996):

$$V_{AB,L1}^{1i,disp} = \frac{{f_2}^2}{{f_2}^2 - {f_1}^2} V_{AB,L1}^{1i} - \frac{{f_2}^2}{{f_2}^2 - {f_1}^2} V_{AB,L2}^{1i} \tag{23}$$

$$V_{AB}^{1i,nondisp} = \frac{{f_1}^2}{{f_1}^2 - {f_2}^2} V_{AB,L1}^{1i} - \frac{{f_2}^2}{{f_1}^2 - {f_2}^2} V_{AB,L2}^{1i} \tag{24}$$

Figure 2.2 shows the concept of the area correction parameters. Each plane is generated using the residual dispersive and non-dispersive effects shown above at the current height of each reference station. The residuals are fit to a surface and the resulting coefficients are sent to the user to interpolate the corrections based on their location. In the areas of overlap the coefficients broadcast by the closest reference stations are used.

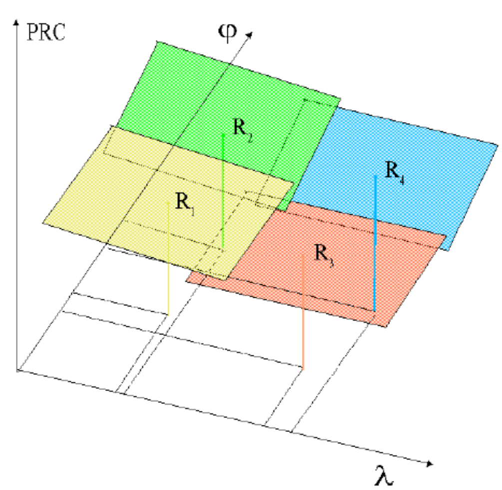

Figure 2.2: Linear FKP planes for four reference stations (Wubbena et al., 2001)

2.3.2 Interpolation to Rover Location

The determined corrections need to be interpolated to the user's location to correct the observations and to position the rover. The interpolation method is the most important step of network RTK, as it has the greatest affect on positioning accuracy (Fotopolous and Cannon, 2001; Dai et al., 2004). There are numerous interpolation methods used.

The distance dependent linear interpolation for the dispersive and non-dispersive correction uses the distance from the reference stations to set weights for the interpolation process. Closest reference station corrections would have the largest weights as an inverse of the distance is used (Dai et al., 2004). The assumption here is that all corrections are double-differenced in between reference stations and all computed with respect to the master station. Dai et al. (2004) shows that the performance of distance dependent linear interpolation interpolation is limited to a certain degree of accuracy and in comparison to other interpolation methods it performs slightly worse due to the estimation of errors in only one dimension.

The linear interpolation method is one of the most commonly used interpolation techniques and is based on obtaining two coefficients (a and b) which represent the spatial extent of the errors. With this method at least three reference stations are required in order to obtain the unknown coefficients, which means one master station differenced with respect to two other reference stations (Wei et al., 2006; Dai et al., 2004; Fotopolous and Cannon, 2001). In the case of having more than three reference stations, a least-squares adjustment is required to obtain the coefficients.

The basic form of this interpolation method from the rover to the master reference station is given by:

$$V_{u,m}^{1i} = (\Delta X_{u,m}, \Delta Y_{u,m}) \binom{a}{b} \tag{25}$$

where $\Delta X_{u,m}, \Delta Y_{u,m}$ are the coordinate differences between the rover's position (or the virtual reference station) to the master reference station and $V_{u,m}^{1i}$ is the double-differenced residual between the rover and master reference station and satellite *1* and *i*. Each set of corrections (for each satellite with respect to the reference satellite) should have a pair of coefficients, which help interpolate the residuals for that particular satellite pair. The coefficients can be estimated on an epoch-by-epoch and satellite-by-satellite basis. Using equation (25), the residual errors can be interpolated to the user's position. This method can perform very well for shorter baselines (20 - 30 km) (Dai et al., 2004).

The linear combination model as outlined by Dai et al. (2004) is based on the computation of a set of coefficients α_i for *n* reference stations:

$$\left.\begin{array}{c} \sum_{n=1}^{n} \alpha_i = 1 \\ \sum_{n=1}^{n} \alpha_i \left(\overrightarrow{X_u} - \overrightarrow{X_n}\right) = 0 \\ \sum_{n=1}^{n} {\alpha_i}^2 = min \end{array}\right\} \tag{26}$$

where α_i is the *i*th coefficient, $\overrightarrow{X_n}$ is the *n*th station's horizontal coordinates and $\overrightarrow{X_u}$ is the horizontal coordinates of the user. The above conditions translate into the following matrix form (Dai et al., 2004; Tekmon, 2012):

$$\begin{bmatrix} 1 & 1 & \cdots & 1 & 1 \\ \Delta X_{1,m} & \Delta X_{2,m} & \cdots & \Delta X_{n,m} & 0 \\ \Delta Y_{1,m} & \Delta Y_{2,m} & \cdots & \Delta Y_{n,m} & 0 \end{bmatrix} \begin{bmatrix} \alpha_1 \\ \alpha_2 \\ \vdots \\ \alpha_{n+1} \end{bmatrix} = \begin{bmatrix} 1 \\ \Delta X_{u,m} \\ \Delta Y_{u,m} \end{bmatrix} \tag{27}$$

where n combinations of reference station pairs exist or $n + 1$ reference stations including the master reference station, m. Like the linear interpolation method, if more than three reference stations exists a least-squares adjustment is required (Dai et al., 2004). Using the coefficients obtained from the matrix solution form, the residual errors can be interpolated to the user's location using the following method:

$$\Delta\nabla V_{u,m} = \alpha_1 \Delta\nabla V_{1,m} + \alpha_2 \Delta\nabla V_{2,m} + \cdots + \alpha_n \Delta\nabla V_{n,m} \tag{28}$$

where $\Delta\nabla V_{u,m}$ is the residual error interpolated to the user's location. The observed carrier-phase can now be corrected using the interpolated residual error:

$$\Delta\nabla\emptyset_{corrected} = \Delta\nabla\emptyset_{u,m} - \Delta\nabla V_{u,m}{}^{disp,non-disp} \tag{29}$$

which can remove dispersive and non-dispersive residual errors from the measurements at the user's location. Linear combination model provides the similar level of performance to that of linear interpolation method.

<u>Low-order surface fitting</u> is used to describe the distance dependent errors, as well as location dependant errors like multipath. The coefficients of this method for more than three reference stations are obtained using a least-square adjustment. This method is based on a second-order Taylor expansion of the GPS error model, much like the first-order surface equation shown below (Dai et al, 2004; Fotopolous and Cannon, 2001):

$$F_{error} = \hat{a} + \hat{b}(\Delta X) + \hat{c}(\Delta Y) + \hat{d}(\Delta Z) \tag{30}$$

where $\hat{a}$ to $\hat{d}$ are the first-order coefficients. However, the model shown includes the change in the Z-axis (taken to be parallel to the local vertical) as well and surface fitting of the errors are normally applied horizontally, which would provide only three coefficients ($\hat{a}$ to $\hat{c}$). After the determination of the surface coefficients, the user based errors can be interpolated. Like all other interpolation methods, each interpolated spatial error corresponds to a satellite, with respect to the reference satellite at common ambiguity level, and the master station for that particular user. The linear interpolation method is in fact a special case of the low-order surface fitting interpolation technique (Dai et al., 2004).

In contrast to other methods, the least-squares collocation method makes use of the covariance matrices to predict distance dependent errors at the user's location (Dai et al., 2004). The computed range for the reference station is subtracted from this carrier-phase measurement:

$$\overline{\emptyset} = \emptyset - \rho \tag{31}$$

and using the following the residuals can be interpolated to the user's location (Dai et al., 2004):

$$V_{u,m} = C_{V_u V_m} D^T \left(D C_{V_m} D^T\right)^{-1} (D\overline{\emptyset} - \lambda \Delta\nabla N) \tag{32}$$

where $V_{u,m}$ is the interpolated residual at user's location with respect to the master station, C_{V_m} and $C_{V_u V_m}$ are variance-covariance (VCV) matrices of the residuals and D is the difference (single or double, depending on the application) operator matrix. In terms of performance least-squares collocation method performs at a similar level as the second-order surface fitting and linear combination interpolation methods (Dai et al, 2004; Fotopolous and Cannon, 2001).

Table 2.1 summarizes the mentioned interpolation methods commonly used in network RTK, shows the main advantage and disadvantage for each technique and displays the relative performance of each.

Table 2.1: Summary of interpolation methods of network RTK

Interpolation Method	**Advantage**	**Disadvantage**	**Performance**
Distance dependent linear interpolation	Simple	Inaccurate	Sub-par
Linear interpolation	Only two baselines needed	Inaccurate over long baselines (> 30 km)	Average
Linear combination	More than two coefficient generated	Inaccurate over long baselines (> 30 km)	Average
Low-order surface fitting	Capable of higher order surface fitting	Low-order surfaces inaccurate over long baselines (> 30 km)	Average
Least-squares collocation	Rigorous	Requires more computation	Good

2.3.2.1 Interpolation in FKP

In the FKP method, a linear interpolation method is used (Wubbena and Bagge, 2006; Tekmon, 2012). This means (as explained above) a set of a and b coefficients (each set for dispersive and non-dispersive errors) are derived for each reference station to describe the linear correlation of the errors in East-West and North-South directions. The surface is taken to be parallel to the WGS84 ellipsoid at the height of the reference station (Wubbena, 1996). However, in reality, any local datum could be used to derive the coefficients.

The interpolation is performed as shown by the equation below for dispersive and non-dispersive residuals alike (Wubbena and Bagge, 2006):

$$\delta r_{u,m,disp}^{1i} = 6.37(a_{disp}(\varphi_u - \varphi_m) + b_{disp}(\lambda_u - \lambda_m)\cos(\varphi_m)) \tag{33}$$

$$\begin{aligned} \delta r_{u,m,non-disp}^{1i} = {} & 6.37H(a_{non-disp}(\varphi_u - \varphi_m) \\ & + b_{non-disp}(\lambda_u - \lambda_m)\cos(\varphi_m)) \end{aligned} \tag{34}$$

where $\delta r_{u,m,disp}^{1i}$ are the dispersive and non-dispersive residuals at the user's location, $a_{disp}, a_{non-disp}, b_{non-disp}, b_{disp}$ are the dispersive and non-dispersive coefficients from the linear interpolation, φ_u and φ_m are latitudes of the coordinates of the user and master station, and $\lambda_u$and $\lambda_u$are the longitudes of the coordinates of the user and master station. *H* is also defined by the following function:

$$H = 1 + 16(0.53 - \frac{\varepsilon}{\pi})^3 \tag{35}$$

Using the following relationships the residuals can be decorrelated for both L1 and L2 measurements (Wubbena and Bagge, 2006):

$$\delta r_{u,m,L2}^{1i} = \delta r_{u,m,non-disp}^{1i} + \frac{f_1}{f_2}.\delta r_{u,m,disp}^{1i} \tag{36}$$

$$\delta r_{u,m,L1}^{1i} = \delta r_{u,m,non-disp}^{1i} + \frac{f_2}{f_1} . \delta r_{u,m,disp}^{1i} \quad (37)$$

Now each carrier-phase observation can be corrected for L1 and L2 using:

$$\emptyset_{corrected} = \emptyset - \delta r \quad (38)$$

2.3.2.2 Interpolation in VRS

For VRS, the correction generation step is typically followed by observation generation, which is generating carrier-phase observations at the master station for the VRS location near the user utilizing a geometric displacement. This process is completed for each satellite with respect to the master station (Wei et al., 2006). Considering that both the position of the master station and the VRS, which is obtained using Single Point Positioning (SPP), are precisely known, the following defines the geometric displacement between the master station and the VRS:

$$\Delta\rho_{m,v}^{s} = \rho_{m}^{s} - \rho_{u}^{s} \quad (39)$$

Also, looking at the single-difference (between satellite *i* and *j*) phase observation at the master station, the single-difference model is shown below:

$$\Delta\emptyset_{m}^{ij} = \frac{1}{\lambda}(\Delta\rho_{m}^{ij} - \Delta I_{m}^{ij} + \Delta T_{m}^{ij}) - \Delta N_{m}^{ij} \quad (40)$$

The same model is valid for the single-difference carrier-phase observation at the VRS. A double-difference can then be formed using:

$$\Delta\nabla\emptyset_{m,v}^{ij} = \Delta\emptyset_{m}^{ij} - \Delta\emptyset_{v}^{ij} = \frac{1}{\lambda}(\Delta\nabla\rho_{m,v}^{ij} - \Delta\nabla I_{m,v}^{ij} + \Delta\nabla T_{m,v}^{ij}) - \Delta\nabla N_{m,v}^{ij} \tag{41}$$

where $\Delta\emptyset_{v}^{ij}$ is the unknown here. $\Delta\nabla\rho_{m,v}^{ij}$ can be obtained from completing the geometric double-differencing and the ambiguity term $\Delta\nabla N_{m,v}^{ij}$ can be solved by using the interpolated $\Delta\nabla T_{m,v}^{ij}$ and $\Delta\nabla I_{m,v}^{ij}$. Typical VRS central facility software would use either linear interpolation or least-square collocation methods or a combination of both. Once the interpolation of the dispersive and non-dispersive effects are complete for the location of the VRS, equation (41) can be used to determine the double-difference ambiguity term between the VRS and master station, allowing the VRS software to determine the single-differenced ambiguity term at the VRS, $\Delta\emptyset_{v}^{ij}$. The rover can position itself using double-differencing between its observables and the VRS generated observables, which should be metres away, to obtain a float solution (Wei et al., 2006). Since, the VRS generated is typically metres from the actual position of the receiver, the spatial errors can be ignored and fixing of the double-difference ambiguity using LAMBDA or any other ambiguity resolution should provide centimetre-level positioning (Teunissen, 1993). Typically the position of the VRS is not changed unless the rover is moved very far (up to a few kilometres).

2.3.2.3 Interpolation in MAC

The MAC interpolation process differs greatly from that of VRS. The interpolation is entirely user dependant. The relevant information is transferred to the user using the Radio Technical Commission for Maritime Services (RTCM) message. This includes the coordinates of the master station and the baselines to the auxiliary stations, as well as the raw master station observations and the single-difference residuals to the auxiliary stations (Lin, 2006). In terms of the correction interpolation MAC is closer to FKP due to its common one-way broadcast design, unlike in VRS where the central facility computes all of the required interpolations without the knowledge of the user of the procedure followed.

One of the main reasons for the development of MAC along with the standardized RTCM 3.0 message was to give the user more control over the interpolation process (Euler et al., 2001). In contrast to the VRS implementation, the aim with MAC has been to improve the system throughput and reduce two-way communications. In this manner, the central processing software can facilitate more users and improve the quality of service. Though, this means that the quality of the coordinates obtained from a MAC network RTK service is dependent on the algorithm that the user is running in the rover receiver. This is one of the weaknesses of the system, as the computations in the MAC approach are "client heavy", which for better accuracy and performance may require more expensive receivers and processors, as opposed to VRS which only requires minimal processing on the user side (Lin, 2006; Tekmon, 2012).

In terms of interpolation, most implementations of MAC from various manufacturers like Leica, use a variation of a very simple distance dependent technique in the older implementations with less processing power, as well as low-order surface and least-square collocation methods in the more powerful receivers (Euler et al., 2003). Lin

(2006) uses these methods as the main technique of interpolation of the corrections on the client side for algorithms using the new RTCM 3.0 message.

2.3.3 Correction Transmission

This step in the network RTK process may not always follow the correction interpolation. In VRS, the corrections are formed and interpolated to the initial approximate position and the raw observations at the master stations are then interpolated to that position using the corrections. All these steps are completed in the central processing facility. The RTCM messages are then formed and sent to the user. With FKP, the corrections are defined using linear interpolation for each individual reference station and broadcast to the user and correction transmission is performed before the actual interpolation by the user. However, the formulation of the interpolation parameters are completed at the reference station, which puts the FKP methodology somewhere in between VRS and MAC. The MAC approach, unlike the other two, requires the correction transmission to be performed before the interpolation process. All required interpolations and correction applications are performed in the rover.

Various techniques exist for the correction transmission to the user in network RTK. However, all of these techniques can be divided into two major categories: one-way communication or two-way communication. In the former, a data link broadcasts the network generated corrections or the network's coefficients every epoch to the user, while in the latter, the user and network's data processing centre are in continuous bi-linear contact (Tekmon, 2012). Essentially, the decision on where the interpolation should take place (rover or central processing facility) is based on the transmission data format used with special consideration given to data bandwidth and computational issues.

2.3.3.1 RTCM SC-104 Protocols

SC-104 is a Special Committee of RTCM that is tasked with setting standard messages for differential GNSS for both maritime and terrestrial applications. In Table 2.2 the different components of RTCM 3.0 can be seen.

Table 2.2: RTCM 3.0 message components

Description	Message Type	Message Name
Observations	1001-1004	L1 GPS RTK Observables, Extended L1 GPS RTK Observable, L1 and L2 GPS RTK Observables
Station Coordinates	1006	Stationary RTK Reference Station ARP with Antenna Height
Antenna Description	1007-1008	Antenna Description and Serial Number
Auxiliary Operation Information	1013	System Parameters

The latest release of RTCM 3.0 is designed to be more efficient in terms of bandwidth use and gives higher integrity in comparison to previous versions, i.e., RTCM 2.3. Like in RTCM 2.3, the first 3 messages in RTCM 3.0 are designed to serve single baseline RTK applications (messages 1001-1003). The RTCM 3.0 messages, as shown in Table 2.2, are divided into 4 main groups: observations, station coordinates, antenna description and auxiliary operation information. In order to provide the minimum network RTK services messages 1001, 1003, 1005, 1007, 1008 and 1011 are required and the rest of the messages provide additional information, such as GPS L1 carrier signal-to-noise ratio, to enhance the performance of the network RTK service (Lin, 2006). RTCM version 3.0 has had 5 amendments, the two most important of which are amendments 2 and 5. The second amendment gives RTCM 3.0 the ability to include residual error messages to support the use of non-physical or computed reference stations, which are included as supplements to facilitate VRS-based network RTK services. The fifth amendment includes the use of SSR, which was discussed earlier, that will eventually enable the reference stations to model undifferenced errors using an approach similar to Precise Point Positioning (PPP).

RTCM has also a standard for Networked Transport of RTCM via Internet (NTRIP), which is an open, non-proprietary protocol developed to facilitate the GNSS correction messages to the client over the Internet (Weber et al., 2006). The NTRIP design has three major components: servers, sources, and casters. An NTRIP source is basically the source that is generating the RTK data stream, which in the case of network RTK would be the main software at the central processing facility. The NTRIP server transfers data from one or multiple NTRIP sources in NTRIP format. And on NTRIP caster acts as a security component for the data providers and also enables the dissemination of data of multiple users. The advantage of using this protocol over the Internet is that it enables centralized network setup, which provides the means to directly interact with the network. However, the issue that arises with the use of this technology is latency, which becomes an issue with network RTK especially in kinematic applications. Though, with the implementation of the new RTCM messages and the emphasis on reduction of bandwidth use, this issue becomes easier to overcome.

Table 2.3 shows a summary of commonly used network RTK that are discussed in this Chapter. The main concept of each technique as well as the major advantages and disadvantages are summarized.

Table 2.3: Summary of commonly used techniques of network RTK

Method	Main Concept	Advantages	Disadvantages
FKP	Correction parameters	One-way communication and no central processing facility required	Cannot keep track of users
MAC	Master-auxiliary	One-way communication and retraceable	More bandwidth use with increasing number of reference stations and more computations on rover side
VRS	Virtual reference station	Users are easily tracked	Two-way communication required

2.3.3.2 One-Way (Broadcast) Communication

One of the biggest issues when implementing a network RTK system is the consideration of bandwidth use (Tekmon, 2012). Since the goal is a real-time positioning system, there is very little room for network latency. As well, the cost of using, e.g., cellular Internet services that typically come with certain legal restrictions should be looked at before the implementation of the network's communication component. However, as mentioned before, the type of communication that is chosen may limit the provider to implement certain methods of network RTK, i.e., the choice of one-way communication rules out the VRS approach.

One-way communication as shown in Figure 2.3 sends the user corrections without prior knowledge of its location. This type of communication does not necessarily require an Internet connection as the broadcast of the correction can be done using a radio link using Ultra High Frequency (UHF) or Very High Frequency (VHF) radio transmitters.

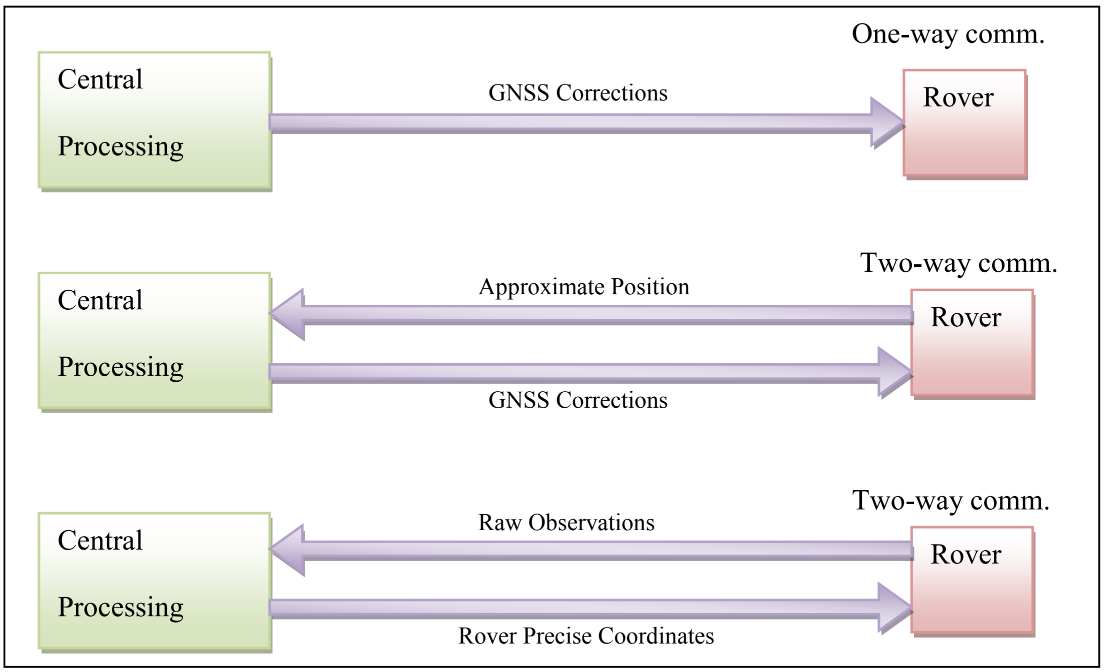

Figure 2.3. Methods of communication for network RTK

The FKP method inherently uses a one-way communication system. The reference station broadcasts its correction parameters using either a radio link or over the Internet. The rover receives corrections from reference stations in its vicinity, permitted by the reach signal if a radio link is utilized, and applies the relevant corrections to its observations using the linear interpolation technique. However, there are implementations of FKP that use the two-way communication system that actually enables the network to act under a centralized architecture; this requires the rovers to send its approximate position to the network, much like VRS. Among the three methods discussed, FKP is the only method that can be used concurrently with MAC or VRS implementations (Tekmon, 2012), i.e., FKP parameters (using message 59 in RTCM 2.3) can be used to enhance VRS kinematic capability.

MAC uses a one-way communication system as well. In this implementation there is no bi-linear communication required between the network and the rover, since the rover is in charge of most computations, interpolation and application of the corrections (Lin, 2006). In variations of MAC the observations from the reference station are used to generate a VRS near the receiver, which uses the VRS methodology at the client side, however the method of communication is still one-way.

MAX (master auxiliary corrections) and i-MAX (individualized master auxiliary corrections) are commercial proprietary implementations of MAC owned by Leica. The i-MAX implementation was developed by Leica to support earlier receivers that are not able to decipher the RTCM 3.0 messages. The difference between MAX and i-MAX in terms of implementation is that MAX is a one-way communication system, which is entirely based on the MAC approach, and i-MAX is a two-way communication system, and much like VRS, the rover is required to transmit its approximate position to the central processing facility (Leica, 2005; Tekmon, 2012). This method differs from VRS in that a virtual reference station is not generated and positioning is performed relative to the master reference station (Leica, 2005). The MAC approach can be demanding in terms bandwidth with larger cells of reference stations, but the i-MAX implementation is independent of the number of reference stations, since it uses a single reference station approach, much like VRS (Brown et al., 2006).

2.3.3.3 Two-Way (Bi-linear) Communication

The two-way or bi-linear communication model (Figure 2.3) is implemented on the basis that the rover communicates with the central processing facility and sends its approximate position or in some variations its raw carrier-phase observations. The central processing facility in turn performs the required computations and transmits the results, be it generated VRS observations or the position of the rover, to the client. VRS is the only method of network RTK that can be achieved strictly through bi-linear communications. The central processing facility requires an approximate position from the rover to generate corrected observations at that position. VRS is a demanding method in terms of communications due to the requirement of parallel transmission of data (Janssen, 2009).

2.4 Summary

In this chapter the development of baseline RTK technology and its expansion to network RTK was introduced. The major steps involved in network RTK were discussed in detail: correction generation, interpolation and transmission. Also, different methods of network RTK and their foremost dissimilarities were presented. The details provided in this chapter are required to provide an overall understanding of network RTK system behaviour. In turn this background information can help explain behaviours and characteristics observed from the static and kinematic evaluation of network RTK in southern Ontario to be presented.

3. METHODOLOGY FOR STATIC AND KINEMATIC EVALUATIONS

In this chapter, other similar studies are examined and their main results briefly discussed, which in turn are to compare to the outcomes of this study. The main goal of this section is to outline the experimental set-up for the static and kinematic tests performed and to show the overall amount of data collected to complete the analyses. The main motivation for the static tests was to analyze the quality of the horizontal solutions and use the results to fulfil the requirements of the MTO project as the specifications are only concerned with horizontal accuracy and precision. The results were used to synthesize a set of procedures and guidelines for the use of network RTK in low-order control surveying. The kinematic data were collected as a secondary analysis in trips made between the static test sites.

3.1 Similar Network RTK Evaluation Studies

Studies of network RTK performance are needed, as the information provided by the service providers is not independent. Also, it is not in the best interest of private network RTK service providers to make all such performance information public. So, there is a requirement for independent studies to characterize the performance of network RTK.

There have been similar studies that investigate the network RTK performance in various locations around the world, for both static and kinematic applications. An example of a comprehensive static evaluation is Edwards et al. (2008) that evaluated network RTK services in Great Britain. Commercial network RTK has been available in Great Britain since 2006 and network RTK services are an expansion of the Ordnance Survey OS Net (OS Net), which differs from Ontario where each private company constructed their own network. Leica and Trimble are the two companies that are licensed to provide network RTK solutions operating SmartNet and VRSNow, respectively. This study focused on the performance of these privately-run networks in terms of solution accuracy and repeatability, improvement with the integration of additional satellite constellations, and performance of the networks at their coverage edges and in presence of significant height differences. A series of tests were completed for this study in March 2008 and solutions of the networks were recorded at each of the chosen test sites. A rather interesting test set-up was employed (Figure 3.1), which utilized a horizontal bar that holds three antennas; the antenna in the centre was connected to a geodetic receiver and the outer network RTK antennas were each at a distance of 25 cm from the centre. The test set-up used can introduce new sources of constant multipath and slightly affect the visibility of low elevation satellites; however, the short and fixed baselines (250 mm) between the antennas can greatly increase the coordination quality of each antenna using physical baseline constraints. Coordinates for the test locations were determined independently using raw data from the central antenna processed with the Bernese version 5.0 software and relative positioning for the two outer antennas with respect to precisely determined central antenna coordinates using Leica GeoOffice software. Filtering of the solutions was employed prior to the analyses using CQ (Coordinate Quality or solution uncertainty), as well as Dilution Of Precision (DOP). The results revealed that both private companies are operating at the same level of accuracy. Also, it was shown that the coordinate quality values indicated by the equipment under more extreme conditions (limited visibility and large multipath) tend to be overly optimistic. The study also concluded that, in general, the accuracies (1σ) of network RTK in Great Britain range from 1.0 to 2.0 cm in the horizontal and 1.5 to 3.5 cm in the height. A set of "proper" field practices for the use of network RTK were defined based on the results of the study.

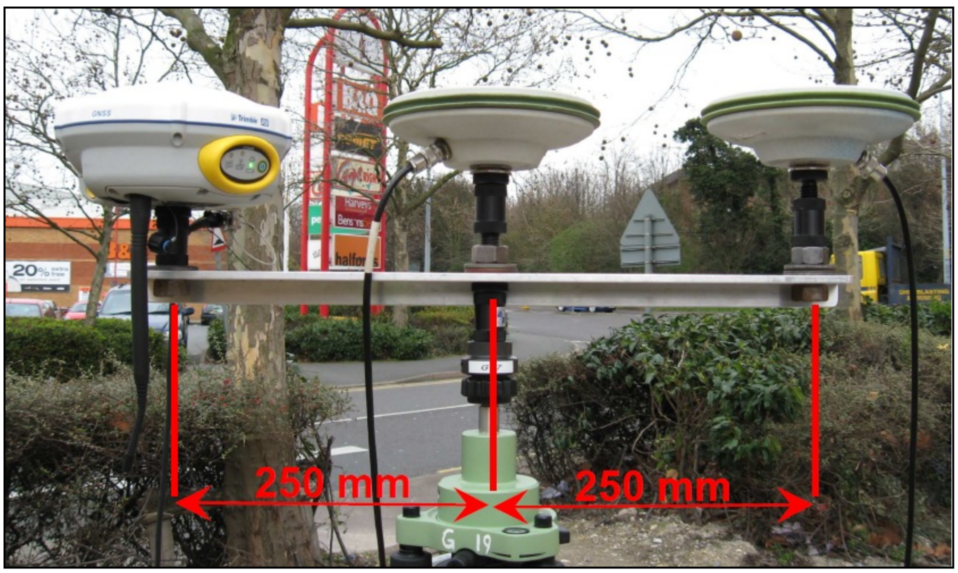

Figure 3.1: Test set up used by Edwards et al. (2008)

Another similar study was conducted by Rubinov et al. (2011) in Victoria, Australia. In this study, both kinematic and static aspects of network services were studied. There are three different networks currently operating in Victoria: VRSNet, using Trimble network software; TopNet, using the Topcon software suite; and Checkpoint, provided by GLOBAL CORS. Three test sites were chosen at various distances. Control points were established at each test site at nominal distances of 250 m and static occupations were performed to determine coordinates for the control points using the Trimble Geo Office

(TGO) post-processing software. The main focus of the study was the quality of height determination at various test locations; however, similar results were shown for the horizontal solution qualities as well. The testing procedure was devised to evaluate the performance of network RTK for two separate applications: general surveying (static testing) and machine guidance applications (kinematic testing). A Temporary Reference Station (TRS) was also introduced to densify the existing Continuously Operating Reference Stations (CORS) network and to evaluate the benefits, if any, of its inclusion on the results. The results showed general height error of 2.5 cm (1σ), which was reduced to 2.0 cm by application of the TRS. The study also showed the performance of the mentioned networks at various distances from the primary reference stations in both horizontal and height accuracy. Generally, a decrease in the absolute accuracy was demonstrated with an increase of the baseline length. For the kinematic portion of the evaluation, a robotic total station was used to track the movement of the vehicle using an omni-directional prism to provide the reference solution. One reason for performing the tests at low speeds (< 5 km/hr) was due to the inability of the total station to track a rapid moving object. In this study, more than one type and brand of network RTK equipment was used. All of the receivers were connected to one dual-frequency antenna mounted on the roof of the vehicle. Three different test runs were performed at 9 km, 23 km and 35 km from the nearest reference station, all of which are approximately 5 - 10 minutes. The height deviation results for each baseline length showed sub-centimetre accuracy at 9 km, as well as ~1 cm and ~2 cm at 23 km and 35 km, respectively. In terms of precision, the baseline length had very little effect on the standard deviation as for all three baselines a standard deviation of ~1.8 cm was observed.

Another study of network RTK in kinematic mode was completed by Aponte et al. (2008) in Great Britain. In this study, two separate kinematic runs were performed of ~60 minute duration using MAC-based equipment with Leica's SmartNet network RTK solution. The equipment was set for a 20 Hz collection rate. The network RTK solutions were compared to relative GPS, as well as coordinates determined using the raw data, though the details of the method that was used to determine the coordinates are unclear. The results of tests in terms of accuracy showed 2D and 3D root mean squared (rms) of ~3.5 cm and ~4.5 cm, respectively. For the precision results of both kinematic runs showed standard deviations of ~2 cm in 3D, with height having twice the standard deviations of easting and northing components. In terms of availability of fixed solutions were during the two 60 minute kinematic runs, ~58% of the network RTK solutions are available compared to the total possible epochs. Other studies involving the performance evaluation of network RTK include: Jonsson et al. (2002), Al Marzooqi et al. (2006), and Delcev et al. (2009). These studies also showed very similar results in terms of availability, accuracy and precision.

3.2 Static Methodology and Fieldwork

The evaluation methodology for the thesis tests was designed to accommodate the three different models of equipment and their respective characteristics, which was a requirement in order to develop procedures and guidelines for use in MTO control surveys. Careful pre-planning and logistics were considered due to the volume of the tasks undertaken. Field practice simulations were held to ensure stability of the proposed methodology and reduce problems during the data collection process. Also, for the thorough evaluation of network RTK services, two separate field campaigns were performed: in December 2010 and in July 2011. The goal of the fieldwork campaigns was to collect as much raw GPS data and network RTK (GPS only) solutions as possible for all active service providers. The fieldwork campaign in July 2011 was performed to test long-term repeatability and also to perform additional tests that were deemed necessary after reviewing the results of December 2011 campaign and consulting with MTO and service providers, such as static timed tests and a control survey test. Only 4 of the sites were revisited due to budgetary and time constraints.

The following tests were performed in each field survey campaign and Table 3.1 shows the amounts of data collected for each portion of the work:

December of 2010 (winter):

- 9 static sites visited (Figure 3.4)
- ~8 hours of raw and network RTK data collected from each receiver at each site.
- Time-to-first-fix tests
- ~50 hours of kinematic network RTK data collected

July of 2011 (summer):

- 4 sites revisited

- ~6 hours of raw and network RTK data collected from each receiver at each site
- Additional tests
    - Static solution tests
    - Control survey tests

The amount of fieldwork carried out for this study provides copious amounts of data, which in comparison to similar literature possesses the largest data set.

Table 3.1: Data types collected during the field campaigns

Field Survey	Data type	Test durations	Total data collected
Winter (Dec. 2010)	Static NRTK	8 hrs	288 hrs (1 Hz, fixed)
	Raw GPS	8 hrs	288 hrs (1 Hz, fixed)
	TTFF	5 trials	135 trials
	Kinematic NRTK	10 hrs	50 hrs (1 Hz, fixed)
Summer (July 2011)	NRTK	6 hrs	80 hrs (1 Hz, fixed)
	Raw GPS	6 hrs	80 hrs (1 Hz, fixed)
	Static solutions	5 trials	369 trials

3.2.1 Test Configuration

The three network RTK rovers were set-up as per Figure 3.2; one receiver / antenna was set up on the selected reference station, which was a forced-centred monument or a brass cap, and the other two receivers / antennas were set up on tripods within a few metres of the reference monument over temporary markers. Network RTK solutions, the associated quality control information, and raw measurements (for post-processing) were recorded for at least 8 hours in the winter campaign and 6 hours in the summer campaign using the auto static solution surveying method, which automatically records network RTK data.

The configuration in Figure 3.2 should minimize biases due to geometrical differences by keeping the geometry and surrounding environment the same. Time-to-first-fix tests were also performed and the measurement for each trial were recorded to be analyzed as a metric of network RTK service performance. Time-to-first-fix was measured from the moment the receiver was fully connected to the Internet to the first network RTK fixed solution. For each trial the receiver was fully restarted to simulate a cold start.

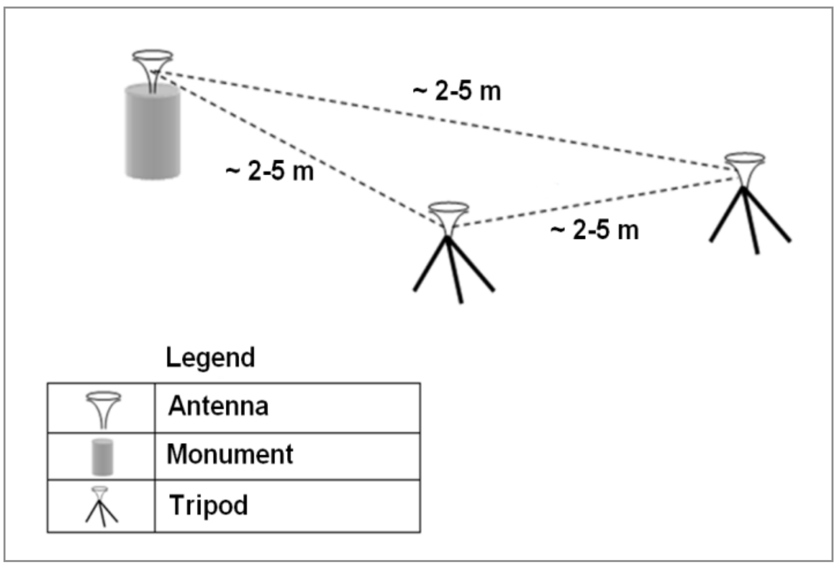

Figure 3.2: Test set up used at each test site

3.2.2 Equipment

The winter campaign was performed from December 2, 2010 to December 15, 2010. All 9 sites were visited. All three service providers participated in this fieldwork campaign. The tested equipment from each service provider is given in Table 3.2. Note that integrated receiver/antenna units were used, as these are typical standard user equipment.

Table 3.2: Models of equipment used for the fieldwork

Service Provider	Manufacturer	Receiver/Antenna
Sokkia	Sokkia	GSR2700 ISX
Leica	Leica	GS15
Cansel	Trimble	R8 Model 2

The summer campaign was performed from July 1, 2011 to July 26, 2011. There were a few equipment changes with some of the service providers, where a variation of the equipment models mentioned in Table 3.2 were used for testing. These changes in the summer were either due to the unavailability of the exact receiver model used at the equipment rental high-season, or due to the request for upgrades by the service provider.

3.2.3 Site locations

Figure 3.3 shows the dense network RTK reference station distribution in southern Ontario. There are a total of over 70 stations covering a span of 900 km from south-western to eastern Ontario. The locations of the nine sites visited during fieldwork for this study are shown in Figure 3.4: Peterborough, Belleville, Kingston, Ottawa, Kitchener, Windsor, London, St. Catharines and Barrie. Each location was chosen in a manner to cover the areas of interest as well as proximity to reference stations in southern and eastern Ontario.

The site names were created based on the closest large municipality and may not represent the actual location of each site. Details of each monument can be seen in Table 3.3, which shows the type and class of the monument occupied. The Coordinated Survey Information Network Exchange (COSINE) station numbers, which are provided in Table

3.3, refer to the monument numbers provided on Ontario's COSINE database. Published coordinates and other details of the abovementioned monuments can be viewed using this database.

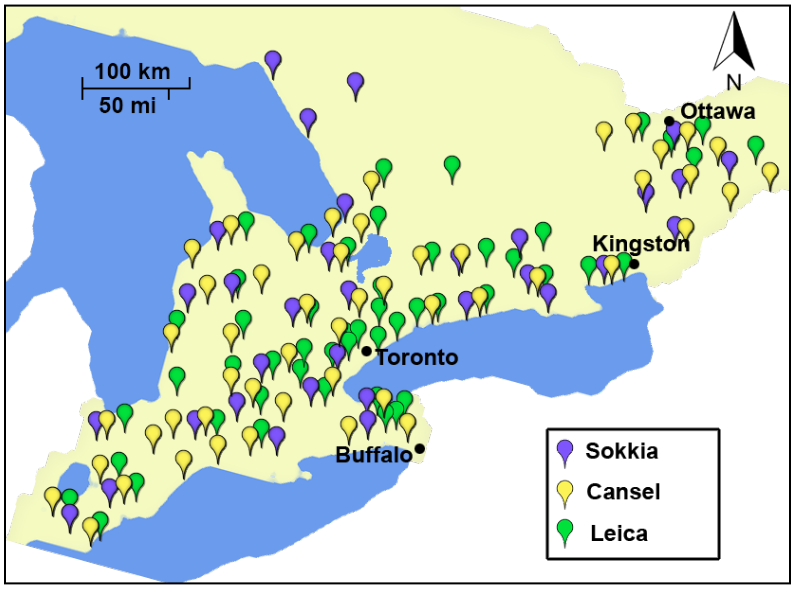

Figure 3.3: Network RTK reference stations in southern Ontario - late 2010

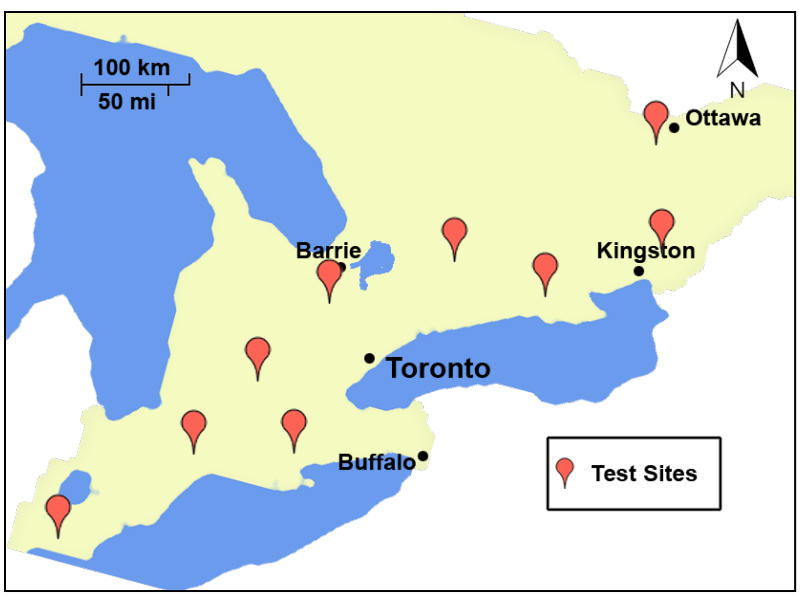

Figure 3.4: Network RTK test locations used in southern Ontario

Table 3.3: Information on the static test site monuments

Name of testing points	Type of monument	Order	COSINE station numbers	Site code
Peterborough	CBN	Class A	00119973002	pet
Belleville	CBN	Class A	00119823033	bel
Kingston	CBN	Class A	00119973001	kin
Ottawa	CBN	Class A	00119833001	ott
Kitchener	CBN	Class A	00119843025	kit
Windsor	Cap	Class C	00819980491	win
London	CBN	Class A	00119813041	lon
St. Catharines	Cap	Class C	00819980031	stc
Barrie	Cap	Class D	00819798415	bar

3.2.4 Reference Coordinates of Test Locations

The monument coordinates used in this study were official coordinates published by Natural Resources Canada (NRCan) (NRCan, 2011) and COSINE (MNR, 2011), the latter of which is a public service provided by the Ontario Ministry of Natural Resources. All of the post-processing of the collected raw GPS data was completed using the Bernese version 5.0 processing software (AIUB, 2005). For coordinate determination, the raw data were used to determine the vectors from the monument to each of the temporary markers. Approximately eight hours of raw data were available from each antenna. The double-differenced vectors were then used with the officially published coordinates (COSINE and NRCan) to determine the coordinates of each temporary marker. Also, each high order monument's coordinates were re-determined and compared to guarantee the quality of these coordinates using raw data from nearby Canadian Active Control System (CACS) reference stations and the eight hours of raw GPS data that were collected over each monument, via static relative positioning. Table 3.4 shows the CACS sites that were used to determine the monument coordinates. These sites were chosen based on the closest pair of active control points to each test site. The monument coordinate determination results show agreement with the published monument coordinates in the sub-centimetre-level.

Table 3.4: CACS sites used in processing and proximity to test sites

Test site	**CACS used**	**Approximate distance from site (respectively)**
Peterborough	Kingston & Peterborough	140 km & 170km
Belleville	Kingston & Ottawa (NRC1)	50 km & 185 km
Kingston	Kingston & Ottawa (NRC1)	30 km & 130 km
Ottawa	Gatineau & Ottawa (NRC1)	20 km & 25 km
Kitchener	Goderich & Port Weller	100 km & 110 km
Windsor	Goderich & Port Weller	200 km & 310 km
London	Goderich & Port Weller	105 km & 110 km
St. Catharines	Goderich & Port Weller	165 km & 80 km
Barrie	Parry Sound & Port Weller	130 km & 115 km

For the control survey monuments the coordinates were determined by occupying each point for approximately one hour and simultaneously setting up a separate receiver over a nearby, higher-order monument. This process was repeated twice and the results were averaged for the control survey adjustment. Also, the relative baselines between the points were surveyed by “leap-frogging” along the traverse. Using Bernese v5.0, a full network adjustment was done to determine coordinates of each monument. Figure 3.5 shows the data collection process that was used for the coordinate determination for the seven control survey points.

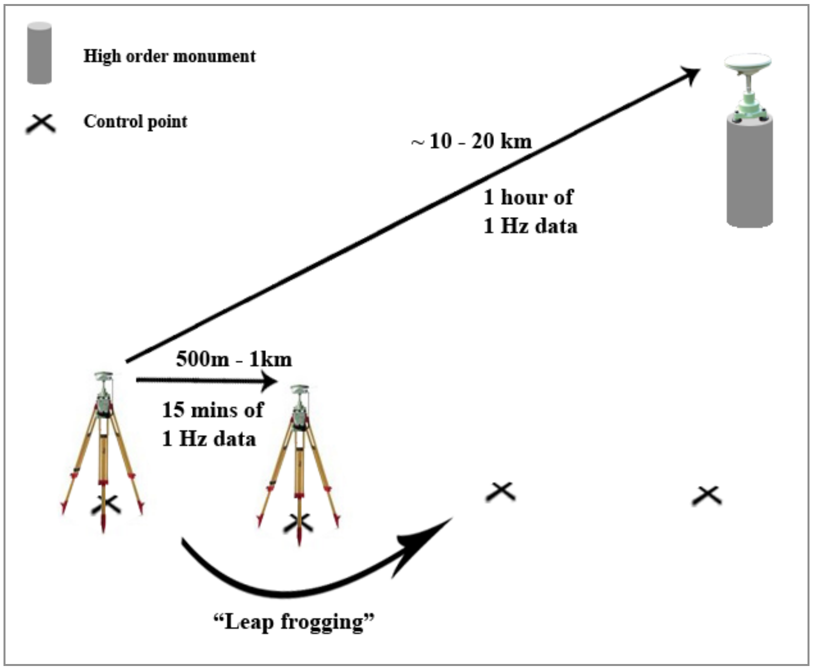

Figure 3.5: Control survey data collection procedure for coordinate determination

3.3 Kinematic Methodology and Fieldwork

The kinematic data collection was performed in parallel to the static tests. Many of the trips made between test locations across southern Ontario were accompanied by kinematic tests. In this section the details of the experimental set-up, as well as the amount of kinematic network RTK data collected are outlined.

3.3.1 Equipment Set-up

The set-up for the kinematic experiment is a rather simple one. The three antennas were mounted on the vehicle's roof, using magnetic mounts. The antennas were approximately 0.5 metres away from each other and organized in a "V" arrangement. The distance between the antennas were not the same for each trial, as the arrangement changes slightly with each kinematic run. The receiver data collectors were placed directly below the antennas inside the car. The Bluetooth connections between data collectors and the receivers proved to function well, even with the physical barrier presented by the vehicle's roof. The overall arrangement of the receivers on the vehicle can be seen in Figure 3.6. The antennas were not surveyed in order to determine the coordinates; however, the network RTK absolute coordinates from each antenna were used to determine the relative baselines, as presented in Chapter 5.

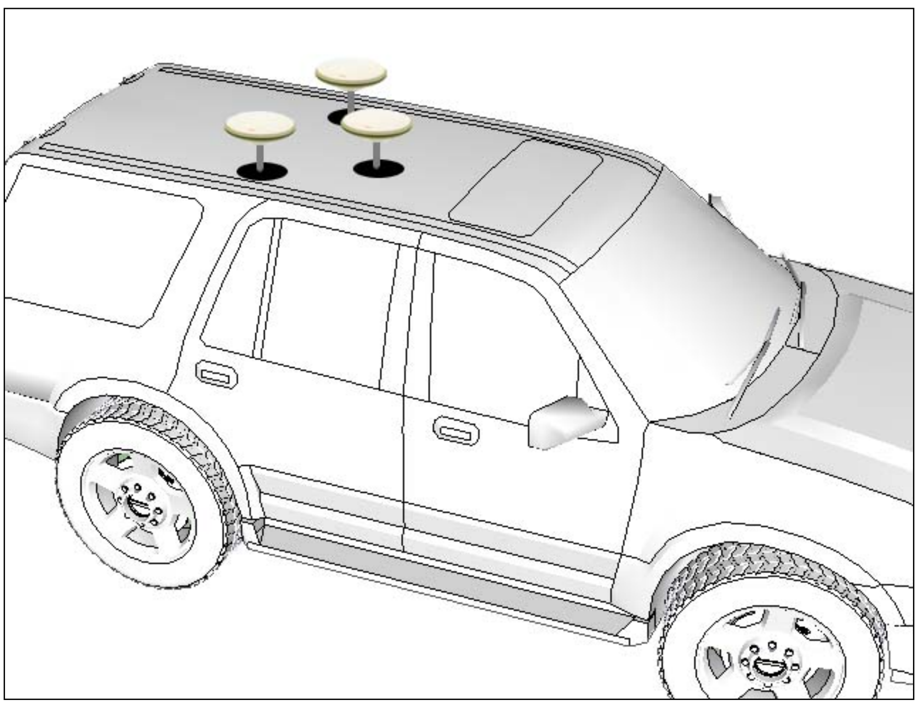

Figure 3.6: Kinematic test antenna arrangement

One of the major difficulties with the experimental set-up shown was the rapid depletion of data collector batteries due to continuous running of the Bluetooth connections. Hence, for longer drives, where applicable, the serial cables were utilized to connect the receivers to their respective data collectors. Another concern was the safety of the equipment at speeds of over 100 km/h.

3.3.2 Test Locations

Five different kinematic data sets were available for the kinematic analysis. Table 3.5 shows the test runs information including destinations, lengths, total number of data points available and active equipment during each test. The trajectories of different data sets described in Table 3.5 are shown in the Figure 3.7 to Figure 3.11. The availability of the data varies with each service provider, which is mainly due to differences in their network coverage. This issue minimizes the amount of common data points available between service providers for comparison. The longest kinematic run is performed over ~350 km drive, which is incomparable to any of the data sets shown in the literature.

Table 3.5: Kinematic test details

Start location	**End location**	**Length**	**Total available solutions**	**Active company equipment**
St. Catharines	Kitchener	3.5 hours	13,054	'A'/'B'/'C'
Kitchener	Windsor	4 hours	20,314	'A'/'B'/'C'
Windsor	London	3.5 hours	15,138	'A'/'B'/'C'
Toronto	Jarvis	2 hours	10,031	'A'/'B'/'C'
Barrie	Toronto	1 hour	4,657	'A'/'B'

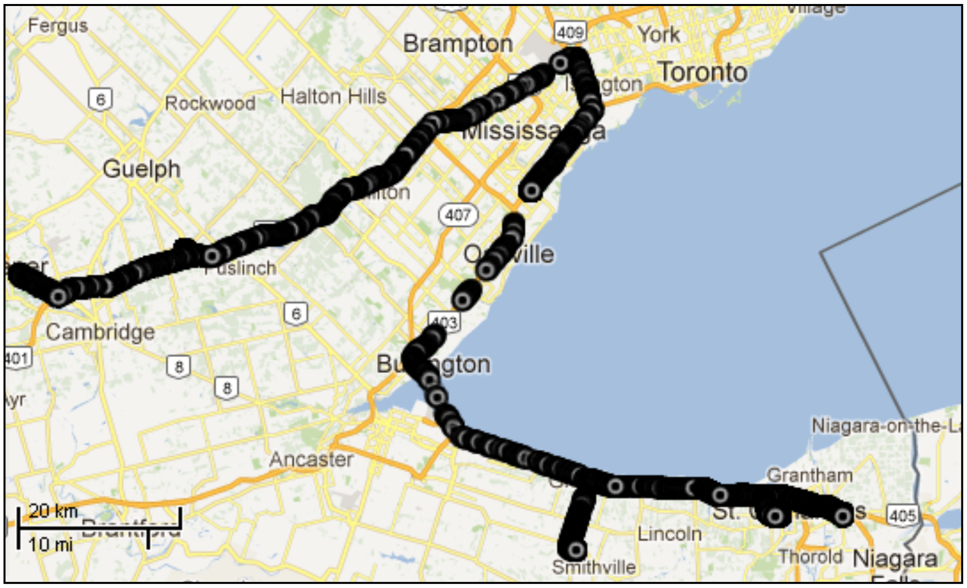

Figure 3.7: St. Catharines to Kitchener test run

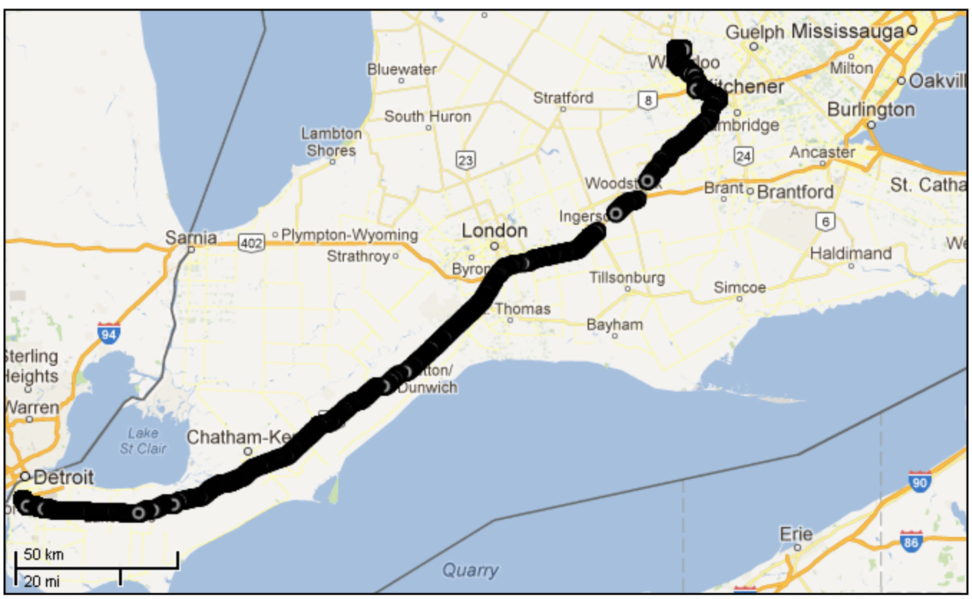

Figure 3.8: Kitchener to Windsor test run

Figure 3.9: Windsor to London test run

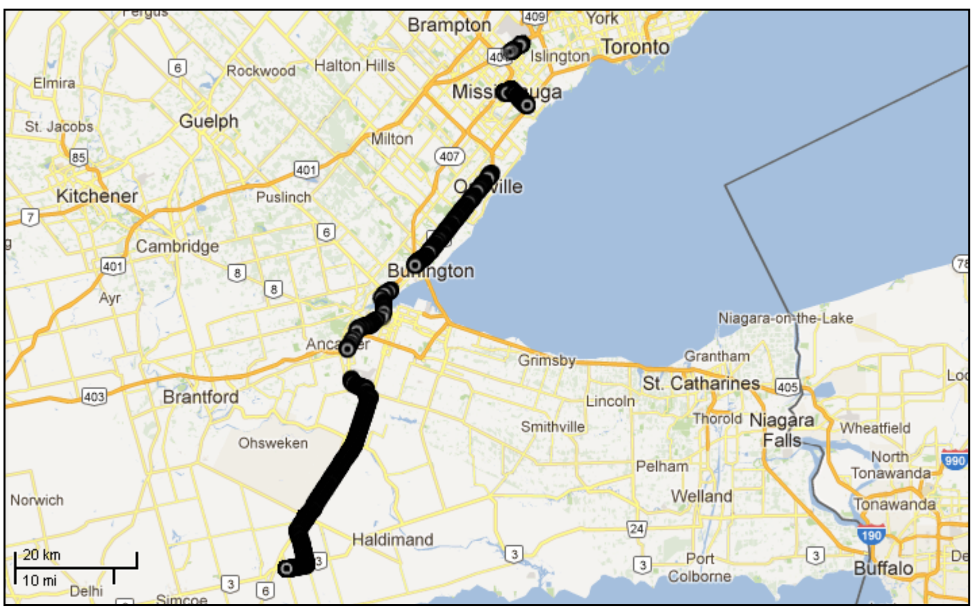

Figure 3.10: Toronto to Jarvis test run

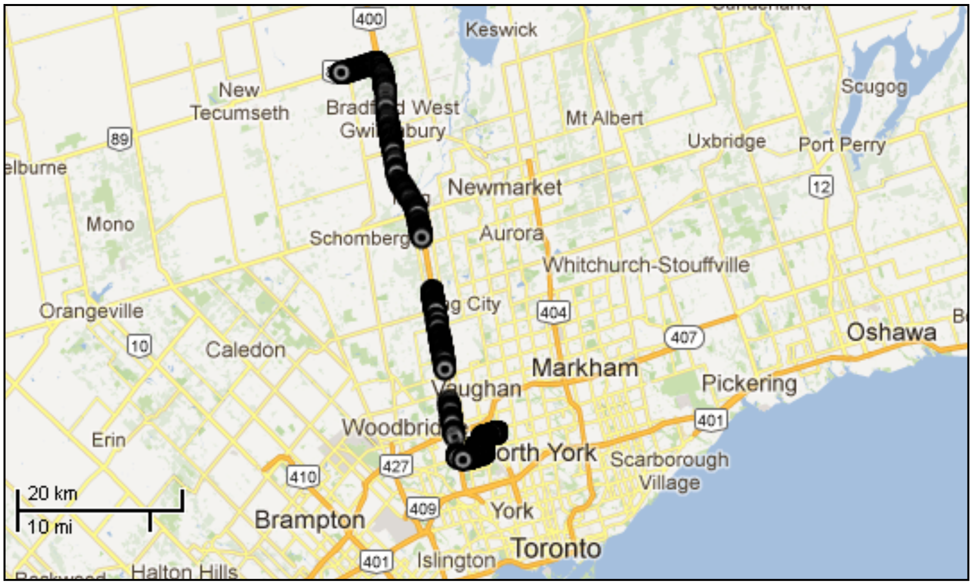

Figure 3.11: Barrie to Toronto test run

As it can be seen from the figures, the data sets are not continuous. In certain situations, the discontinuities can be up to 30 minutes. The changing environment during the test and the existence of obstructions cause disruptions in the availability of the solution. However, discontinuities are expected with any kinematic data set of this kind.

3.4 Performance Analyses Metrics

In order to define ‘performance’ of network RTK, performance metrics need to be defined. For the purpose of this analysis, the metrics selected are: availability, time-to-first-fix, precision, accuracy and solution integrity. Also, the effect of moving average filtering is studied on precision and maximum error. These metrics were chosen to help quantify the performance of network RTK as well as aid in the setting of guidelines and procedures for the utilization of network RTK in control surveying.

3.4.1 Availability

The purpose of the availability analysis is to show the amount of usable data that were collected for each test site. The network RTK availability percentage is computed by comparing the number of network RTK records available against the number of records that should be available at the 1 Hz data collection interval over the period of observation.

3.4.2 Time-To-First-Fix

The time-to-first-fix (TTFF) analysis shows the average time to first network RTK position fix for each service provider at each test site. The TTFFs were recorded from a "cold start" (turning on the receiver after a complete shutdown) to the time when the first fixed solution is obtained. This test was repeated at least 5 times for each equipment.

3.4.3 Precision

The purpose of the precision analysis is to compare the collected 1 Hz solution with respect to its own mean, using the auto static solution setting, which allows the receiver to automatically record network RTK data. The standard deviations of the time series characterize the data as "precise" or "imprecise" within 1σ of the normal distribution.

3.4.4 Accuracy

The accuracy analysis compares the network RTK solutions from service providers against the published and determined coordinates. For these analyses, the service provider's internal quality control variances are used to filter the network RTK solutions, with the results being shown in NEU (North, East and Up) components.

3.4.5 Solution Integrity

The solution integrity analysis is an in-depth look at coordinate quality covariances and attempts to determine the reliability of the coordinate quality values that are given by equipment processing outputs. This study provides comparisons of absolute errors against coordinate quality values, and correlation plots.

3.4.6 Moving Average Filtering

The moving average filtering analysis compares different size averaging windows of the 'raw' network RTK solution with respect to each determined coordinate. An average of the 1 sec filtered network RTK solutions collected for the service providers with different sized time bins (5 sec, 10 sec, 30 sec, 60 sec and 5 min) to show how this moving average can be used to filter solutions further and obtain better results.

4. STATIC NETWORK RTK EVALUATIONS

This chapter focuses on characterizing the performance quality of network RTK in southern Ontario in static mode. The following metrics are used to examine the performance of network RTK: availability, time-to-first-fix, precision, accuracy, solution integrity and moving average filtering. Some of these metrics, such as moving average filtering, were chosen to aid in developing the guidelines and specification for the MTO project. Examples of plots for each performance metric are shown in this chapter, though the complete set of solution quality, solution integrity and moving average filtering plots at each test site for each service provider can be found in Appendices A, B and C.

4.1 Solution Quality

Figure 4.1 shows a "good" network RTK solution time series plotting solution error versus local time. Horizontally, a maximum error of ~1 cm can be seen and the time series shows very little variation. Statistically, there are no significant positional biases seen in the solution. As expected, the up component shows approximately twice as large an absolute error as the horizontal components. For 8 hours of network RTK records, a standard deviation of 0.6 cm in the horizontal and 0.8 cm in the height component was observed. Also, solution biases of 0.1 cm, 0.2 cm and 0.8 cm bias can be seen in the north, east and height components respectively. The variation seen in the time series are due to the residual noise in the measurements.

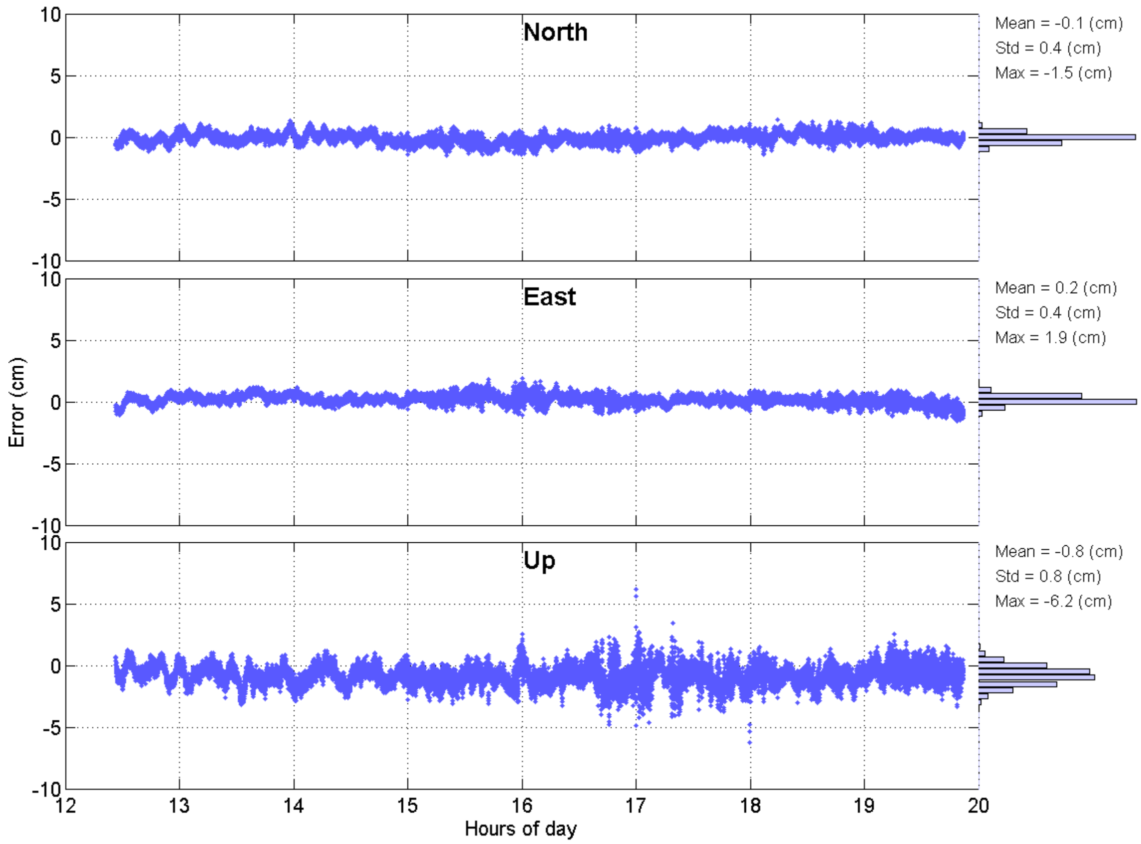

Figure 4.1: Example of “Good” quality network RTK solution

In contrast to Figure 4.1, Figure 4.2 displays a “not so good” solution showing larger variations of a few centimetres from the reference coordinates. The standard deviations in the north, east and height components are 1.3 cm, 1 cm and 2 cm respectively. The biases are 0.5 cm, 0.4 cm, north, east and 1.2 cm for the height component, respectively. The uncertainty is almost three times worse than the previous "good" solution. A gap of 10 - 15 minutes can be seen between hours 14 – 16 of the data. This gap is not due to a discontinuation in the available solutions and is a result of removing outliers using the equipment provided coordinate variances. Furthermore, some sinusoidal structure is present in some portions of the “not so good” time series. This is due to the fact that the test site, Kingston or 'kin', is at the very edge of all of the networks and the network RTK software is actually extrapolating the residual errors instead of interpolating them.

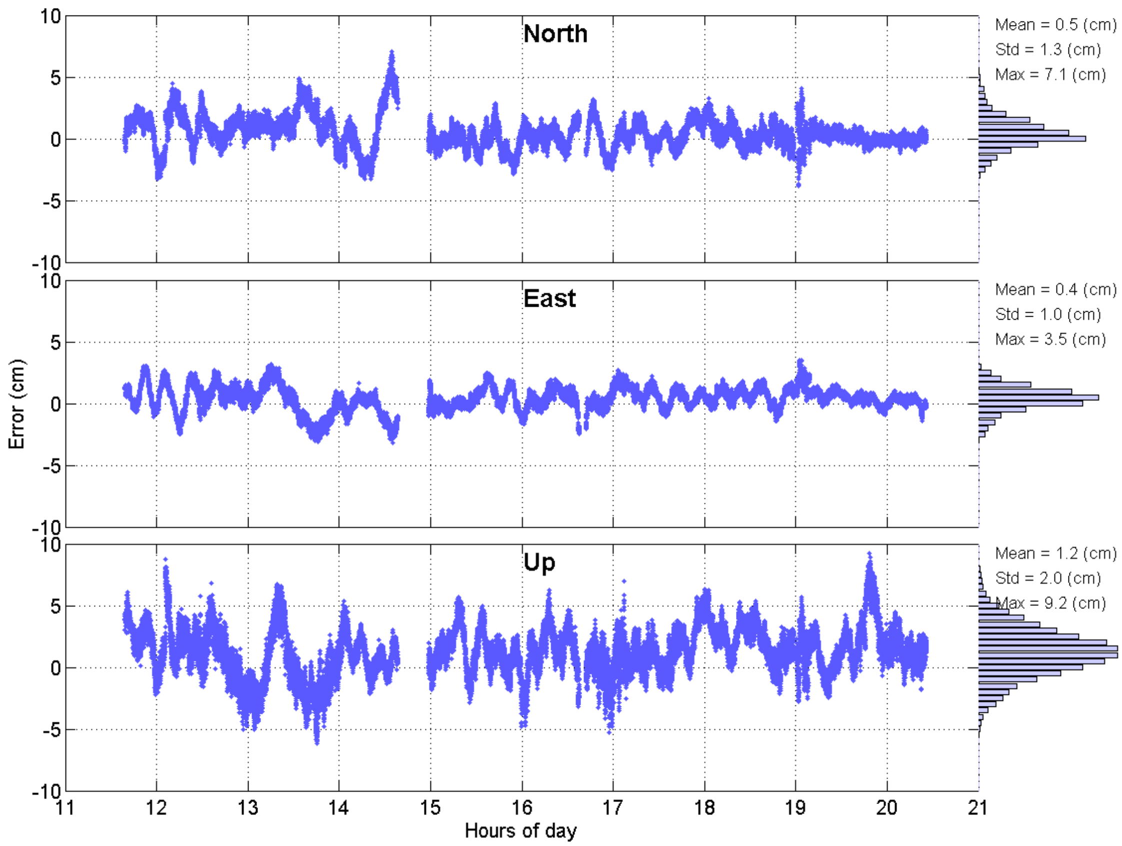

Figure 4.2: Example of "Not so good" quality network RTK solution

Figure 4.3 shows the existence of biases in some of the network RTK solutions. The time series in each component have sizeable non-zero means. The solutions are very precise in the horizontal component, as illustrated by the associated histograms and standard deviation values. The standard deviations for north and east components are 0.9 and 0.6 cm, respectively. A large maximum error can be seen due to a 8 cm spike in vertical component. However, large overall biases of 1.5 and 3.1 cm in the north and east components, respectively, paint a picture of a precise but not so accurate solution. Also, the same sinusoidal behaviour is seen, but with a higher frequency than shown in the previous results. These biases are not due to any issues involving error estimation, as the solution is still fairly precise. The biases are directly related to the coordination procedure for reference stations of each network. In this particular case, the network is showing a 4cm horizontal bias with respect to Ontario's official reference datum (NAD83 CSRS epoch 1997.0).

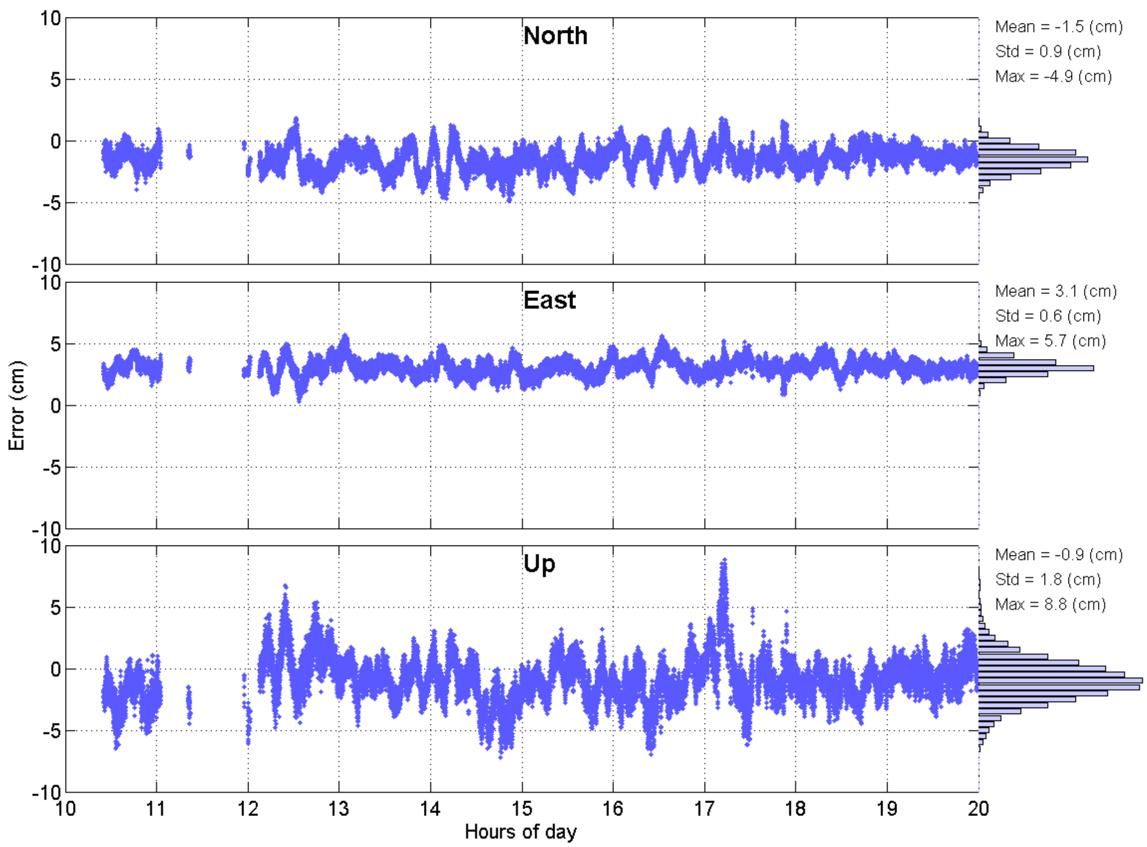

Figure 4.3: Biases in network RTK solution

Figure 4.4 demonstrates low frequency sinusoidal structure in the network RTK position solution. The solutions show a longer period (~20 minute) oscillation through most of each time series, as compared to a ~15 minute period in Figure 4.3. Most of the solutions collected as part of this study are affected by this pattern; however, characteristics differ from location to location, as well as service provider. This sinusoidal effect is an excellent example of why the user should collect more than one set of observations, offset by minutes or hours, to determine accurate network RTK based coordinates. For example, in Figure 4.4, if hours 14 to 14.5 are considered, the solution varies from -5 cm in northing to +5 cm within a 15 minute window. This means that if a user were to collect just a single position fix, or if the results were to be averaged using 5 minute windows, solutions would differ by ~10 cm in this one component.

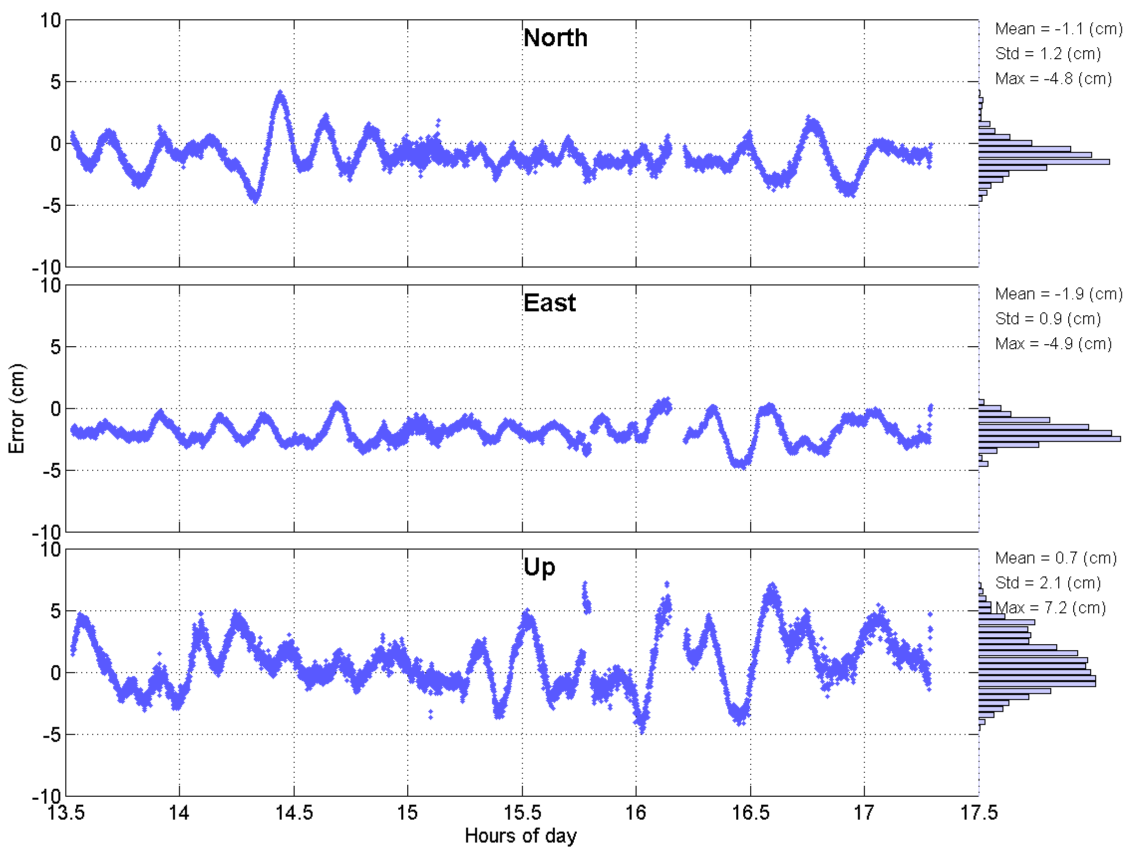

Figure 4.4: Sinusoidal behaviour in network RTK solution

Large fluctuations in a matter of minutes indicate that the interpolation of the residual errors is not completely successful and a large portion of the residual errors in the rover's observations are left uncorrected. These results should provide sufficient evidence to take more than one set of observations for each survey and to also separate the observation trials by at least tens of minutes (possibly at different times of day) to avoid relying on observations that are not completely independent.

4.2 Availability

Solution availability is one of the first issues that needs to be addressed when evaluating the performance of network RTK. This section describes the availability percentages of each service provider at various test locations. Results are subject to a variety of issues that affect the network RTK users. Cellular coverage and access latency are the most prominent causes of data gaps. Another major issue is processing lag: epoch skips and data lags may exist due to older hardware and software. Bluetooth issues are also troublesome: when using a data-collector and recording solutions at 1 Hz, Bluetooth connections tend to disconnect even at metre-level distances. However, it is important to consider that occupying a point for up to ten hours while collecting ambiguity-fixed network RTK solutions at a rate of 1 Hz is far from typical for the average user. Though, this unorthodox method of testing is necessary to push the system performance, and to observe and characterize the availability of the services.

4.2.1 Winter Campaign

The winter availability results can be seen in Figure 4.5 to Figure 4.7 for the service providers at different test locations around Ontario. Typically, for a fully operational network RTK service, an availability of 97% to 99% is expected (Aponte et al., 2009). Though, as Figure 4.5 illustrates, this is the case for only three of nine locations for this particular service provider (Company 'A'), with the average solution availability being 86% ±11% (1σ). During the course of the field work, the equipment was checked every 30 minutes. Some of the missing data here is due to losing Internet connection and the inability of the user equipment to automatically reconnect to the Internet, therefore requiring manual restarts. This issue presents a major short coming of network RTK equipment and service availability for long hours of data collection. So, the major limiting factor of network RTK availability is the two-way communications between the receiver and network server. Reliable network latency and cellular coverage is needed to be considered and remedied to be able to render network RTK as a 100% available service. Also, visibility affects availabilty; however, due to the locations of these test sites, this was not a major issue. It can be seen from Figure 4.5 for sites in Ottawa ('ott'), Windsor ('win') and London ('lon') show an availability of almost 99%. Availability percentages of 99% suggests that this network and equipment is capable of providing this level of availability, which validates the point made above that the network availability (cellular coverage, network latency and equipment problems) is, normally, the major issue.

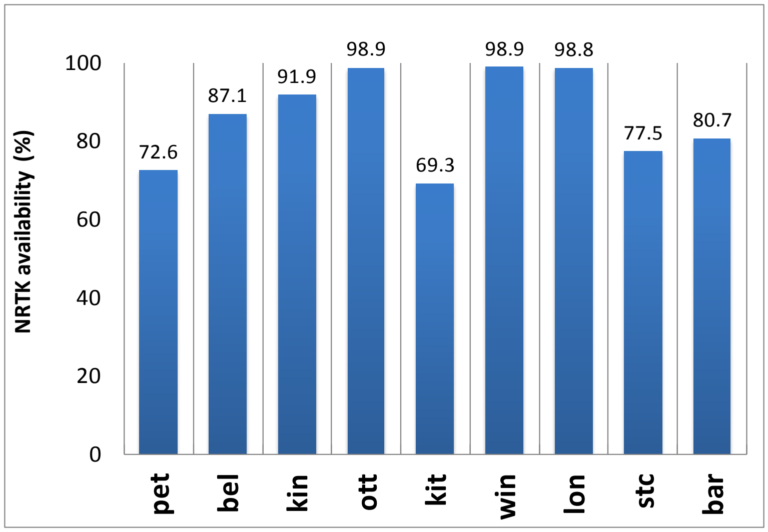

Figure 4.5: Availability percentage in winter campaign for Company 'A'

Results for Company 'B' can be seen in Figure 4.6. The average availability in the winter campaign is 42% ±7% (1σ). This is less than half of what the availability for a robust network RTK system should be. There are no data available for test site Belleville ('bel') due to a hardware corruption issue. An unstable Bluetooth connection is the cause of the equipment disconnecting from the cellular modem and interrupting the Internet connection (mainly at sites 'pet' and 'kit'). A serial cable was used as an alternative when Bluetooth issues persisted. Also, the lack of robustness of the network RTK software may have caused lags in the estimation of the error corrections, which can lead to skipped epochs in solutions. The majority of the data gaps are due to regular skipping of records, for example every other second or every 5 seconds. In the next section it can be seen that a slight change in hardware and software can increase the availability of the network RTK solutions. Solution availability is also affected by the user location within the network. Further details of missed epochs due to network lag or reduced software robustness are shown in Section 4.2.3.

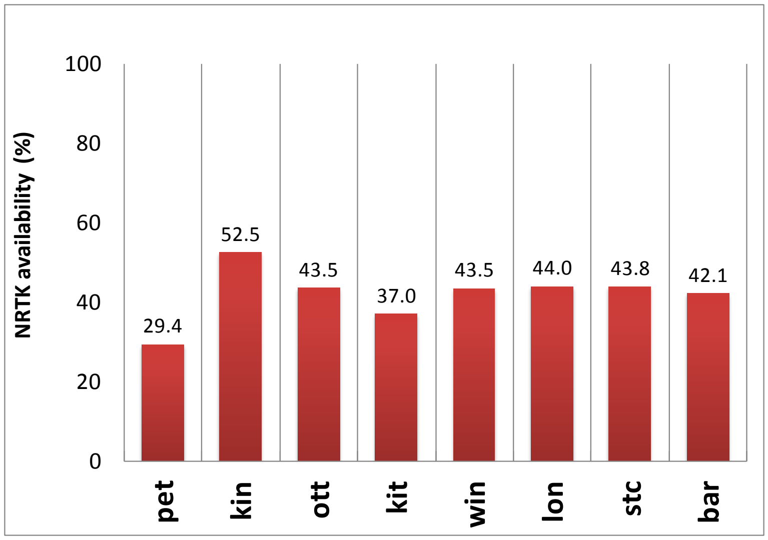

Figure 4.6: Availability percentage in winter campaign for Company ‘B’

Solution availability for Company 'C' can be seen in Figure 4.7. Availability is within acceptable levels at all sites except at Kingston (‘kin’), which is located at the edge of this network. The average availability is 98.5 ± 2% (1σ), which is very high and consistent.

This section shows that there is no uniform network RTK performance when it comes to solution availability from various service providers. The figures show that percentages of available solution can change with location and service provider. Also, data gaps due to cellular connections and equipment malfunction over long periods of data collection (e.g., many hours) can cause lower availability. Furthermore, remote locations will be adversely affected by sparse wireless network coverage, as opposed to densely populated areas that tend to have significantly better coverage. The results seen above represent data availability percentage for extended periods of observation (many hours) and may not represent what the average user will encounter during their much shorter periods of observation.

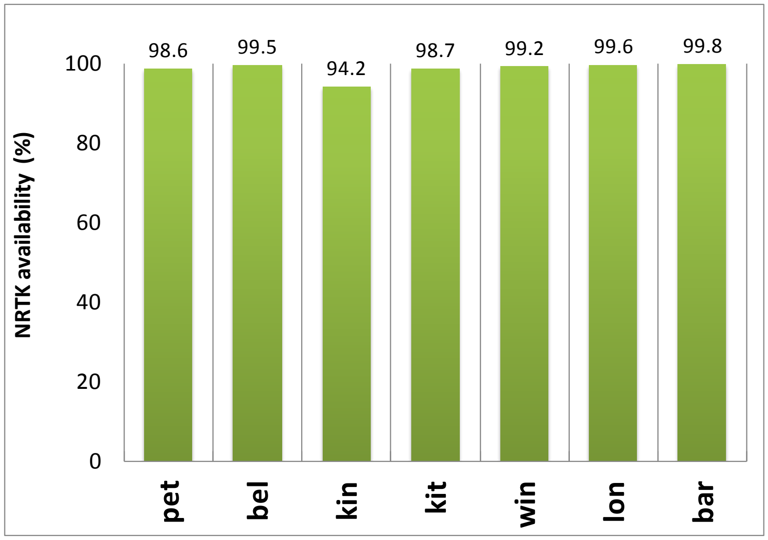

Figure 4.7: Availability percentage in winter campaign for Company 'C'

4.2.2 Summer Campaign

Figure 4.8 to Figure 4.10 show the percentages of solution availabilities from the test sites revisited in the summer. Figure 4.8 shows significantly better results for Company 'A' than the winter results. The average availability in the summer is 88% ± 9% (1σ). This is closer to what the ideal case should be (>97%), but still leaves room for improvement. The improvement seen here may be due to slight changes in hardware and software.

The results for Company 'B' in Figure 4.9 indicates that this particular service's availability was increased significantly to acceptable levels with a hardware upgrade. The average for the summer results is 90% ±20% (1σ). This average would be 99.8% ±0.1%

(1σ) if the Kitchener (‘kit’) site is ignored. The data shortage at this site was due to significant cellular issues and high connection latency.

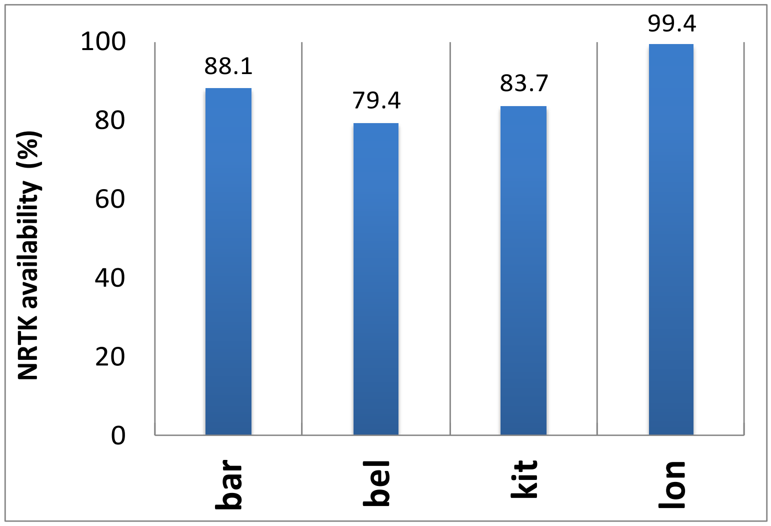

Figure 4.8: Availability percentage in summer campaign for Company ‘A’

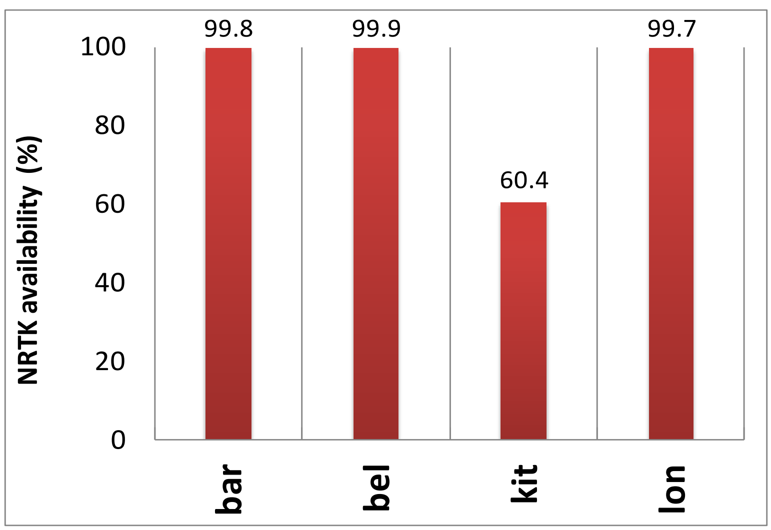

Figure 4.9: Availability percentage in summer campaign for Company ‘B’

Figure 4.10 shows results that are consistent with the winter results for Company ‘C’. The average for the service availability is 98% ±1.4 (1σ), which is very good and slightly above expected published levels. However, for 'bel' Company 'C' is experiencing slightly below expected availability, which is not consistent with the winter results.

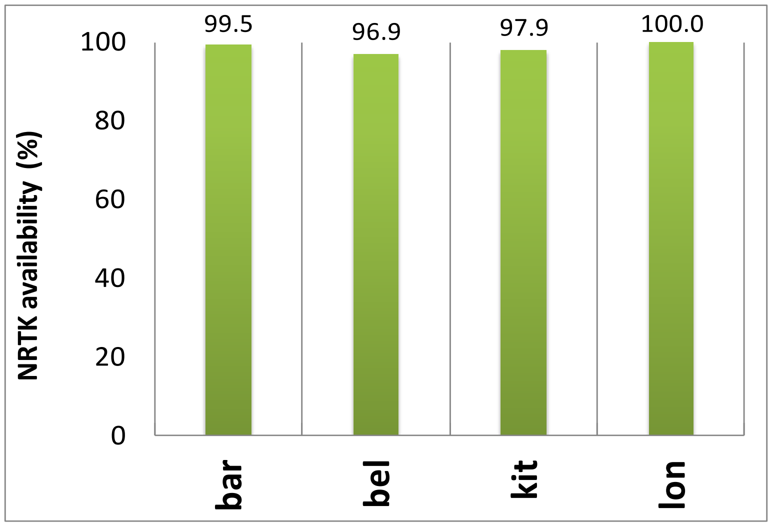

Figure 4.10: Availability percentage in summer campaign for Company 'C'

4.2.3 Data Gap Analysis

This section illustrates some of the data gaps that exist within the records collected. Table 4.1 shows the results for Company 'A', indicating that the majority of data gaps are 1 second gaps. Also, a few 2, 3, 4 and 5 second data gaps were observed. The majority of gaps larger than 5 seconds are actually one minute up to isolated cases of 10s of minutes in duration. This result, as mentioned, is most likely due to weaknesses in the robustness of the hardware and software used during the fieldwork, and could also be caused by delays in the cellular network connection. However, these magnitudes of data gaps should not affect the user experience significantly, as the average user will not collect this amount of data for control and engineering surveys. Missing records can affect the availability of the solution significantly. From almost 60 hours of data, more than one hour is missing due to 1 to 5 second data gaps.

Table 4.1: Data gaps in winter campaign for Company 'A' (1 Hz data rate)

Site	1 sec skips	2 sec	3 sec	4 sec	5 sec	Epochs missing	>5 sec	Epochs available
pet	374	2	3	0	8	427	3	20521
bel	231	1	2	0	6	269	1	21858
kin	458	0	1	0	2	471	0	23509
ott	327	2	3	1	7	379	4	20735
kit	573	0	0	0	0	573	0	30886
win	654	2	0	0	4	678	0	27547
lon	510	49	18	4	20	778	5	21283
stc	403	11	7	2	6	484	4	23990
bar	415	9	12	1	16	553	3	29984
Overall	3945 (85%)	76 (3%)	46 (3%)	8 (1%)	69 (7%)	4612 (100%)	20	220313

Table 4.2 shows the data gap analysis results for Company 'B,' and as the availability results suggest, significant data gaps exist. The first noticeable issue is that there are more data missing from 1 to 5 second gaps than epochs available. Available epochs make up about 44% (typical availability results) of the total epochs that should be available, assuming 100% availability. Also, the majority of the data gaps are 2 second gaps (59% of missing data). With 1 to 5 second gaps, it can be expected that the availability of the data should almost double, and place well above 80%. However, other major issues such as long periods of disconnects play a significant role in the low availability.

Table 4.3 shows the excellent results for Company ‘C’. Throughout the field campaign only five 1 second gaps were observed. Also, the majority of the gaps are 5 second gaps. Only two major interruptions occurred - both at site ‘bel’. The overall solution availability, as seen in the previous section and in Table 4.3, is above 98%, which puts the results at typical network RTK levels.

Table 4.2: Data gaps in winter campaign for Company ‘B’ (1 Hz data rate)

Site	1 sec skips	2 sec	3 sec	4 sec	5 sec	Epochs missing	>5 sec	Epochs available
pet	3205	2521	206	18	16	9017	4	7919
kin	3475	1330	1	0	4	6158	0	7104
ott	3983	3414	117	0	3	11177	2	9715
kit	4751	4734	536	0	1	15832	0	11960
win	5120	4870	623	2	4	16757	0	12897
lon	4334	4595	306	2	5	14475	0	11381
stc	4933	4564	591	0	2	15844	0	12366
bar	4215	4643	376	5	4	14669	2	11433
Overall	34016 (32%)	30671 (59%)	2756 (8%)	27	39	103929 (100%)	8	84775

Results from each service provider are different, as with most results from this study. From various external studies, it can be seen that network RTK services are largely outperforming the services in Ontario in terms of availability. Only the results from Company ‘C’ demonstrate acceptable data availability for network RTK.

Table 4.3: Data gaps in winter campaign for Company 'C' (1 Hz data rate)

Site	1 sec gaps	2 sec	3 sec	4 sec	5 sec	Epochs missing	>5 sec	Epochs available
pet	1	0	0	0	11	56	0	28377
bel	3	0	0	0	11	58	2	29756
kin	0	0	0	0	32	160	0	30815
kit	0	0	0	0	6	30	0	28897
win	0	0	0	0	7	35	0	26627
lon	0	0	0	0	4	20	0	28421
bar	1	0	0	1	11	60	0	32742
Overall	5 (1%)	0	0	1	82 (98%)	419 (100%)	2	205635

4.3 Time-To-First-Fix

Figure 4.11 to Figure 4.13 show the average TTFF for each test site and their standard deviations recorded during the winter campaign. TTFF is heavily affected by the quality of the cellular coverage at any location. Figure 4.11 shows the average values and standard deviations of Company 'A' TTFF results. The majority of the results are under 25 seconds, with the one major exception of site 'kin'. Figure 4.12 shows the average and standard deviations of TTFF for Company 'B'. By examining Figure 4.11 and Figure 4.12, it can be seen that the results at various locations are very different. For example at site 'kin' Company 'B' has fast and consistent TTFF results, as opposed to the very large and inconsistent results from Company 'A', while the reverse results can be seen for the Peterborough ('pet') test site. This may be due to the fact that companies are using different wireless carriers.

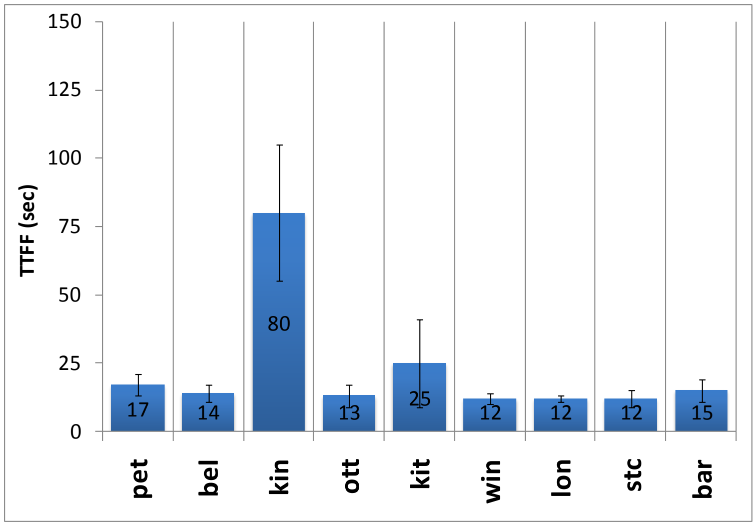

Figure 4.11: TTFF in winter campaign for Company 'A'

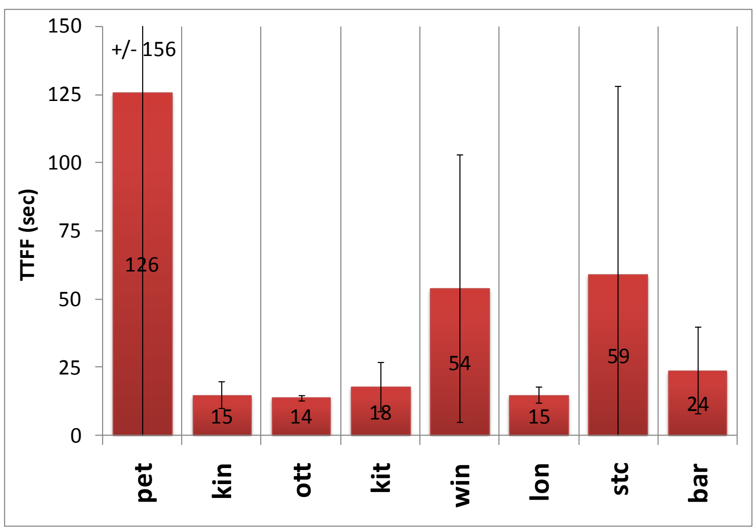

Figure 4.12: TTFF in winter campaign for Company 'B'

Company 'C', as it can be seen from Figure 4.13, produced similar results to Company 'A', which includes poor TTFF results at site 'kin'. Interestingly, the mean and standard deviation of TTFF for site 'kin' are almost identical to the results shown in Figure 4.11. Generally, for most locations around Ontario approximately 15 to 30 seconds can normally be expected for the equipment to produce a network RTK position fix from a cold start. At some locations, there are isolated situations where the value can be as large as one to two minutes.

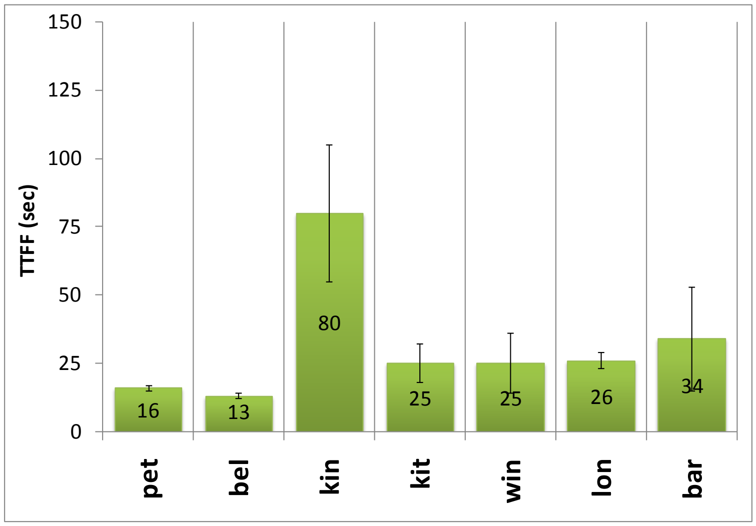

Figure 4.13: TTFF in winter campaign for Company 'C'

4.4 Horizontal Precision

The precision of network RTK data gives the user an indication of the repeatability of network RTK solutions over the short-term, where short-term is defined in terms of hours. In the next few sections, figures illustrating precision for both the winter and summer campaigns are presented. The precision calculated here is the standard deviation about the mean of each time series, for each test site, from each service provider, computed in northing and easting components (and vertical component in Section 4.5). The values have been appropriately scaled to illustrate the 2σ (95%) confidence level. In order to transform the 1σ (68%) horizontal precision into the 95% horizontal precision a scale factor of 2.45 for two-dimensional data is used (GSD, 1996; Harre, 2001).

4.4.1 Winter Campaign

Figure 4.14 to Figure 4.16 show of the per site precisions for the three service providers. The precision statistics are calculated with approximately eight hours of network RTK data for each service provider in the horizontal component. Figure 4.14 shows the horizontal network RTK precision (95%) for Company 'A' at each test site. As can be seen the results vary between 1.4 to 3.7 cm with a mean precision of 2.3 ±0.8 cm over all test sites. These results are very similar to published values from other similar studies on network RTK.

Figure 4.15 shows the horizontal network RTK precision (95%) for Company 'B'. The overall precision from all test sites is 3.0 ±1.1 cm, which is slightly worse than the results from the other service providers. Interestingly, 'lon' sites shows consistent high levels of precision for all service providers and some of the best results for Company 'B'. This may be due to the surrounding environment at this site, with great visibility and no significant source of multipath nearby. Also, consistent with the precision of Company 'A' and Company 'C' at test site 'pet' similar level of precision is demonstrated.

There are some common trends in Figure 4.14 and Figure 4.15. For example, both results suggest that positioning precision at sites 'pet' and 'kin' is lower than at 'ott', 'kit' and 'lon'. This may be due to network geometry similarities between both service providers. However, at the site 'bar', a difference can be observed. The precision for Company 'B' at this site is almost half of that obtained with Company 'A': 4.3 cm versus 2.3 cm. The possible cause for this difference is the proximity of the closest reference station for Company ‘B’ compared to Company ‘A’.

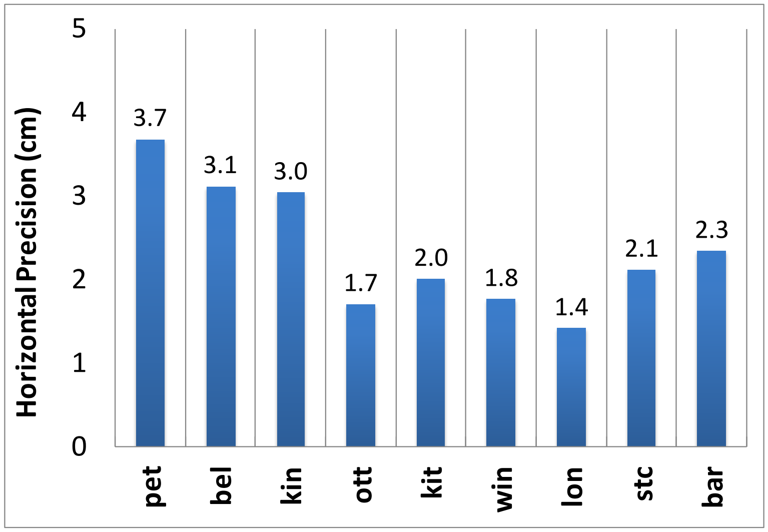

Figure 4.14: Horizontal precision (95%) in winter campaign for Company ‘A’

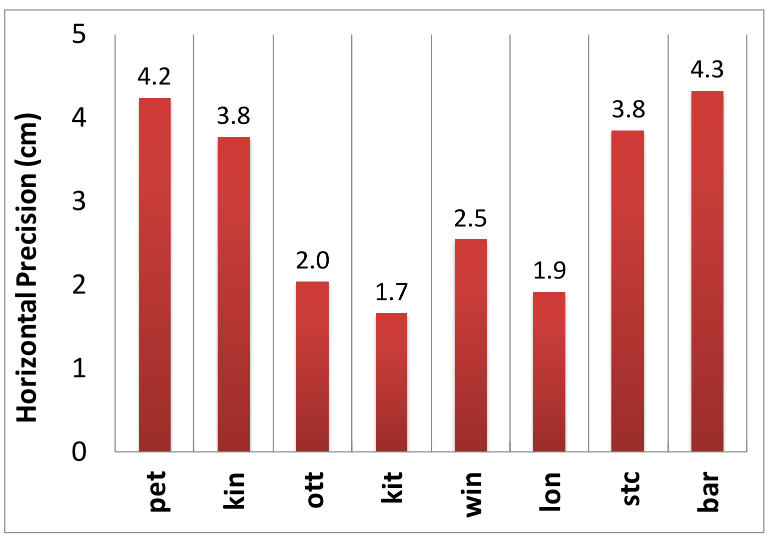

Figure 4.15: Horizontal precision (95%) in winter campaign for Company ‘B’

Figure 4.16 shows the horizontal network RTK precision (95%) for Company 'C'. The overall precision computed over all test site is 2.4 ± 0.9 cm. Missing sites, as mentioned before, are due to solution unavailability resulting from service provider network maintenance. The precision for Company 'C' is at similar levels as the other service providers, which all show 2-3 cm (95%) precision. However, site 'kin' is seen here as having a lower precision than the rest of the results for Company 'C'. This result is in fact the case for all networks at that particular location, which was at the edge of each company's coverage during the time of the surveys.

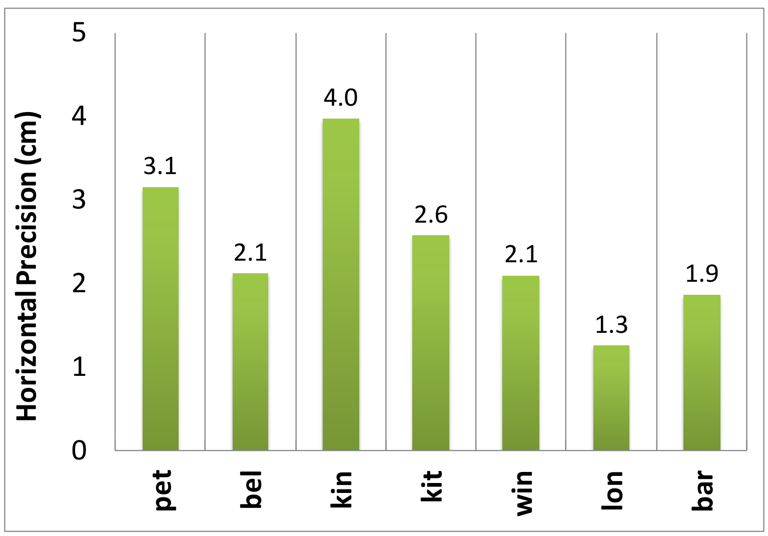

Figure 4.16: Horizontal precision (95%) in winter campaign for Company 'C'

As can be seen, all three service providers offer very similar precision levels (on average 2-3 cm) in almost all locations around southern Ontario. This suggests that in terms of network RTK methods and network architecture there is no significant difference between various methods of network RTK put forward by the service providers. Also, the results indicate horizontal precision (95%) below 5 cm at all locations.

4.4.2 Precision Repeatability

The similarity of the winter horizontal precision results lead to the expectation of seeing similar levels of precision from the summer results as well which would be an indication of long-term coordinate repeatability and consistency; however, Figure 4.17 to Figure 4.19 illustrate that the horizontal precision of network RTK solutions for the revisited sites in the summer campaign are systematically worse in comparison with the winter precision values. Figure 4.17 shows up to 1.5 cm worse results in the summer than the winter. This is possibly due to the collection of smaller number of data points in the summer campaign compared to the winter campaign (25% less data were collected in the summer), which could cause the standard deviation of the solutions to be larger.

Precision statistics for Company ‘B’ in Figure 4.18 indicate an improvement in the winter precision for the site ‘bar’, while every other result from Company ‘B’ follows the trend seen in Figure 4.17. The lack of availability of winter data for site ‘bel’ caused a gap in Figure 4.18 and therefore no comparison between the summer and winter was possible at this location. Test site ‘bar’ does not exhibit the pattern of worsening precision from winter to summer. However, for ‘kit’ and ‘lon’, this behaviour is consistent with the results from Company ‘A’.

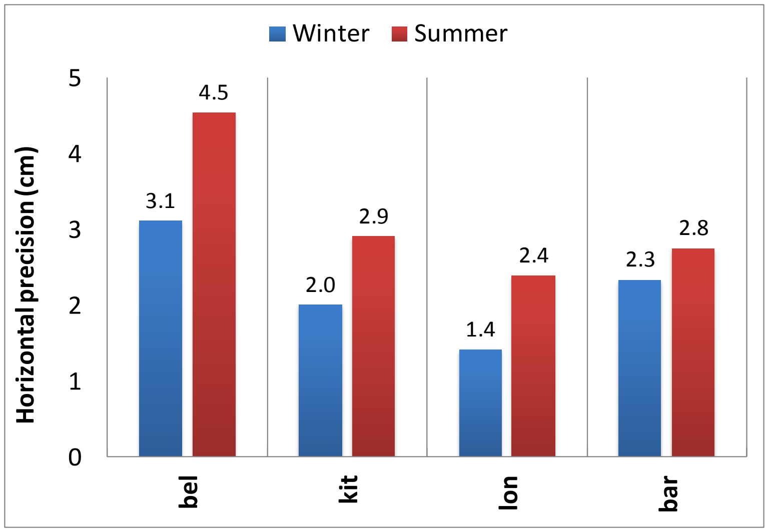

Figure 4.17: Comparison of winter and summer campaign precision for Company ‘A’

Figure 4.19 displays the comparisons for Company ‘C’. These results also consist of up to 1 cm higher values for 95% horizontal precision in the summer. These results follow the same trend seen from Company 'A' and 'B'.

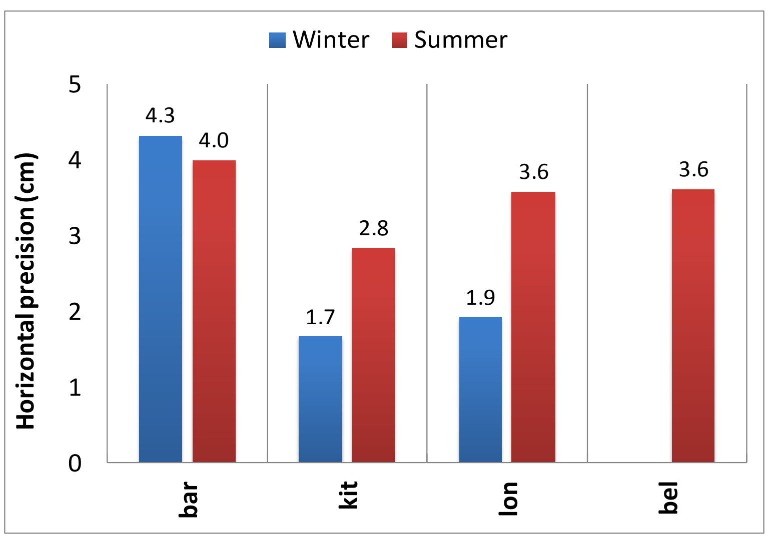

Figure 4.18: Comparison of winter and summer campaign precision for Company ‘B’

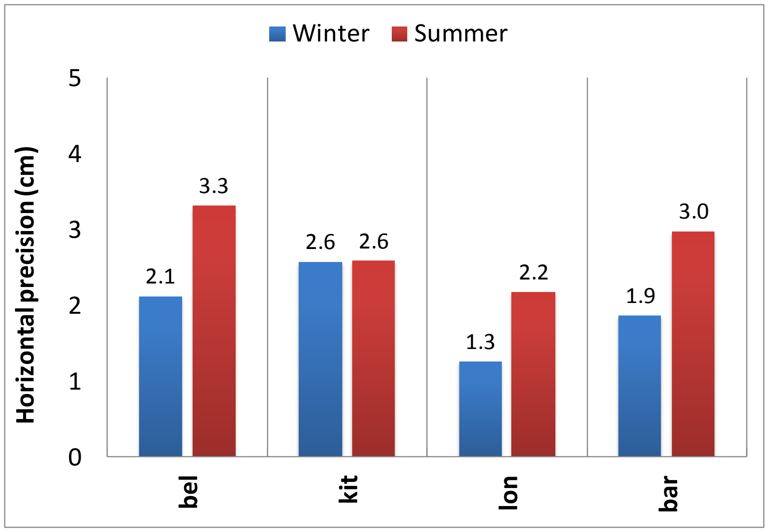

Figure 4.19: Comparison of winter and summer campaign precision for Company ‘C’

In order to further examine the consistency of the precision levels between the winter and summer results, a statistical test of the standard deviations at each site is performed. The test of the standard deviations, the statistical F-test, was carried out with the null hypothesis being that the two standard deviations are equal. Table 4.4 shows the results of each test for the horizontal standard deviations at each revisited site for each service provider. As is seen from the results, all of the null hypotheses are rejected. None of the precisions obtained in the winter visits are statistically the same as in the summer campaign. This result is primarily due to the large number of samples taken with each visit. On average, over 18,000 data points were recorded at each site for each service provider and for the precision to be deemed as statistically repeatable, the standard deviations need to be the same at the millimetre level. For a two-tailed F-test at a 5% significance level, the test statistic must lie in the range of 0.97 to 1.03 to accept the null hypothesis. This result indicates that the precision values obtained from network RTK are only reliable in short-term and may not be repeated in the long-term.

Table 4.4: Statistical test for repeatability of horizontal precision

		Sites			
		bel	**kit**	**lon**	**bar**
Company 'A'	Winter	1.1 cm	0.8 cm	0.6 cm	1.0 cm
	Summer	1.9 cm	1.2 cm	1.0 cm	1.1 cm
	F-test	2.7	2.1	2.9	1.4
	Status	Rejected	Rejected	Rejected	Rejected
Company 'B'	Winter	N/A	0.7 cm	0.8 cm	1.8 cm
	Summer	1.5 cm	1.2 cm	1.5 cm	1.6 cm
	F-test	N/A	2.9	3.5	0.9
	Status	N/A	Rejected	Rejected	Rejected
Company 'C'	Winter	0.9 cm	1.0 cm	0.5 cm	0.8 cm
	Summer	1.4 cm	1.1 cm	0.9 cm	1.2 cm
	F-test	2.4	1.0	3.0	2.6
	Status	Rejected	Rejected	Rejected	Rejected

4.4.3 Overall Horizontal Precision

In order to another perspective of how precise the network RTK in Ontario can be, a plot of records of ambiguity fixed network RTK solutions collected from all companies in the winter campaign are shown in Figure 4.20. With over 510,000 fixed network RTK solutions, a horizontal precision of 2.6 cm is obtained. Note that this level of precision may not be achievable unless significant amounts of data are collected. Figure 4.21 shows the histogram for the horizontal precision of network RTK solution from the winter campaign.

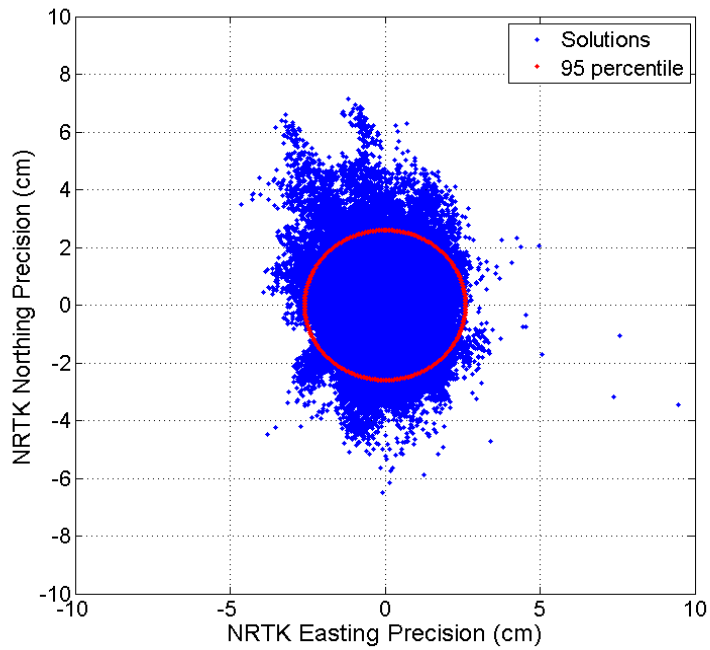

Figure 4.20: Overall precision of all data points collected in winter campaign

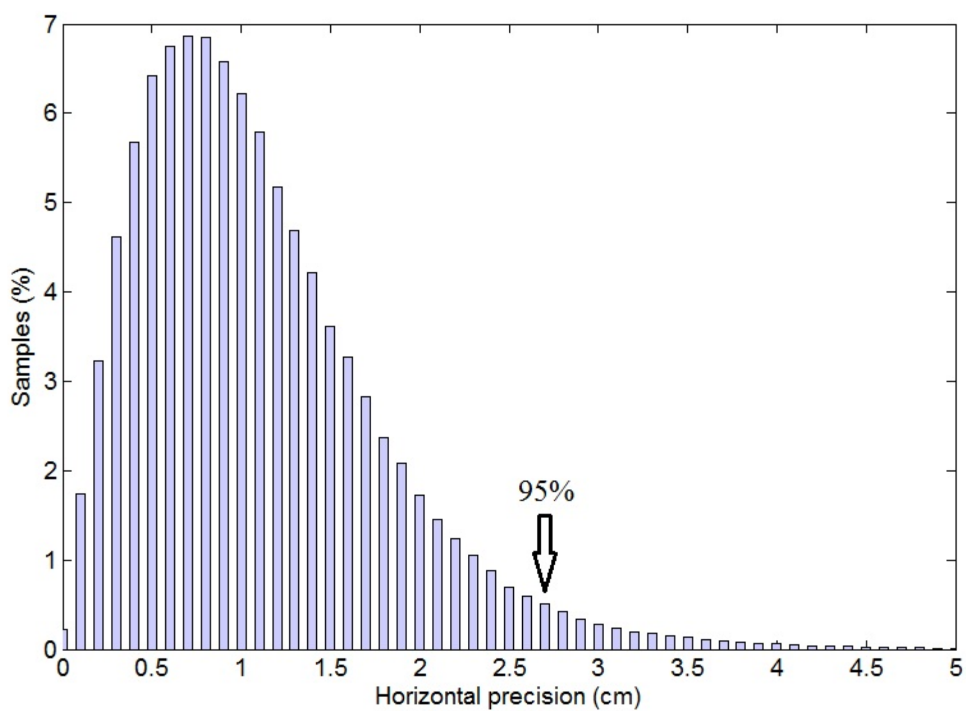

Figure 4.21: Winter horizontal precision histogram showing 95% confidence interval

To compare the level of precision that can be seen in Figure 4.20, the summer overall precision results are also plotted in Figure 4.22. Over 250,000 fixed network RTK solutions were collected over the summer campaign. Figure 4.23 shows the histogram of the horizontal precision from all data collected in the summer. In comparison to the winter, the combined horizontal precision (95%) is 2.3 cm, which is 3 mm lower than the previous site-by-site comparison showing the summer precision value to be significantly larger than the winter in almost all locations revisited. This discrepancy in the results is mainly due to scaling of the precision of the summer results using a scaling factor of 2.45 standard deviations to achieve 95% confidence level as opposed to using the actual 95th percentile using a much larger sample pool for the overall precision. This also reveals that the 2.45 scaling factor provides a more pessimistic confidence interval (~98%) in comparison to the actual results.

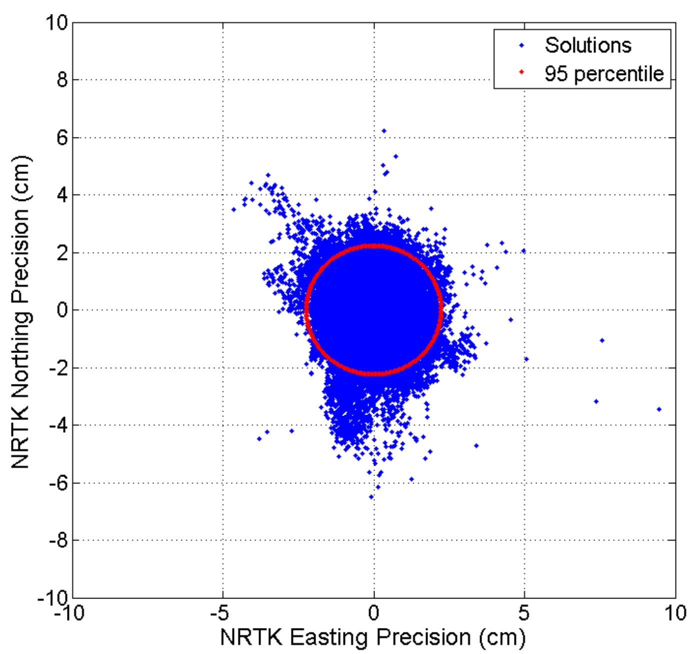

Figure 4.22: Overall precision of all data points collected in summer campaign

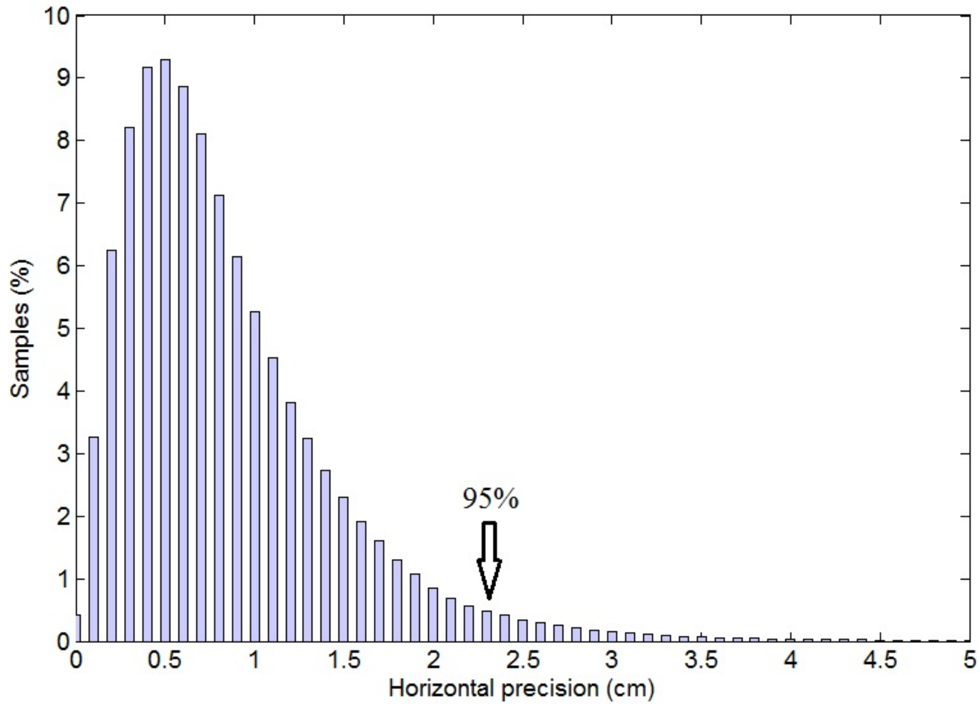

Figure 4.23: Summer horizontal precision histogram showing 95% confidence interval

4.5 Vertical Precision

Similar to the horizontal precision results shown in the previous section, the vertical precision results are divided into the winter and summer campaigns and precision repeatability. The vertical solution precision are first computed at the 1σ (68%) level by calculating the standard deviation of the solution about the mean and then the results are scaled to represent 2σ (95%). Unlike the horizontal results, where the computed standard deviations were scaled using 2.45 (due to 2D), a factor of 2 is used to scale the vertical (1D) results (Harre, 2001).

4.5.1 Winter Campaign

Figure 4.24 to Figure 4.26 display the precision results for vertical precision in the winter campaign. Figure 4.24 shows the company 'A' 95% precision results. The vertical precision, as expected, is higher than the horizontal precision shown earlier in this section; however, the magnitudes are raised only by a few millimetres in comparison. Typically, vertical precision and accuracy results are expected to be up to 2 times worse than the horizontal. The overall shape of the plot indicates that the vertical components perform consistently with the horizontal precision results. The average precision shown by company 'A' for the winter campaign is 2.8 ±0.7 cm, which is slightly better than expected values for vertical precision of network RTK.

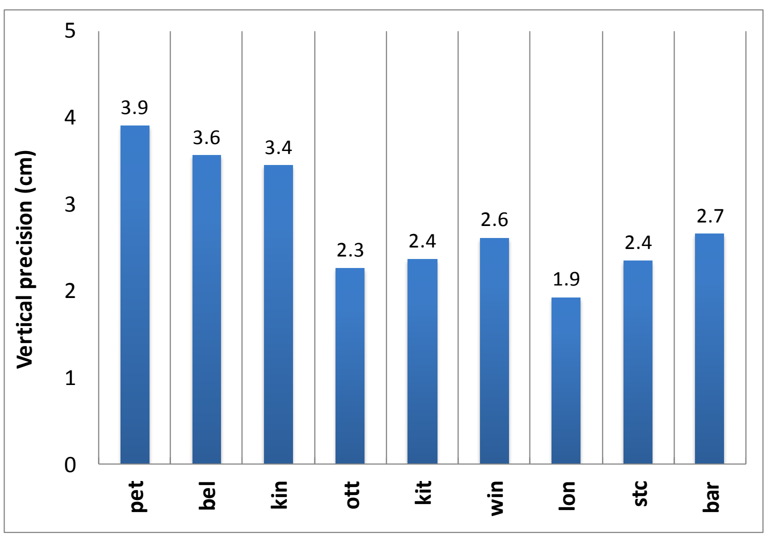

Figure 4.24: Vertical precision (95%) in winter campaign for Company ‘A’

Figure 4.25 shows the vertical precision results for Company 'B'. The mean precision over all sites for this data set is 3.2 ± 1.1 cm. The precisions at sites 'kit' and 'ott', like Company 'A', are excellent and at the 2 cm level. This high quality can be seen in the horizontal results as well. Though, the vertical precision results for Company 'B' are less consistent with the horizontal results, e.g., site 'ott' is showing a higher vertical precision than horizontal precision.

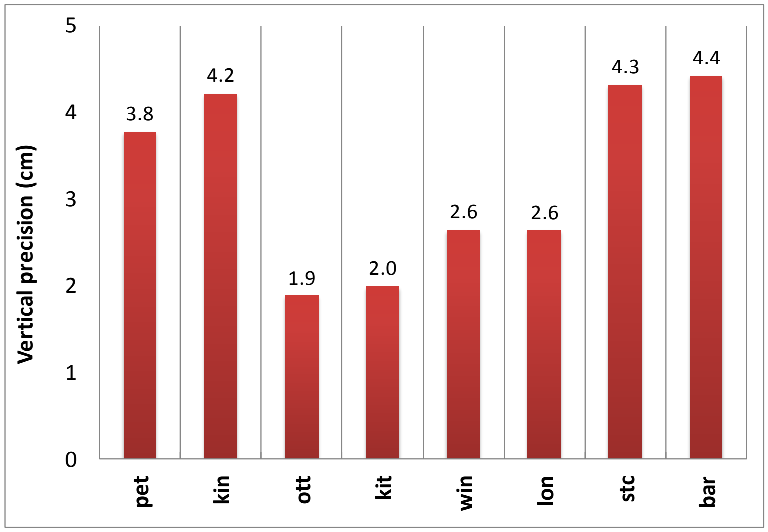

Figure 4.25: Vertical precision (95%) in winter campaign for Company ‘B’

Test results at the sites 'pet' and 'kin' consistently show low precision for all three service providers. The testing environment around these two sites are not ideal. There are a significant number of trees and vegetation around the CBN pillar at the 'kin' site which affect visibility, as well as produce near-field multipath. The consistency between horizontal and vertical results suggests that one of the most important factors in using network RTK, as with all other GNSS dependent methods of surveying, is the surrounding environment. Network RTK is able to remove and reduce the magnitudes of common mode errors though the use of double-differencing. Multipath profiles and hardware and software countermeasures are utilized to mitigate the error of multipath in the reference stations; however, multipath in the immediate area surrounding the rover is one factor which cannot be effectively mitigated. Figure 4.26 shows the precision results for the winter campaign for Company 'C'. The results show a mean of 2.8 ± 0.9 for all test sites, which is in the 2.5-3.5 cm range seen with the other service providers. Also, the site 'lon' shows the highest precision, as with Company 'A', with a precision of 1.5 cm (95%).

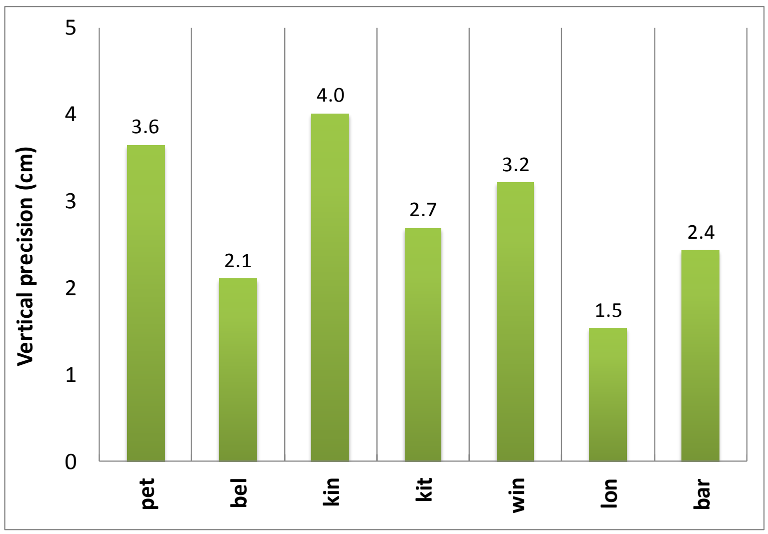

Figure 4.26: Vertical precision (95%) in winter campaign for Company ‘C’

4.5.2 Precision Repeatability

Figure 4.27 shows the change in precision for the four revisited sites in the summer. The vertical results show lower precision for all the service providers. Even though in the summer about 25% less data were collected, this fact alone cannot explain the significantly lower precision values. For example, Figure 4.27 shows a decrease of 4.6 cm (95%) in the precision, which is up to 2.5 times worse than the obtained precision for the winter visit. Other factors such as raised levels of ionospheric activity and tropospheric delay due to extreme weather conditions can be used to explain the lower precision in the summer results, which are explained later this section.

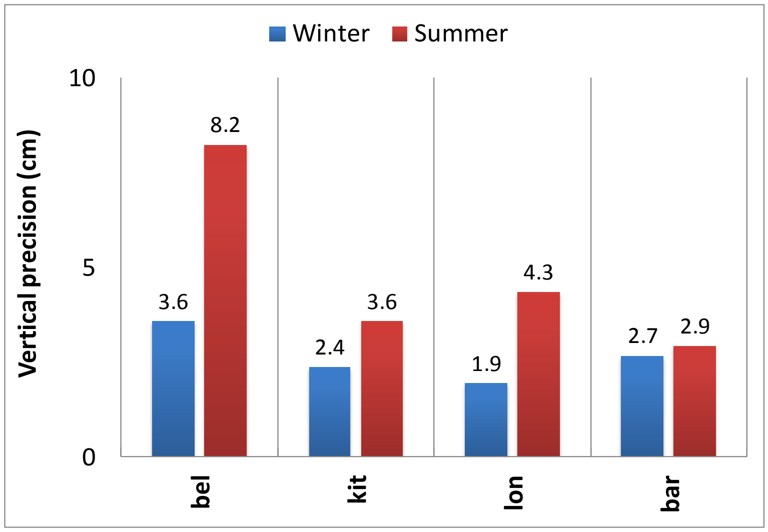

Figure 4.27: Comparison of winter and summer campaign vertical precision for Company 'A'

Figure 4.28 shows similar results for Company 'B'. Site 'bel' shows a precision of 6.5 cm, which compared to the previously shown results in the winter, is an extreme case. The raised precision values for 'bel' are consistent throughout all service providers' results, which suggest that a local environmental factor is most likely causing the problem.

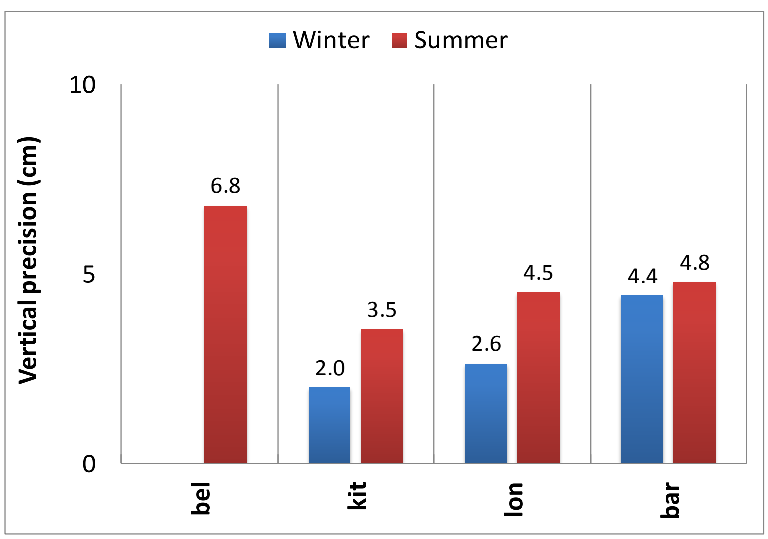

Figure 4.28: Comparison of winter and summer campaign vertical precision for Company 'B'

Figure 4.29 shows the Company 'C' results for precision repeatability. Site 'bel' shows the highest value as with the other data sets. The precision levels are close to Company 'A' results in the summer and 'bel' is showing the worse precision with value of 8.3 cm.

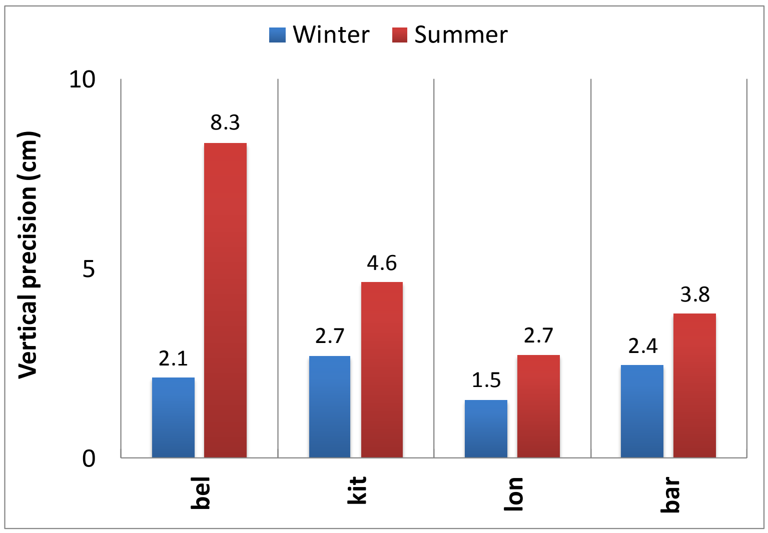

Figure 4.29: Comparison of winter and summer campaign vertical precision for Company ‘C’

In order to examine the significant degradation of vertical precision a comparison of ionospheric activity can be made. Total electron content plots can provide the quantity of electrons present along a path through the ionosphere and are very good indications of ionospheric activity. By examining the Total Electron Content (TEC) maps provided by the National Oceanic and Atmospheric Administration (NOAA) for the winter and summer test date (Figure 4.30) it can be seen that the summer revisit was performed during a significantly raised level of ionospheric activity, which affects height more than any other component. This can partially explain for the significantly decreased levels of precision in the summer revisit of site 'bel'. Table 4.5 shows the rejection of all vertical precision comparison statistical tests performed on the data from each service provider.

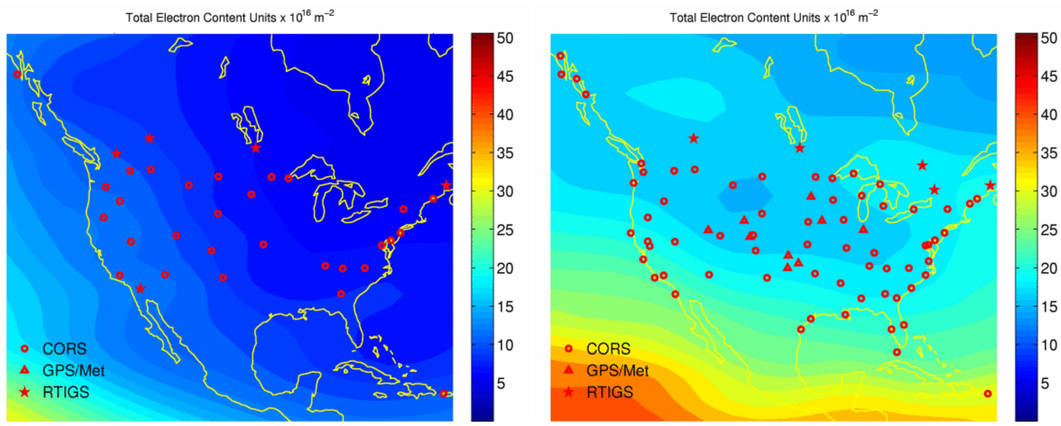

Figure 4.30: Ionosphere activity on site 'bel' test dates in winter (left) and in summer (right) at 12:00 pm

Table 4.5: Statistical test for repeatability of vertical precision

		Sites			
		bel	**kit**	**lon**	**bar**
Company 'A'	Winter	1.8 cm	1.2 cm	1.0 cm	1.3 cm
	Summer	4.1 cm	1.8 cm	2.2 cm	1.5 cm
	F-test	5.3	2.3	5.1	1.2
	Status	Rejected	Rejected	Rejected	Rejected
Company 'B'	Winter	N/A	1.0 cm	1.3 cm	2.2 cm
	Summer	3.4 cm	1.8 cm	2.3 cm	2.4 cm
	F-test	N/A	3.1	2.9	1.2
	Status	N/A	Rejected	Rejected	Rejected
Company 'C'	Winter	1.1 cm	1.3 cm	0.8 cm	1.2 cm
	Summer	4.2 cm	2.3 cm	1.4 cm	1.9 cm
	F-test	15.6	2.9	3.1	2.4
	Status	Rejected	Rejected	Rejected	Rejected

Like the horizontal results, the standard deviations need to be the same value at millimetre-level in order to pass the statistical repeatability tests. It can be seen that for site 'bar', a pass is almost produced from the statistical test for all three companies;

however, due to the slight difference in precision the null hypotheses are rejected in all cases.

4.6 Horizontal Accuracy

In this section, the observed mean error and rms of the network RTK solutions are detailed. The reference coordinates used and their determination were described in the previous chapter. Mean errors that are repeatable in network RTK are mainly caused by the quality of integration of the networks with the official datum, which in Ontario is NAD83 CSRS. Network RTK performance should be very consistent in the horizontal and indeed it is the height performance that contains the most variability (Rubinov et al., 2011). In this section, the horizontal quality of network RTK coordinate fixes will be investigated to check its consistency and accuracy in southern Ontario.

4.6.1 Winter Campaign

Typical network RTK accuracies should range from 1-3 cm horizontally (Edwards et al., 2008; Rubinov et al., 2011), though with various other effects taken into consideration, such as distance from the closest reference station, multipath environment and user's location within the network, this accuracy range can be larger. Furthermore, private network operators continuously advertise complete coverage within their network, which suggests that typical network RTK accuracy can be expected anywhere within a network. Since the main objectives of this study is to evaluate the accuracy of network RTK services as a whole, the details of the abovementioned effects will not be discussed in detail. Instead focus will be placed on significant accuracy issues and network distortions within each service provider's network. Figure 4.31 to Figure 4.36 display the mean error of the solutions for each service provider. Figure 4.31 shows the mean errors at each test location, determined from the Company 'A' network RTK position time series compared against each site's reference coordinates. In terms of the components of the mean error, it is clear that the northing and easting both show systematic behaviour. In most cases, typical network RTK accuracy can be seen with the exceptions of 'bel', where the horizontal accuracy exceeds 3 cm in the horizontal. The systematic behaviour in the direction of the biases may be due to distortions in the integration of the network in the official datum. Also, long-term repeatability comparisons are made later in this section to show that the biases seen in the results are not products of short-term systematic behaviour, and are, in fact, due to distortions in the networks.

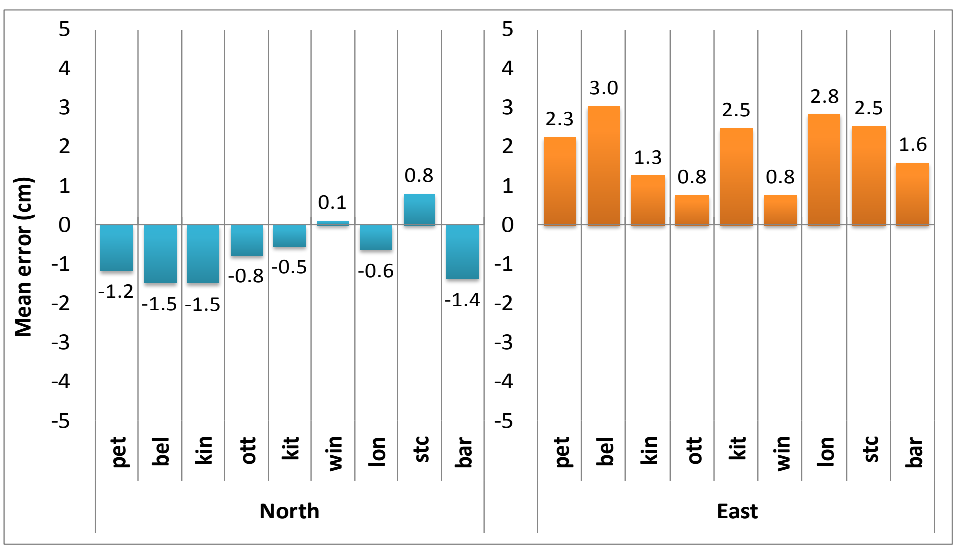

Figure 4.31: Mean error in winter campaign for Company 'A'

In Figure 4.32, the bias magnitudes and their directions are shown for the Company 'A' results. For the most part, the biases are directed towards the southeast and the majority of the biases have magnitudes of 1-2.5 cm. This illustrates that the Company 'A' network has a linear distortion of up to 3 cm horizontally. The reference station coordinates have a direct effect on the solutions and with closer alignment with a high order network (e.g., CSRS network) these biases could be reduced. The reference stations coordinates should be determined more rigorously and more than one high-precision monument should be utilized.

Figure 4.32: Horizontal biases in winter campaign for Company 'A'

Figure 4.33 shows the results of the mean error for Company 'B' at the test sites. As mentioned previously, the data for the winter visit to 'bel' are not available due to on-board receiver memory failure. The level of accuracy seen from these results is up to 1 cm worse than shown in Figure 4.31. However, the horizontal accuracy is still within expected levels of typical network RTK accuracy, though closer to the upper bound. Sites ‘ott’ and ‘bar’ with almost 4 cm biases in the horizontal are outside the expectations of network RTK-defined accuracies. Similar to the previous results, there is systematic behaviour that seems to suggest network misalignment with respect to the Ontario datum. This fact is displayed further in Figure 4.34.

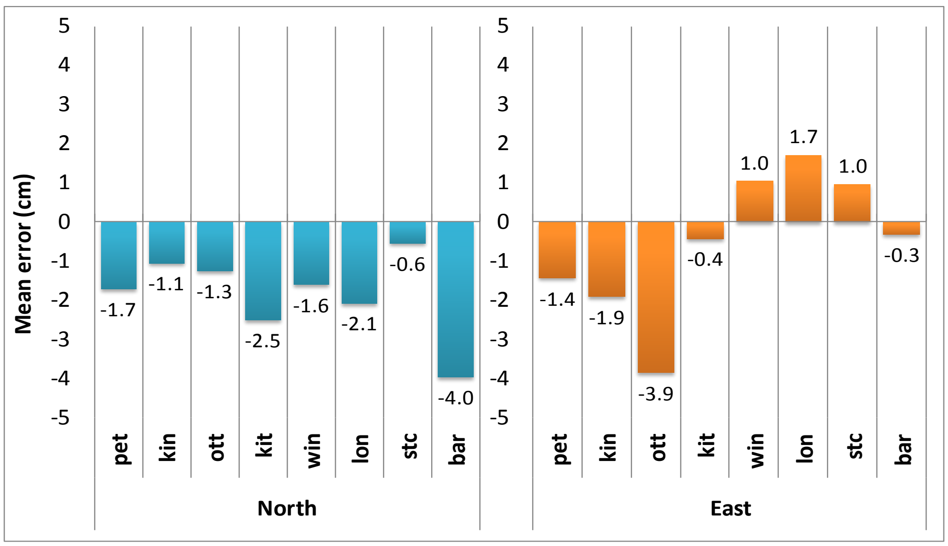

Figure 4.33: Mean error in winter campaign for Company ‘B’

The interesting phenomenon that can be seen in Figure 4.34 is that the network distortion has a completely different pattern than that for Company ‘A’. These distortions describe a more rotational pattern about a pivot point near the city of Toronto, indicating again how well this network is “tied” into the Ontario’s official NAD83 CSRS datum.

Figure 4.34: Horizontal biases in winter campaign for Company ‘B’

Figure 4.35 shows the mean biases in the solutions of Company ‘C’ at the test sites. As mentioned before, sites ‘ott’ and ‘stc’ are not available for this particular service provider due to issues with service availability. The biases shown in Figure 4.35 are all within typical network RTK accuracy. Test site ‘win’ shows the largest bias with a magnitude of 1.7 cm. Figure 4.36 illustrates that there is no significant network alignment within the Company ‘C’ solutions as compared to the reference coordinates. For the most part, the biases tend to behave randomly and almost all are at or below 1 cm in the horizontal. Indeed, the biases are too small and random to conclude any significant network misalignments. Although the missing data lacks the ability to show the network’s behaviour around areas close to Ottawa and St. Catharines.

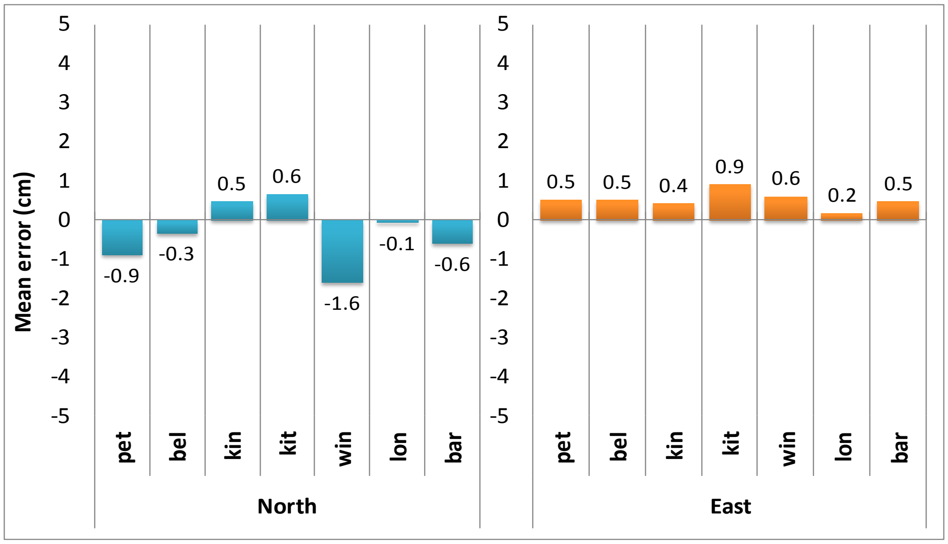

Figure 4.35: Mean error in winter campaign for Company ‘C’

Figure 4.36: Horizontal biases in winter campaign for company ‘C’

The overall rms has also been computed to show the level of accuracy of the networks under examination. The combination of short-term precision and solution bias display a better picture of the performance of each network. Figure 4.37 shows the rms at the test sites for Company ‘A’. These results are typically affected by the mean biases present in each solution at each location. Test site ‘bel’ has not only the largest bias, but also the largest rms value, and site ‘win’, with the smallest bias, has the smallest rms. This is mainly due to the similar levels of precision within the same network.

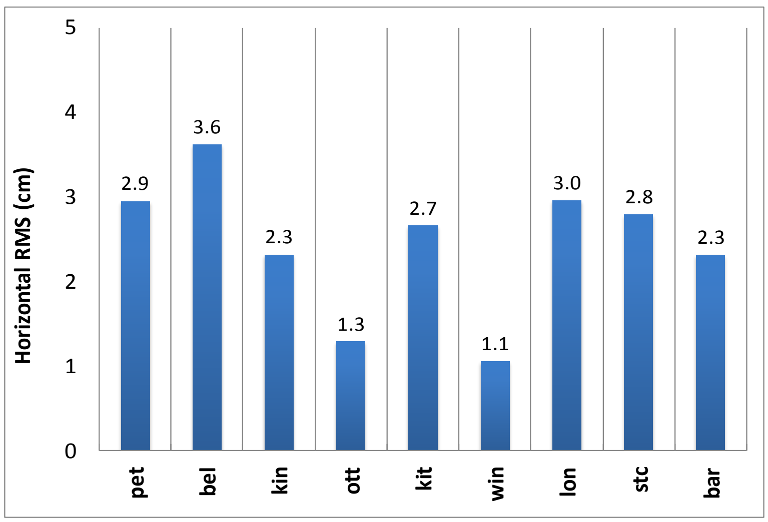

Figure 4.37: Horizontal rms in winter campaign for Company ‘A’

Figure 4.38 shows the rms at the test sites for Company ‘B’. The rms is larger than the one shown in Figure 4.37. Also, similar to the effect of biases on Company ‘A’ results, sites ‘ott’ and ‘bar’ with the largest mean biases are causing the largest rms values.

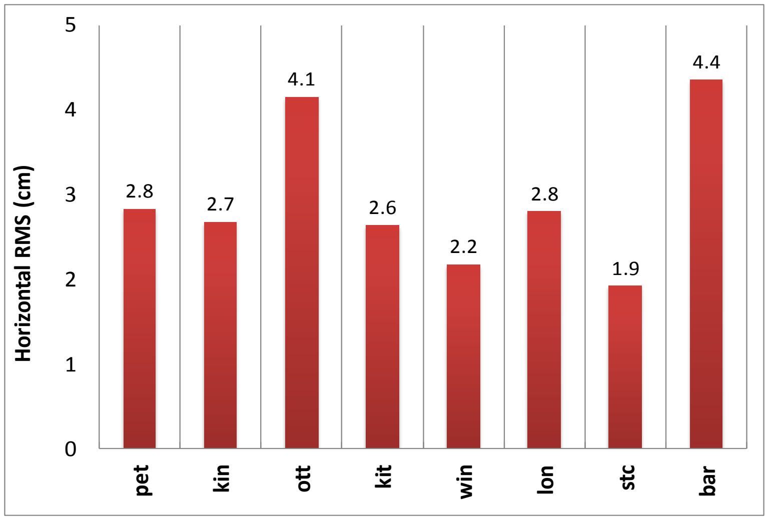

Figure 4.38: Horizontal rms in winter campaign for Company 'B'

Figure 4.39 shows the rms at the test sites for Company 'C'. Test site 'lon' has the lowest rms of all the results shown at ~0.5 cm. Though, the results are still showing a large rms at 'win' due to larger mean errors in the solutions with respect to other test locations.

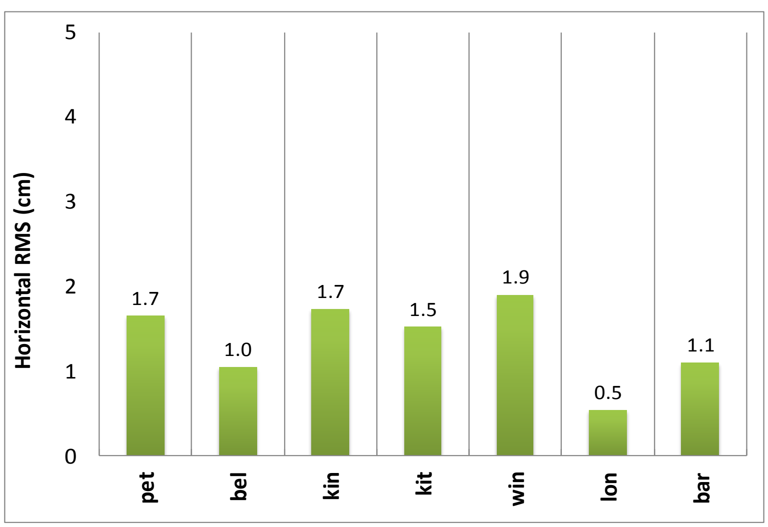

Figure 4.39: Horizontal rms in winter campaign for Company 'C'

4.6.2 Repeatability: Summer versus Winter

In this section the results of the summer campaign will be compared to the winter. The main goal is to examine and separate any long-term systematic behaviour in the networks from the short-term errors that can affect the solutions. Also, the long-term repeatability of the solutions needs to be evaluated in order to be able to deem these network RTK services as "repeatable" methods of few centimetre-level positioning. This evaluation involves looking at the accuracy of the solutions collected over 6 months to a year apart. In this case the winter and summer results are being compared.

Figure 4.40 compares the mean errors from the winter campaign with respect to those of the summer for Company 'A'. The biases, though in some cases large, display a repeatable pattern. The magnitude of the biases over time may change from a few millimetres up to a centimetre. An anomaly can immediately be seen in the northing of site 'bel' with a difference of ~2 cm. This is an expected result and the systematic tendency of these biases reinforces the assumptions made earlier in this section: accuracy of solutions of each service provider is mainly influenced by network reference station misalignment, and the degree of integration of each network into the local high-accuracy datum. The results seen in this chapter so far show that the immediate sources of error (geometry, visibility, multipath, etc.) can be categorized as random errors affecting the short-term quality of the solutions. And the larger sources of error, such as network misalignments, can be categorized as systematic errors that affect the long-term repeatability of the solutions. Figure 4.41 compares the mean errors from the winter campaign with respect to the summer for Company 'B'. Site 'bel' has no equivalent results from the winter to be compared with. The behaviour displayed is matching at the few millimetre-level in almost all test sites.

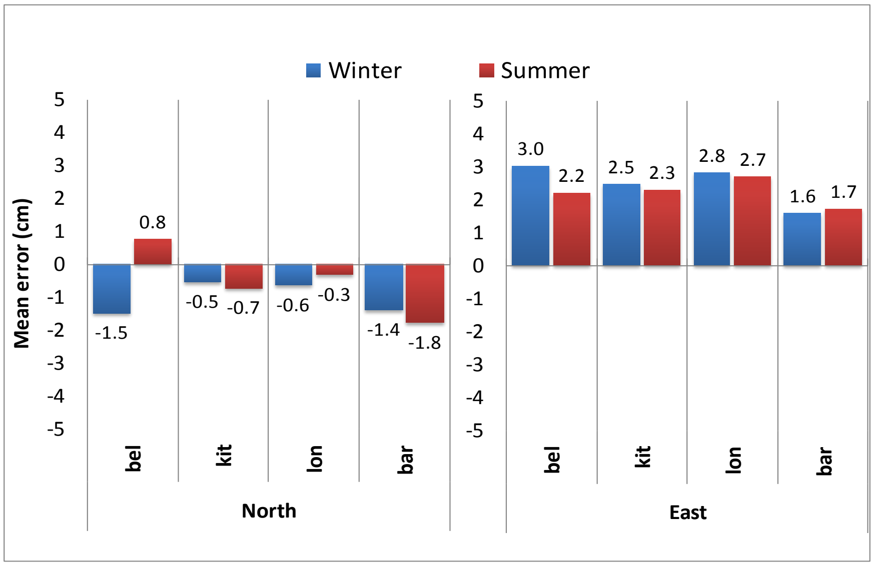

Figure 4.40: Long-term repeatability for Company 'A'

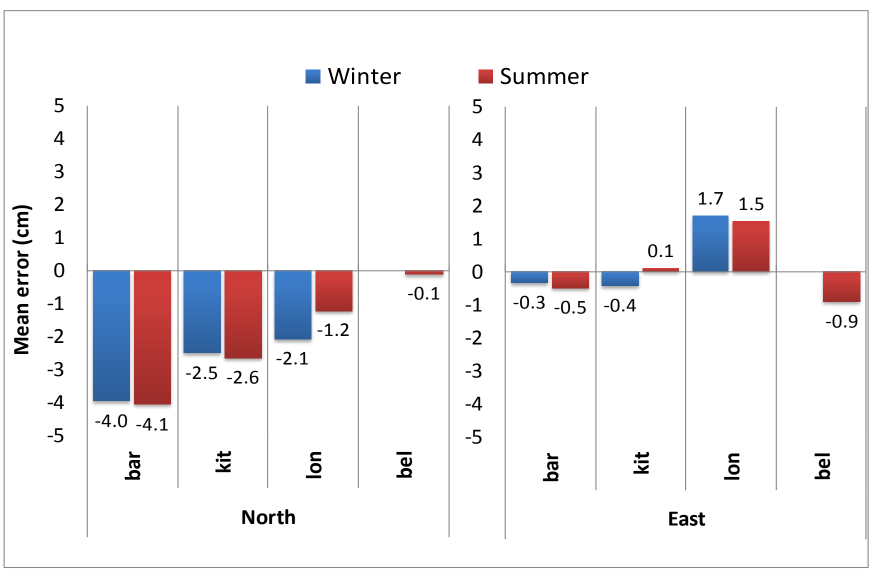

Figure 4.41: Long-term repeatability for Company 'B'

Figure 4.42 compares the mean errors from the winter campaign with respect to that of the summer for Company ‘C’. It is interesting that even with sub-centimetre biases, over large data sets, the biases tend to repeat themselves between seven-month campaigns. Site ‘bar’ displays this phenomenon to the millimetre. This means that network RTK has developed to the state that, for large data sets, it can potentially remove most other sources of error from the solutions, leaving only the need for proper coordination of the network reference stations. Of course, this averaging would not have a major effect on smaller and shorter data sets as the GPS measurement noise and errors in the network RTK corrections would dominate solution accuracy.

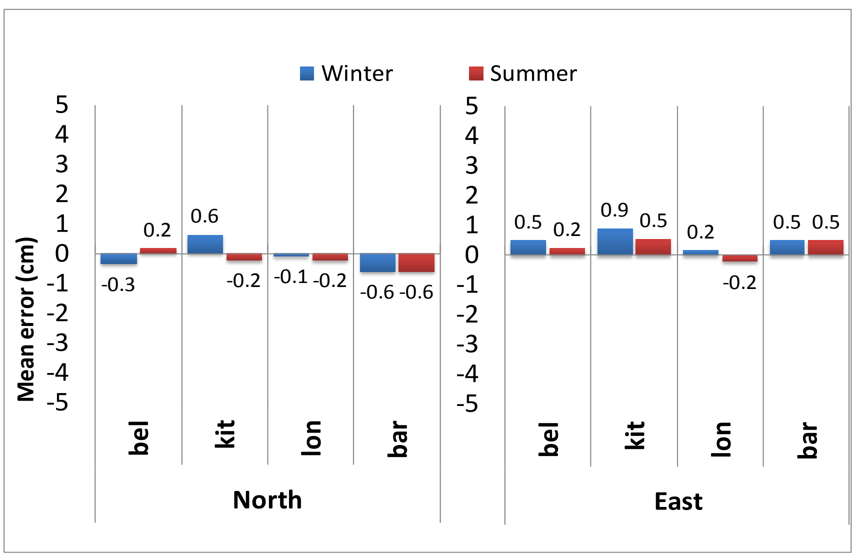

Figure 4.42: Long-term repeatability for Company ‘C’

The horizontal means of the winter and summer results can be statistically tested to examine the repeatability of the mean error. A statistical t-test is used to determine the repeatability of the horizontal means. The standard deviations and number of samples are also used in the t-test. With the high number of degrees of freedom for a two-tailed 5%

significance level, the t-test value should be contained within a range of -2.2 and 2.2. Table 4.6 shows the results of the statistical testing on the mean horizontal errors at various sites. The degrees of freedom for each test are a function of each data set's number of samples and its standard deviation. As can be seen, all the tests rejected the null hypothesis of the winter and summer means being equal.

Table 4.6: Statistical test of repeatability for mean error

		Sites			
		bel	**kit**	**lon**	**bar**
Company 'A'	Winter Samples	29984.0	20735.0	27547.0	23990.0
	Summer Samples	18748.0	24476.0	22786.0	18872.0
	Winter Mean	3.4 cm	2.5 cm	3.0 cm	2.1 cm
	Summer Mean	2.3 cm	2.4 cm	2.7 cm	2.5 cm
	DoF	26537	45283	32785	42318
	t-test	71.2	11.9	36.2	-35.8
	Status	Rejected	Rejected	Rejected	Rejected
Company 'B'	Winter Samples	N/A	11960	11381	11433
	Summer Samples	N/A	15730	21630	21843
	Winter Mean	N/A	2.6 cm	2.7 cm	4.0 cm
	Summer Mean	0.9	2.6 cm	2.0 cm	4.1 cm
	DoF	N/A	26133	32999	21661
	t-test	N/A	-8.6	59.0	-6.0
	Status	N/A	Rejected	Rejected	Rejected
Company 'C'	Winter Samples	32742	30815	26627	28421
	Summer Samples	18583	26172	21275	21676
	Winter Mean	0.6 cm	1.1 cm	0.2 cm	0.7 cm
	Summer Mean	0.3 cm	0.6 cm	0.3 cm	2.1 cm
	DoF	27356	55438	32259	34227
	t-test	27.4	58.3	-18.9	-153.3
	Status	Rejected	Rejected	Rejected	Rejected

Much like the F-test performed for the horizontal precision repeatability, the high number of degrees of freedom causes the tests to leave very little room for a difference between each set of results. The mean errors, like the standard deviations, have to match exactly to the millimetre to confirm statistical repeatability.

4.7 Vertical Accuracy

It is typical to see mean errors of 2-3.5 cm in the vertical solutions (Rubinov et al., 2011; Edwards et al., 2008). The precision values are generally smaller and this makes the mean errors the largest contributor to rms of a solution. In Figure 4.43 vertical mean errors of 3 mm to 5 cm in the solutions for Company 'A' are seen. Common patterns can be seen for site 'bar', where the mean error has the same magnitude and direction for all data sets. For Company 'A', mean errors behave much less systematically in the vertical than the horizontal, ranging from -3 cm to +3 cm. From the previous section, the horizontal error shows biases in the same direction for both east and north components throughout southern Ontario, which suggest a linear translation in their network coordinates (Figure 4.31). However, the vertical biases have a random behaviour in terms of direction and magnitude. The magnitudes of the mean errors are within the expected range shown in similar studies of network RTK.

Figure 4.44 shows the vertical mean errors across southern Ontario for Company 'A'. It is difficult to deduce any particular pattern shown by these vertical translations; however, it can be seen that the eastern test sites show smaller mean errors than the western test sites, and that the direction of the biases vary with no particular pattern.

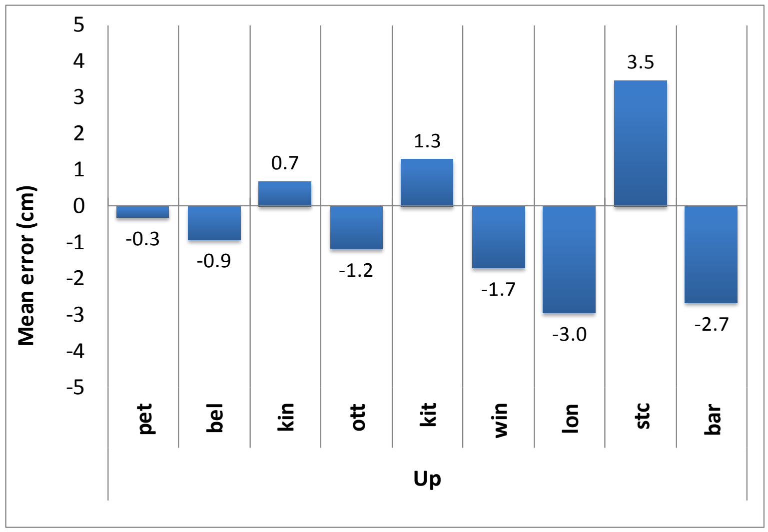

Figure 4.43: Mean vertical error in winter campaign for Company ‘A’

Figure 4.44: Vertical biases in winter campaign for Company ‘A’

Figure 4.45 illustrates the mean error results for Company 'B'. Same magnitude for the mean errors can be seen here. However, most of the errors are positive, which suggests a possible vertical translation of the network coordinates. In terms of magnitude, the errors are within expected range of 1.5-3 cm in the vertical (Edwards et al., 2008; Rubinov et al., 2011). Figure 4.46 illustrates the vertical biases for Company 'B' on the map of southern Ontario. Except for sites 'bar' and 'pet', all other biases are in the positive direction. Also, as with the Company 'A' results, the eastern test sites show smaller mean errors compared to the western sites. However, the distinct rotational pattern seen by the horizontal results from Company 'B' is not shared by the vertical mean errors seen here. Lack of high-precision calibration monuments in south western Ontario can be partially responsible for the large errors seen in the western results.

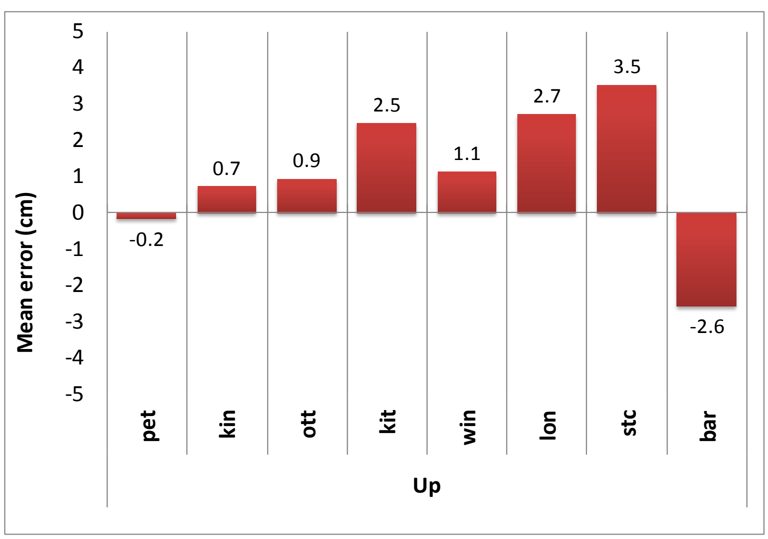

Figure 4.45: Mean vertical error in winter campaign for Company 'B'

Figure 4.47 illustrates the Company 'C' results for the vertical mean error. These results show more of trend than the other service providers. Except at site 'bar', the eastern (west of Toronto) sites are producing positive results and the western sites are in the negatives.

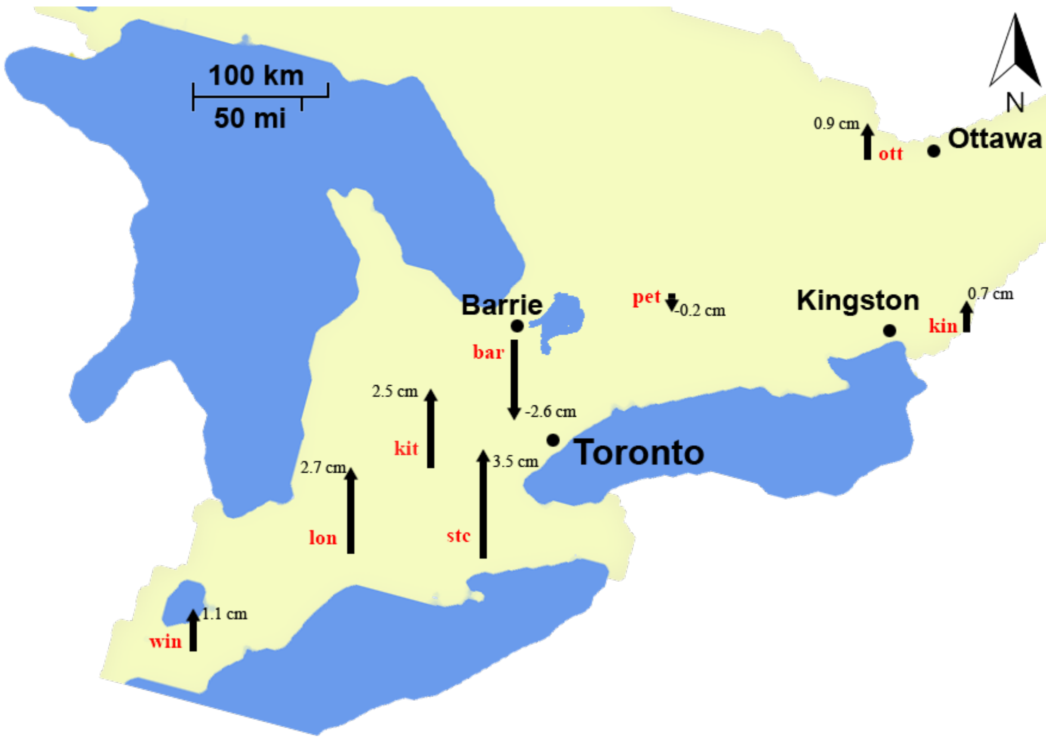

Figure 4.46: Vertical biases in winter campaign for Company 'B'

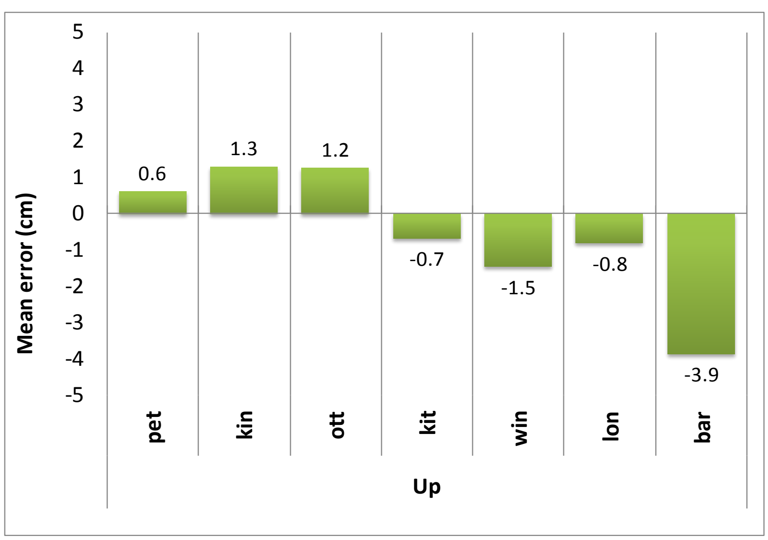

Figure 4.47: Mean vertical error in winter campaign for Company 'C'

Figure 4.48 illustrates the vertical biases for Company 'C'. All of biases are below 2 cm, with the exception of site 'bar'. The outlier seen in 'bar' may be due to the low quality of the test site (third-order monument, trees nearby, etc.). Also, a tilt in the reference coordinates exists as the western test sites have negative biases and eastern test sites have positive mean errors. However, the magnitudes of the biases are too small to be considered as a definite bias in the coordinates.

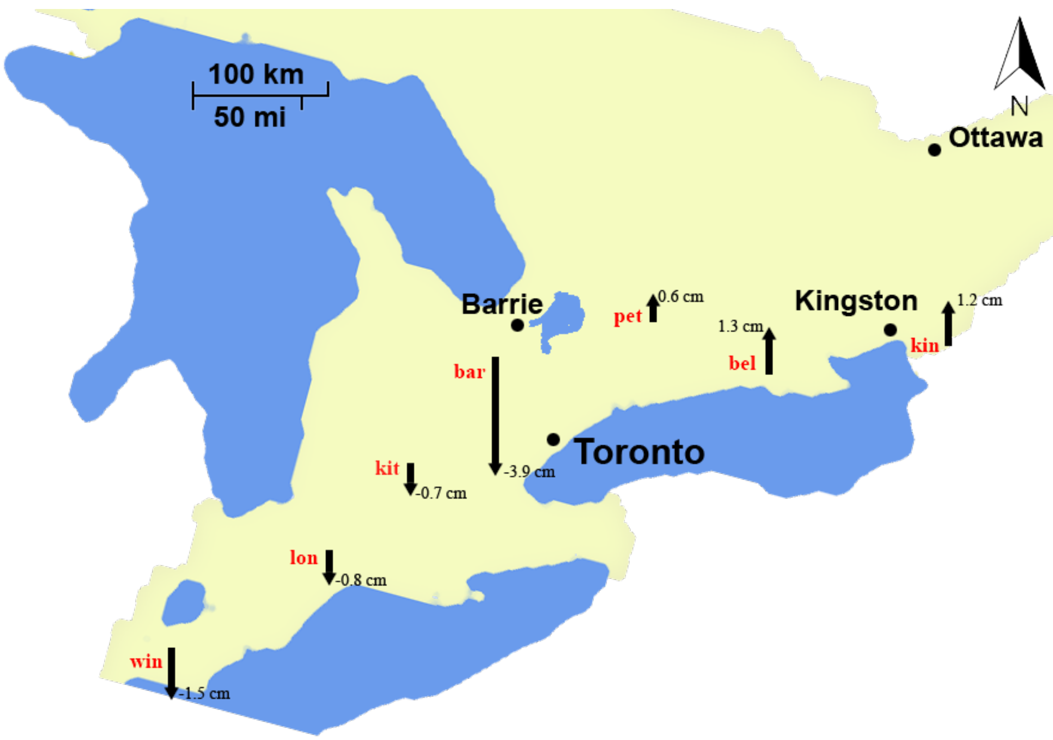

Figure 4.48: Vertical biases in winter campaign for Company ‘C’

The rms of the solutions can also be looked at to examine the accuracy of the solutions by combining the short-term and long-term biases into one comparison. Figure 4.49 shows the rms values for all winter sites for Company 'A'. The levels of accuracy seen here are better than the rms values obtained for the horizontal results. A range of ~2-3 cm can be seen across southern Ontario for Company 'A' with the exception of site 'stc', where the large mean error of 3.5 cm in the vertical solution is causing the outlier.

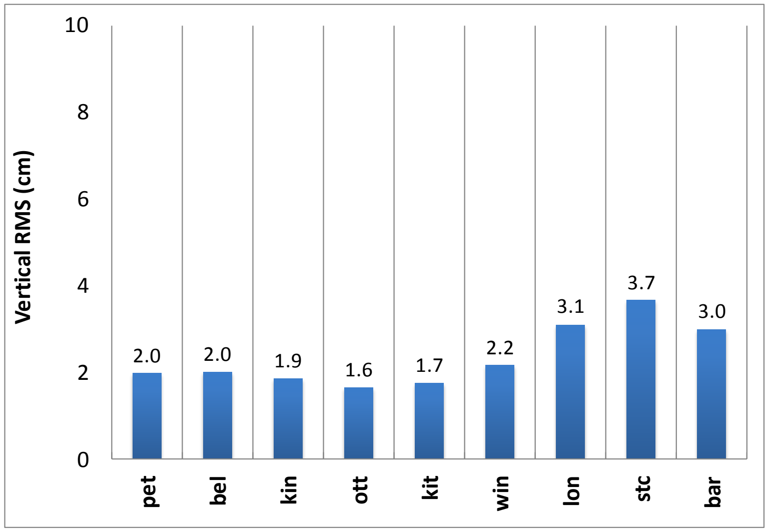

Figure 4.49: Vertical rms in winter campaign for Company 'A'

Figure 4.50 illustrates the vertical rms values for Company 'B'. The same rms range as Company 'A' can be seen and the site 'stc', with a mean error of 3.5 cm, is the contributor to the large rms. Also sites 'pet', 'win' and 'ott' have excellent accuracy results for both service providers, ranging in 1.5-2.2 cm, which is most likely due to the similarities in their network architectures in eastern Ontario.

Figure 4.51 illustrates the Company 'C' rms values, which are smaller than those of the other service providers. This is primarily due to the small vertical mean errors, as well as higher precision in the solutions. However, site 'bar' has an uncharacteristically large rms, which is due to the high mean error of -3.9 cm in the vertical.

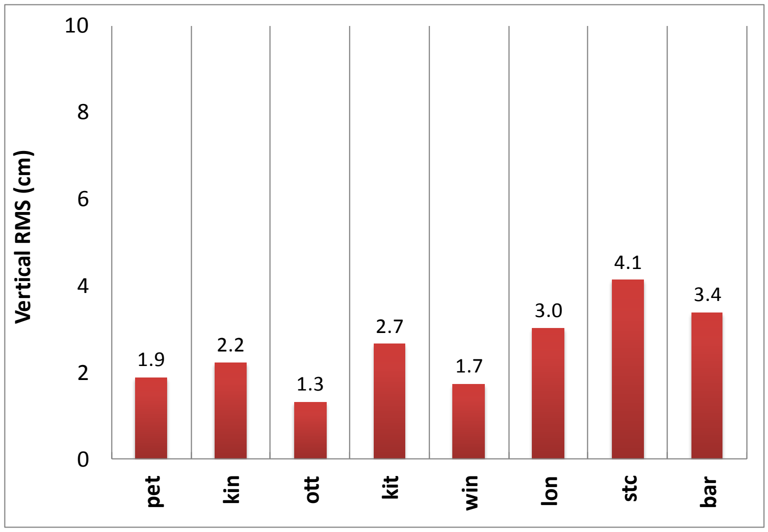

Figure 4.50: Vertical rms in winter campaign for Company 'B'

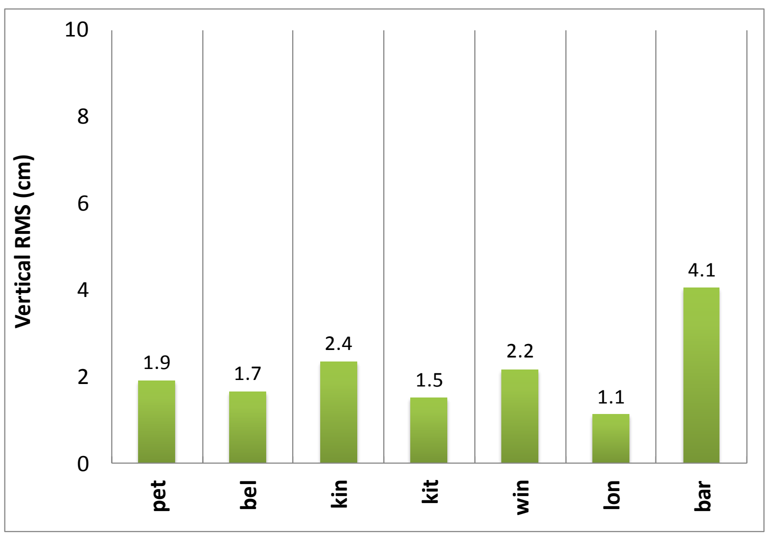

Figure 4.51: Vertical rms in winter campaign for Company 'C'

4.7.1 Repeatability: Summer versus Winter

In order to determine the repeatability of the mean errors in the coordinates, further statistical testing needs to be done. Tests involving the standard deviation and mean can reveal whether the accuracy seen from the results of this study are significant and repeatable. Figure 4.52 to Figure 4.54 show the repeatability in vertical mean error between winter and summer visits. The directions of the results tend to be the same while the magnitudes vary. However, for sites 'bel' and 'kit' in Figure 4.52, the magnitudes and directions of vertical mean errors changes. An extreme example of changing magnitude for the vertical error can be seen in Figure 4.54, which shows an increase of 4.1 cm in the vertical mean error. That particular test site, especially for Company 'C', has a very large (5.4 cm) vertical error for the summer revisits. This can be confirmed by examining the correlation solution integrity plot of the site 'bel' revisit in the summer in the Appendix C which shows that a staggering 72% of the solutions exceed the estimated error by the equipment. This large mean error is most likely due to a bias in the vertical coordinate of the reference station.

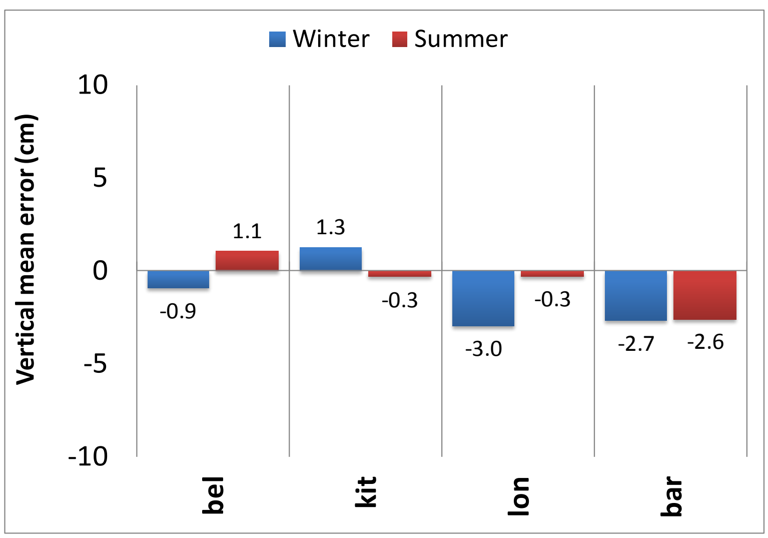

Figure 4.52: Long-term vertical repeatability for Company 'A'

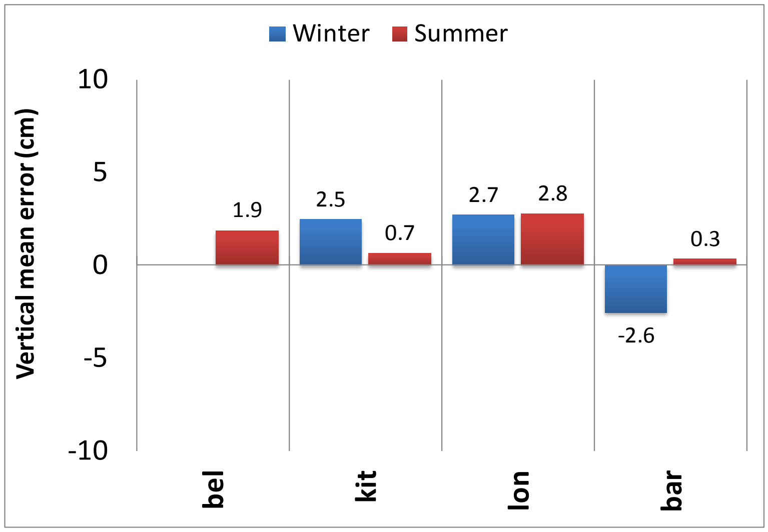

Figure 4.53: Long-term vertical repeatability for Company 'B'

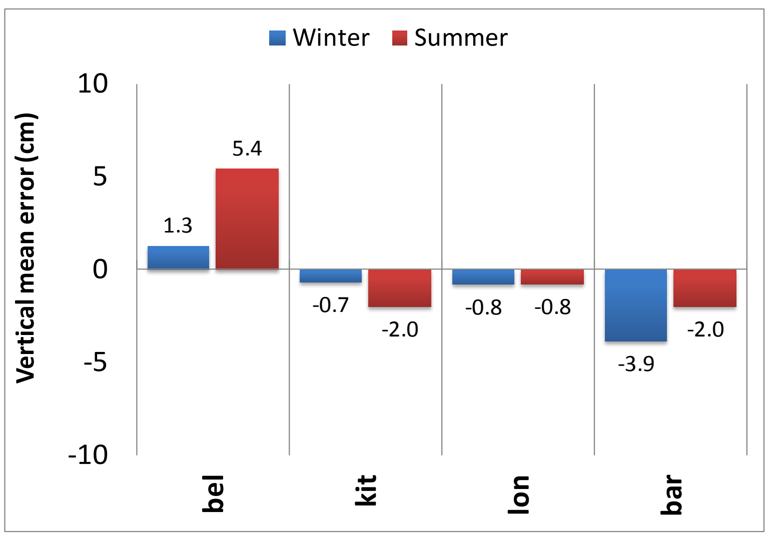

Figure 4.54: Long-term vertical repeatability for Company 'C'

The vertical mean errors can be tested for repeatability using the t-test. Table 4.7 shows the results of statistical testing for vertical mean errors. Only one test did not reject the null hypothesis for the two-tailed t-test. Company 'C' at site 'lon' shows the same vertical bias and close standard deviations. These results indicate that the vertical mean errors are mostly not statistically repeatable.

Table 4.7: Statistical test of repeatability for vertical mean error

		Sites			
		bel	**kit**	**lon**	**bar**
Company 'A'	Winter Samples	29984.0	20735.0	27547.0	23990.0
	Summer Samples	18748.0	24476.0	22786.0	18872.0
	Winter Mean	-0.9 cm	1.3 cm	-3.0 cm	-2.7 cm
	Summer Mean	1.1 cm	-0.3 cm	-0.3 cm	-2.6 cm
	DoF	23201	42890	30175	38589
	t-test	-63.0	116.1	-170.5	-7.5
	Status	Rejected	Rejected	Rejected	Rejected
Company 'B'	Winter Samples	N/A	11960	11381	11433
	Summer Samples	N/A	15730	21630	21843
	Winter Mean	N/A	2.5 cm	2.7 cm	-2.6 cm
	Summer Mean	1.9 cm	0.7 cm	2.8 cm	0.3 cm
	DoF	N/A	26133	32999	21661
	t-test	N/A	107	-4	-111
	Status	N/A	Rejected	Rejected	Rejected
Company 'C'	Winter Samples	32742	30815	26627	28421
	Summer Samples	18583	26172	21275	21676
	Winter Mean	1.3 cm	-0.7 cm	-0.8 cm	-3.9 cm
	Summer Mean	5.4 cm	-2.0 cm	-0.8 cm	-2.0 cm
	DoF	19940	40560	31983	34790
	t-test	-133.6	80.8	-1.8	-126.0
	Status	Rejected	Rejected	Accepted	Rejected

4.8 Horizontal Solution Integrity

The solution integrity analysis consists of comparing our independently determined errors in the network RTK solution with the estimated coordinate uncertainty values that are provided to the user by service provider equipment. These coordinate quality (CQ) values vary from one service provider to another. The plot in Figure 4.55 shows the actual network RTK determined horizontal error (blue) in comparison with the 1σ, 2σ and 3σ values (red, yellow and green, respectively) determined from the network RTK estimation filter covariances for a period of two hours for Company ‘C’ at site ‘lon’ in the winter. The network RTK horizontal solution error is predominantly within the boundaries of the one standard deviation values. This is an example plot of the solution integrity: internal solution estimated error versus independently calculated error. More such plots for various service providers at each test location can be found in the report appendices. CQ values tend to follow the shape of the calculated solution errors, that is, they are usually within the 1σ level. However, the expanded portion of the plot shows the solution error being almost entirely outside the 1σ and for a small period time close to the 2σ boundaries.

The results from Figure 4.55 in comparison to the calculated errors are actually overestimated for the most part. The 1σ values actually contain ~85% of the actual data points, which contains ~17% more results than the 68% of the normal distribution. In this section of the report, the focus will be on showing correlation plots that can compare the distribution of estimated error by the equipment with respect to the actual errors in the solution. The results shown here for each company represent typical levels of quality and are not ‘worst’ or ‘best’ case scenarios.

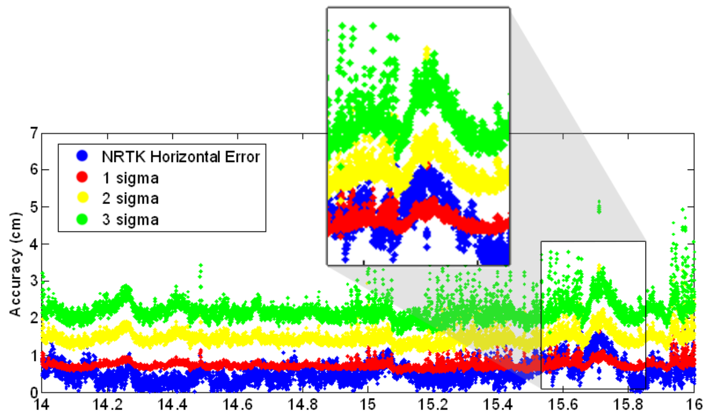

Figure 4.55: Company ‘C’ network RTK errors versus 1, 2 and 3 σ for ‘lon’

Each epoch of data is accompanied by its corresponding horizontal estimated rms provided by the equipment. These values are plotted against the calculated horizontal error for Company ‘C’ for site ‘kit’ in Figure 4.56. The horizontal rms values for these plots have been scaled appropriately to the 95% confidence interval. The green line represents one-to-one correlation. Any data point on the left side will be deemed to be an overestimation of the error and the right side would represent underestimation of the actual error in the solutions. Approximately 94% of the equipment-provided uncertainty values are larger than the actual errors. Figure 4.56, as the statistics indicate, shows that for the most part this solution set has overestimated rms values, since the large bulk of the data points are on or to the left of the highly correlated line. Correlation plots from other service providers can be viewed to demonstrate of typical behaviour in terms of solution integrity for each network.

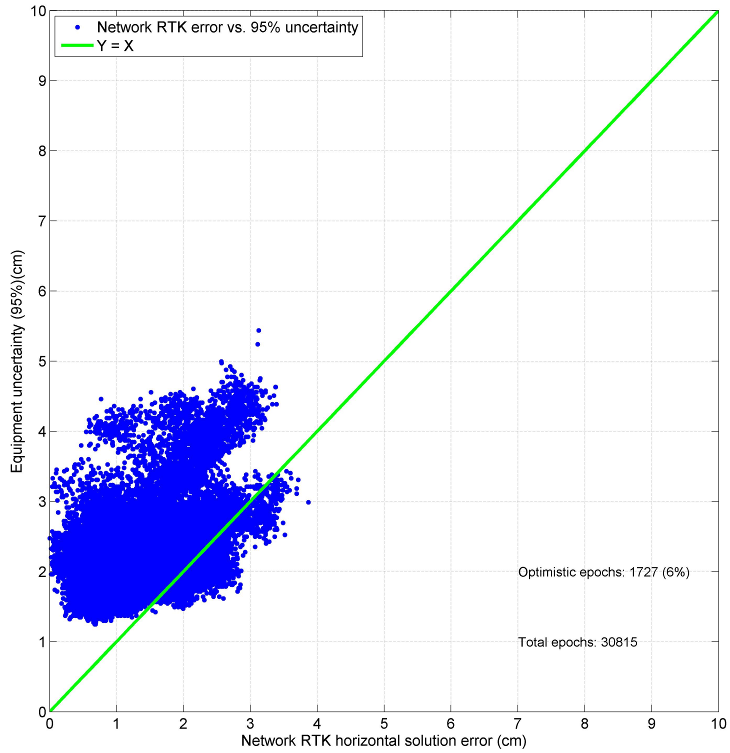

Figure 4.56: Solution integrity for Company 'C' at 'kit'

Figure 4.57 shows the correlation plot for Company 'B' at site 'win'. Approximately 8% of the equipment-provided uncertainty values are larger than the calculated errors. This result is very similar to that in the previous Figure. However, due to lack of solution availability, the number of epochs presented is less than half. Discreet lines can be seen due to millimetre rounding of output values by the equipment. Also, vertical lines appear above the 2-4 cm horizontal error that is typical for Company 'B' results. The vertical shape shown is in every solution integrity result for Company 'B' and is usually focused around a specific interval of absolute error. It is not clear why this pattern in the estimated error exists, however it may be due to issues in the error estimation process. The majority of the epochs recorded do not show a significant amount of error underestimation, which is to be expected.

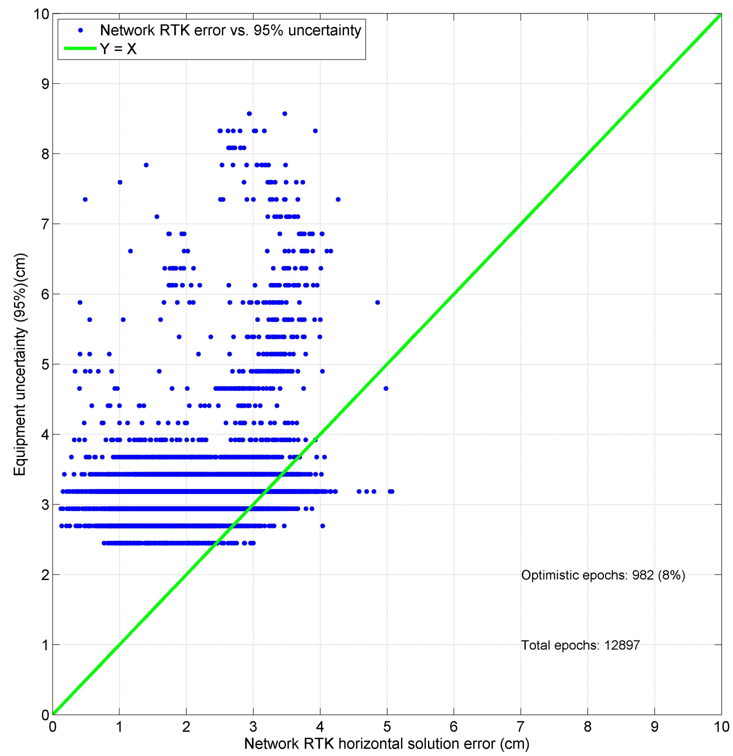

Figure 4.57: Solution integrity for Company 'B' at 'win'

Figure 4.58 shows the correlation plot for Company 'A' at site 'kin'. Typically, a significant percentage (>7%) of the equipment estimated errors are under-estimations. In isolated cases, close to all of the epochs collected are to the right of estimated error at 99% confidence. Also, the same discreet lines can be seen that are due to millimetre rounding of the Quality Control (QC) output. From the results presented in this section, it can be concluded that as with like most other analyses, there is no unified pattern shown in the behaviour of various providers in Ontario. Each service provider's estimated error shows individual characteristics, which indicates that a single process for error estimation and reporting is not used. Without following a standard procedure for error estimation as each service provider uses different network RTK processing algorithms, results in different uncertainty estimates, it is very difficult to rely on the provided rms values as the only source of quality control of the solutions. Also, proper scaling of the estimated errors (at 95% uncertainty) need to be performed and reported to the user to avoid any confusion in terms of confidence levels of the solutions provided. The errors computed will take into consideration the estimated parameters when calculating the position of the user. However, these estimated values do not consider sources of errors, which in certain conditions may dominate the measurement noise. Hence, the user needs to be very careful when using the equipment coordinate quality indicators, as under certain conditions these values will be extremely optimistic and unrealistic.

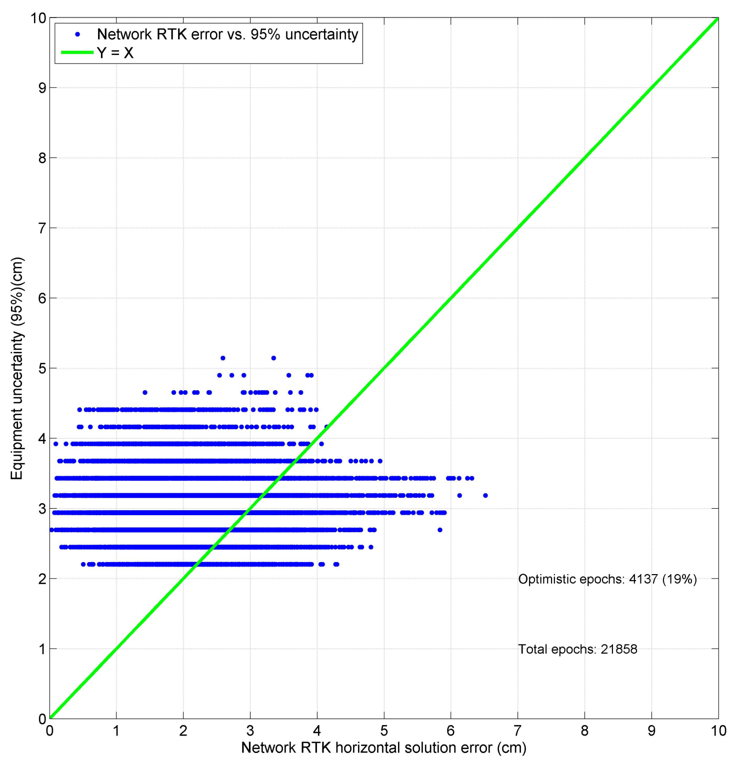

Figure 4.58: Solution integrity for Company ‘A’ at ‘kin’

4.9 Vertical Solution Integrity

Typically, the internal solution uncertainties with network RTK equipment are provided as horizontal and vertical uncertainties, separately. In some cases the equipment is also able to provide the user with all 3D components of the uncertainties for north, east and up (or x, y, z). In this section the equipment provided vertical uncertainties will be compared to the computed vertical error in the network RTK solution. Much like the horizontal integrity analysis, the main analysis consists of two types of plots. The solution integrity plots will be showing the solution error time series against the 1σ, 2σ and 3σ vertical rms. Figure 4.59 shows an example plot for Company 'C' vertical error displayed against the internally computed rms values. As it can be seen the 1σ (red) line contains the majority of the solutions, which is expected for the 1σ value as it should contain ~ 68% of the normally distributed errors. Like the horizontal integrity plots, the network RTK error does not follow the general shape of the equipment provided uncertainties at all times. For example in Figure 4.59, between 12:00 and 12:30, the initial spike in the computed rms values is not followed by a spike in the vertical error. This behaviour is characterized by over-estimation of the error in the solution. Under-estimation of the error occurs as well and can be seen in the vertical solution integrity plots; however, they usually occur in instances where a large bias in the vertical solution is visible. The network RTK vertical error in most cases, rarely steps out of the 3σ rms provided by any of the equipment. If an outlier occurs, it is usually for a brief periods of time (1-2 minutes).

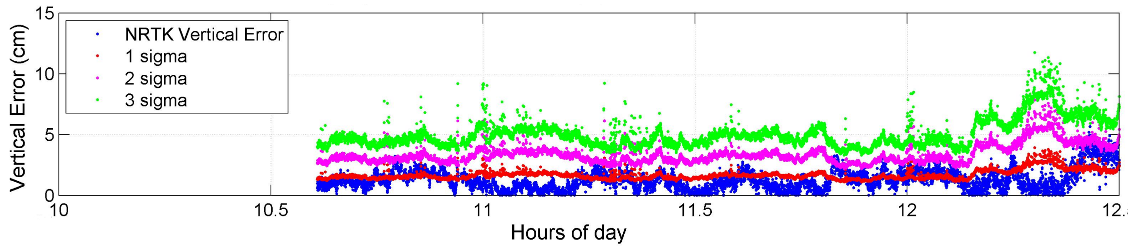

Figure 4.59: Company ‘C’ vertical error versus 1, 2 and 3σ for ‘pet’

Another set of plots are generated as part of the solution integrity analysis, which show the correlation between the independently computed errors in the solutions against the 95% scaled uncertainty (~ 2σ). For the vertical analysis the same sort of behaviour is shown as in the horizontal analysis in the correlation plots. A larger number of points are situated near the correlated line (green) and typically the rest of the points are above it, indicating that the actual error is smaller than the estimated uncertainty. Figure 4.60 shows an example correlation plot for Company 'C' in site 'bel'. In this particular site, as the figure indicates, ~20% of the total epochs are optimistic. This means that in 20% of the solutions, the vertical error in the solutions exceeds the 95% scaled rms value. For a normally distributed data set, the optimistic uncertainties should not exceed 5% of the total epochs available; this would signify that the provided uncertainties contain at least 95% of the solution errors.

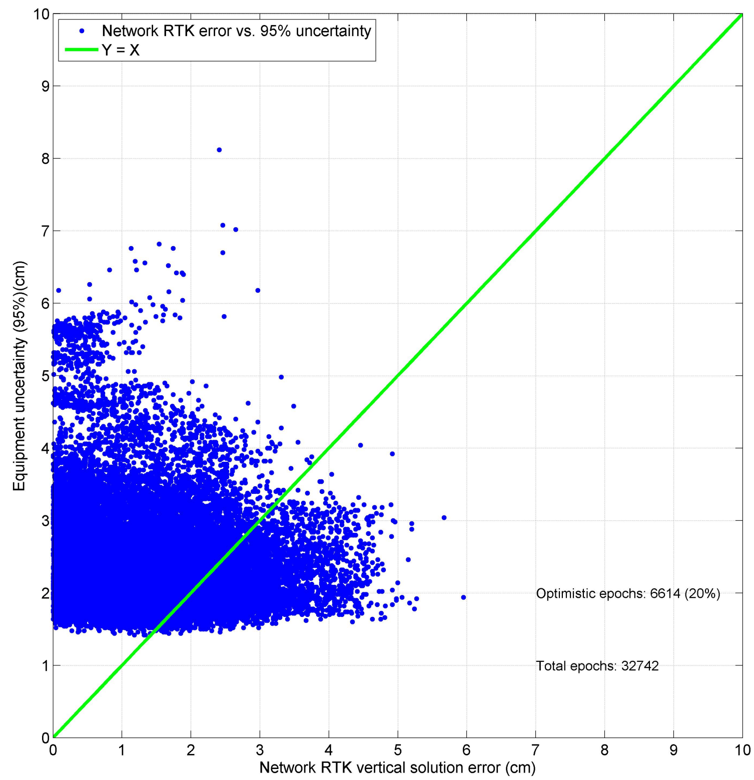

Figure 4.60: Solution integrity for Company ‘C’ at ‘bel’

Figure 4.61 shows the results for Company 'B' in the summer revisit of site 'bel'. The pattern shown here is completely different from the previous figure. Over 58% of the epochs are optimistic and the equipment uncertainties tend to vary only between ~2-3 cm range, as opposed to Figure 4.60 where the range of uncertainties are ~1.5-7 cm. The wide and narrow data points moving along the X-axis illustrates the fact that there is a weak relationship between the actual errors in the vertical solutions and the internally computed uncertainties. Also, the estimated errors in the solutions are predominantly optimistic.

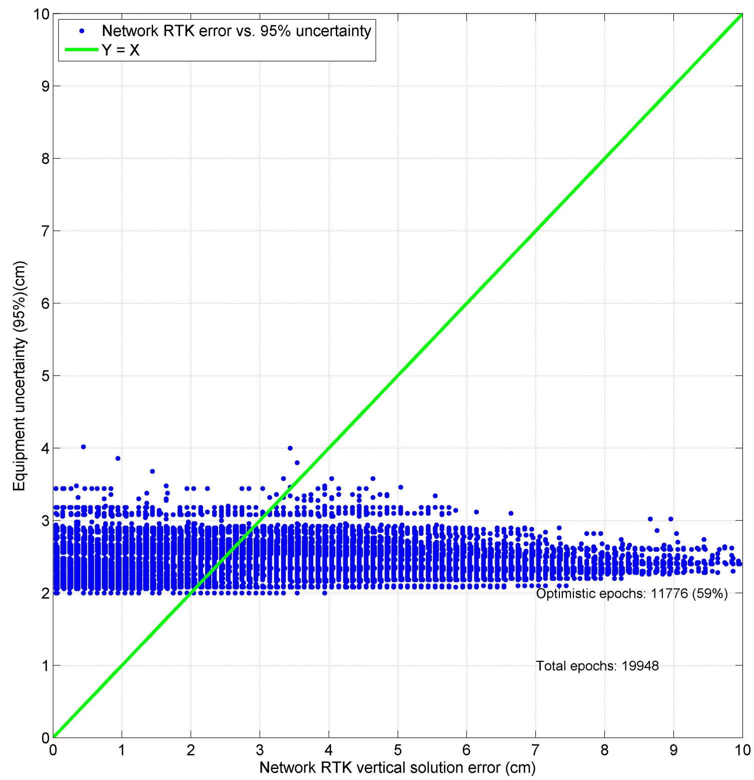

Figure 4.61: Solution integrity for Company 'B' at 'bel'

4.10 Horizontal Moving Average Filtering

This section shows the quality of the filtered solutions with network RTK coordinates computed from moving averages of 5 seconds, 30 seconds, 60 seconds and 300 seconds of network RTK position fixes, for each test site. These periods were selected to examine the effect of moving average filtering on the time series in terms of precision and maximum error. The main goal of this analysis is to use the averaging time bins as a filter to compute an acceptable duration for a static network RTK survey to accommodate precision and accuracy specifications, such as those given by MTO. However, this analysis can also be used to examine the effect of longer observation windows on solution precision and accuracy. The largest window was selected as 300 seconds, as with longer periods of observation the viability and efficiency of utilizing network RTK tends to lose its lustre and also the average user may not deem network RTK a significant benefit over the older methods of relative positioning. The accuracy of the solutions over periods of several hours (observed in some time series) will contain biases that cannot be removed by averaging windows of up to 5 minutes. The mean biases are completely unaffected by this type of short-term averaging. The precision of the solution though can be significantly improved, as wider each window will dampen the results of the individual points into one single solution.

4.10.1 Precision

Figure 4.62 through to Figure 4.64 illustrate the effect of moving average filtering on the 95% confidence level precision of the solution. Figure 4.62 shows the results for the precision of Company ‘A’ results at the winter test sites. The precision tends to improve with larger window sizes. The largest window size (300 seconds) provides the most significant improvement over the rest of the results. Large windows of observation (300 seconds) should be repeated to provide the user with at least two sets of independent solutions. For example, an improvement of 1 cm in horizontal precision can be seen for site ‘kin’ with respect to the 5 second window size and 1.2 cm improvement over the original 1 second solution set precision.

Figure 4.63 shows the moving average filtering results for Company ‘B’. The site ‘stc’ results show that the precision has improved 1.3 cm with the 300 second filtering window. However, Company ‘B’ shows smaller improvements overall from moving average filtering with respect to Company ‘A’ results. This may be due to the fact that the Company ‘B’ solution time series have a lower sinusoidal period much greater than 5 minutes, and small window sizes of a few minutes cannot have a major impact on improving the precision.

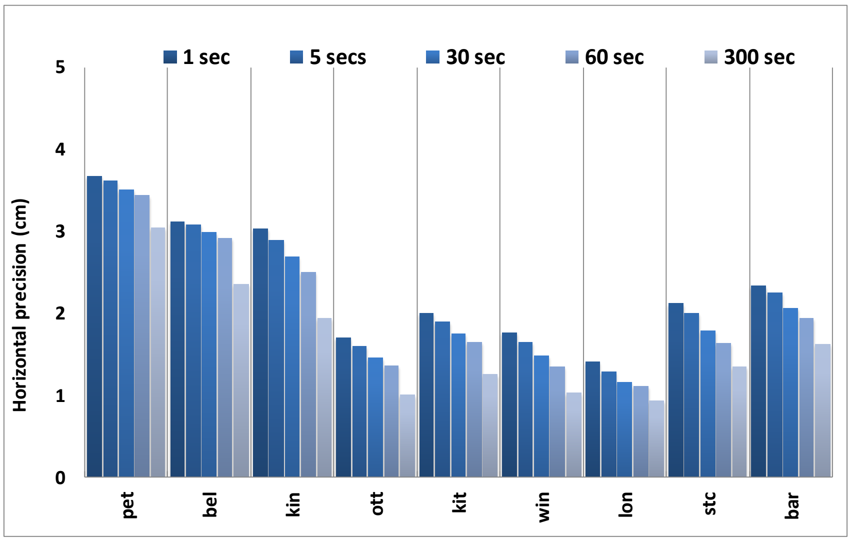

Figure 4.62: Moving average filtering vs. precision for Company ‘A’

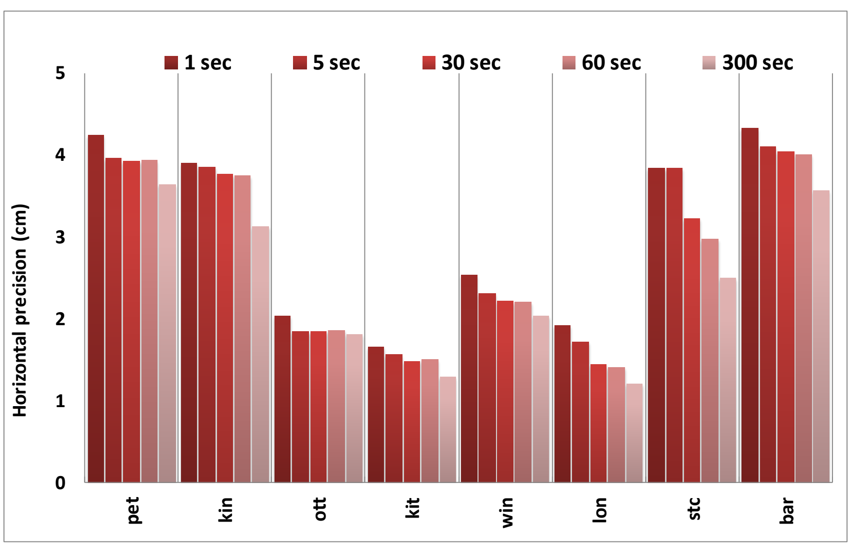

Figure 4.63: Moving average filtering vs. precision for Company ‘B’

Figure 4.64 shows the effect of moving average filtering on Company ‘C’ precision. The most significant enhancement is at site ‘win’ with a 1 cm improvement. The results are not at all systematic. In some cases the solution precision is affected significantly for the 5 minute time window filter. If the solution set is spread out over a small interval, it is expected that the precision will not change significantly with larger time bins.

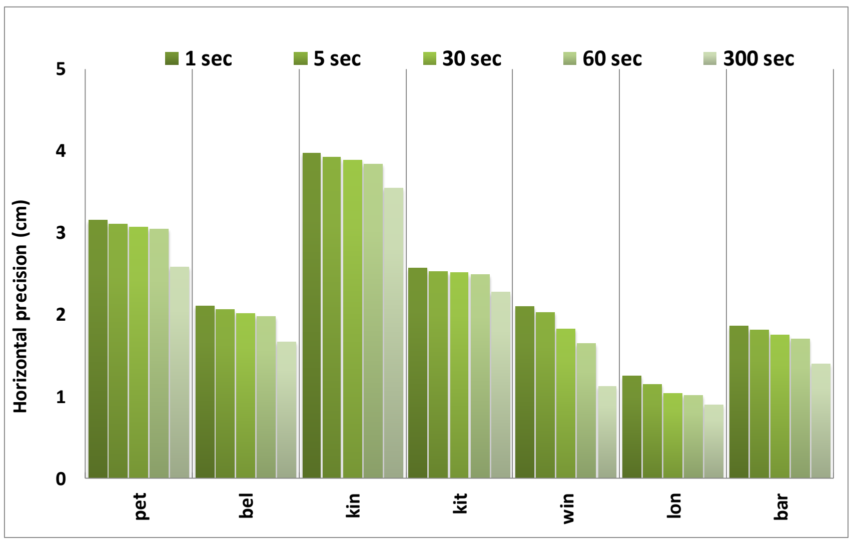

Figure 4.64: Moving average filtering vs. precision for Company ‘C’

Significant precision improvements here indicate that there may have been large isolated errors that have been dampened by the larger moving average window sizes. Table 4.8 shows a table of the improvements over the original 1 Hz data set in terms of precision for each of the service providers. The improvement of 300 second averaging is superior to the all other time bin sizes, on average doubling the results of the next largest time bin (60 seconds), and increasing precision by more than 25% over the original solution precision. An improvement of 6 mm in precision (95%) over the original solution is significant and cannot be ignored.

Table 4.8: Statistics for improvement of precision with various time bin sizes

Time bins	Company ‘A’ (cm)	Company ‘B’	Company ‘C’	Overall
5 sec	0.1	0.2	0.1	0.1
30 sec	0.3	0.3	0.1	0.2
60 sec	0.4	0.4	0.2	0.3
300 sec	0.7	0.7	0.5	0.6

4.10.2 Maximum Error

This section displays the effect of moving average filtering on the horizontal maximum error of each solution set. Figure 4.65 shows the change in magnitude of maximum horizontal error with various window sizes of moving average filtering for Company ‘A’. The maximum error is affected more by the moving average filtering than precision. In some cases, improvements over 5 cm in the horizontal maximum error can be observed. This result is of great importance to the average user, given their very limited period of observation. The results indicate that with up to 300 seconds of observations, the maximum error can be reduced significantly. For example, maximum horizontal position error at site ‘bel’ is shown to improve by of 5.8 cm with a 300 seconds time bin as opposed to a single 1 Hz position fix.

Figure 4.66 displays the improvement of maximum error with moving average filtering for Company ‘B’. A very large reduction in the maximum error can be seen for the site ‘stc'. The largest error has a magnitude of 78 cm in the horizontal, which was not filtered properly by the equipments' quality control mechanisms. With 300 seconds of averaging, a significant improvement can be seen that reduces this error to 4.1 cm in the horizontal. Similar behaviour is noted for sites 'lon' and 'bar' that demonstrates the effectiveness of averaging through larger windows of observations on reducing the magnitude of maximum horizontal errors.

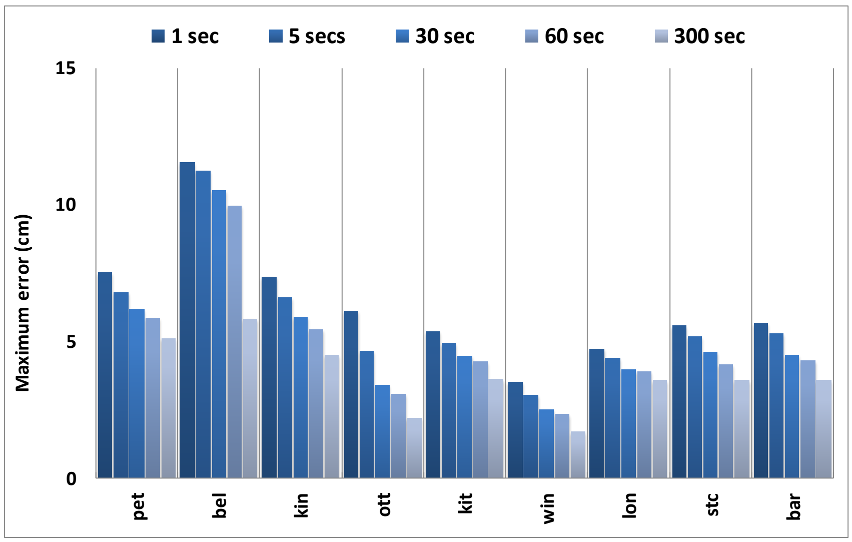

Figure 4.65: Moving average filtering vs. maximum error for Company 'A'

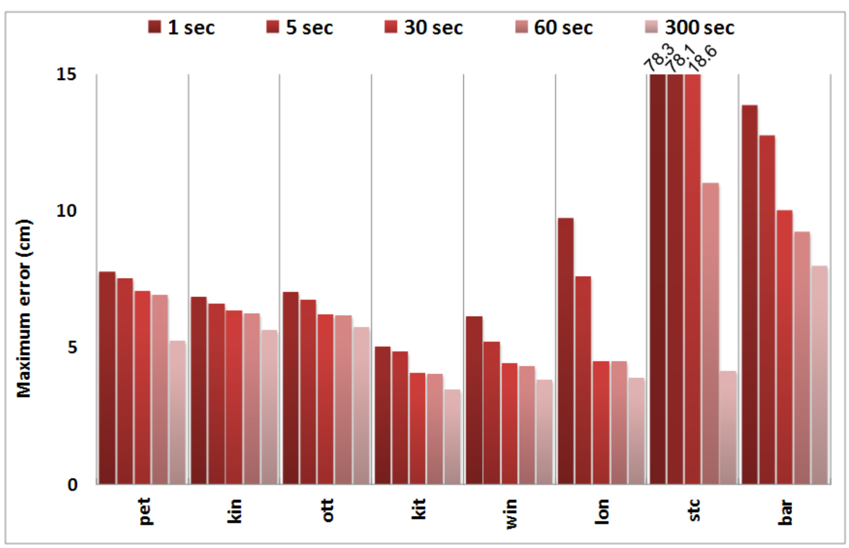

Figure 4.66: Moving average filtering vs. maximum error for Company 'B'

For Company ‘C’, Figure 4.67 shows smaller improvements for maximum error in comparison to the other service providers. This is mainly due to the significantly lower maximum error in the horizontal. However, notable improvements are still made for various sites such as ‘bel’ and ‘kin’. A reduction of 2.8 cm in the horizontal maximum error can be seen for both sites ‘bel and ‘kin’.

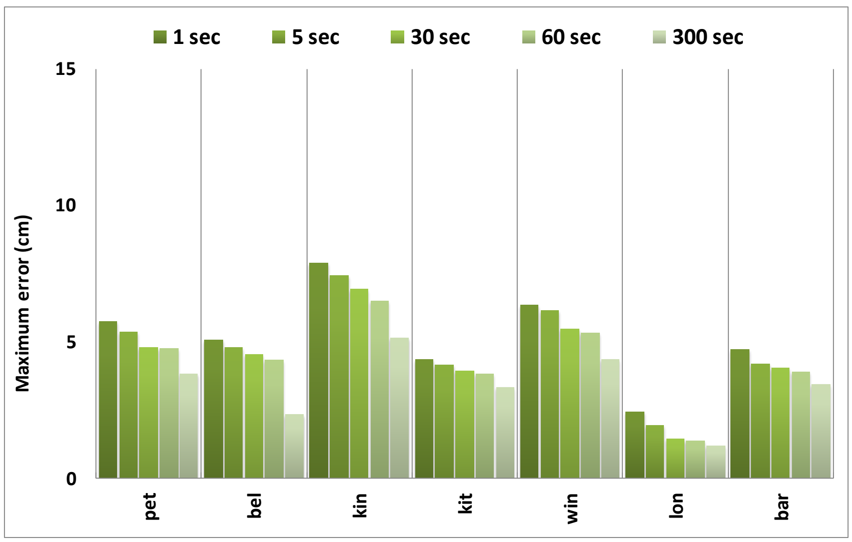

Figure 4.67: Moving average filtering vs. maximum error for Company ‘C’

Table 4.9 shows the improvement of the network RTK solution in terms of maximum errors for all three service providers. The maximum is significantly reduced by moving average filtering as can be seen from Table 4.9. Only 300 seconds of averaging of the solutions is able to reduce the magnitude of the maximum error by close to 40%. Of course, each network behaves differently when it comes to maximum error.

Table 4.9: Statistics for improvement of maximum error with various time bin sizes

Time bins	Company ‘A’ (% improvement)	Company ‘B’ (% improvement)	Company ‘C’ (% improvement)	Overall (% improvement)
5 sec	10.3	7.4	8.9	8.9
30 sec	21.4	29.3	18.5	23.0
60 sec	25.8	31.6	21.9	26.4
300 sec	49.2	41.7	38.9	43.3

The same effect, as precision, can be seen here with Figure 4.64 as in Figure 4.67: the moving average filtering dampens very large maximum errors in each data set. In some extreme cases, the maximum error is reduced from decimetre level to a few centimetres (for Company ‘B’ in site ‘stc’). This type of behaviour suggests, as outlined in the previous section, the existence of isolated large errors that affect the precision of the solution significantly and can be overcome by just using a larger pool of measurements. However, the averages of the 30, 60 and 300 seconds results are heavily skewed by the large maximum present in the Company ‘B’ solution at site ‘stc’ (~80 cm horizontal maximum error).

4.11 Vertical Moving Average Filtering

Much like the horizontal section, this section examines the effect of moving average filtering on the vertical precision. Also, the improvements of the vertical solutions in terms of precision and maximum error will be summarized. The precision shown for the vertical results are scaled to the 95% confidence interval.

4.11.1 Precision

Moving average filtering has a profound effect on improving precision of the solutions. This was shown in the horizontal analysis section, where the filtering process improved the precision on average by 25% using 60 second time bins. The improvement of the vertical precision using the same process is shown here. Figure 4.68 shows the effect of moving average filtering on vertical precision over 8 hours of network RTK solutions for Company 'C'. The improvements are noticeable, e.g., site 'kin' shows an improvement of 1.2 cm precision with 300 second filtering. The maximum errors need to be examined in order to further understand the increase in precision.

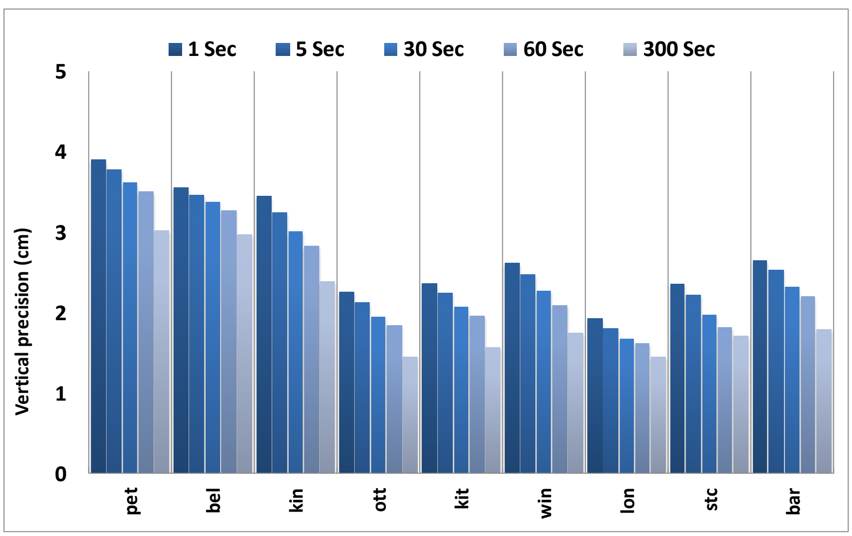

Figure 4.68: Moving average filtering vs. vertical precision for Company ‘A’

Figure 4.69 shows the results of moving average filtering for Company 'B'. The improvements are less than 3 mm for some of the sites such as 'ott' and 'kit'. This is due to how closely solutions are positioned for these sites. The 1 second precision is already below 2 cm and there is not much more room for improvement. For site 'kin', the large variations in the solution are spread throughout the 8 hours and the averaging windows are not large enough to dampen the effects. Overall, results from Company 'B' are lightly affected by moving average filtering compared to the results from Company 'A'.

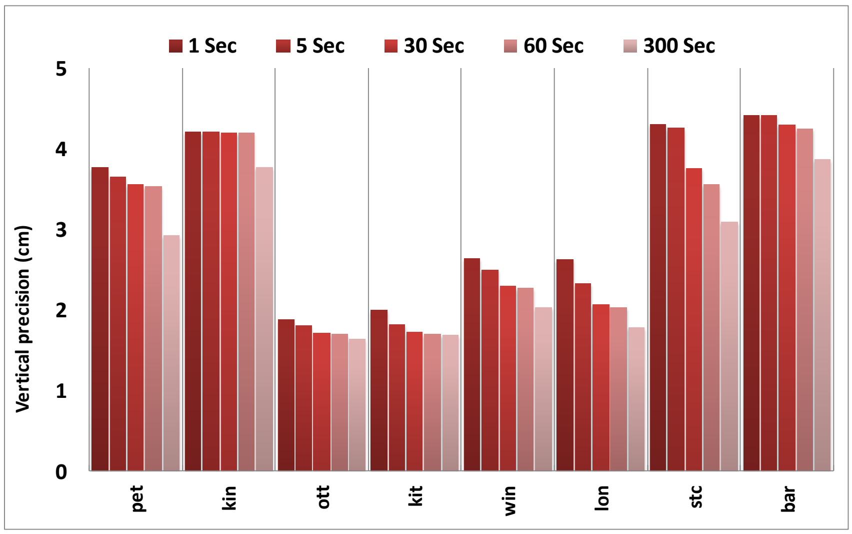

Figure 4.69: Moving average filtering vs. vertical precision for Company ‘B’

Figure 4.70 shows the Company 'C' precision results. The improvements in precision are very similar to Company 'A'. However, much like company 'B' very little improvement is seen in precision in site 'kit'.

Table 4.10 shows the average improvements to vertical precision using moving average filtering. The comparisons are made to the original 1 Hz 95% precision available. As it can be seen, the 300 second time bin averaging can improve the original precision by up to ~7 mm. This may not be a significant improvement; however, the averaging process significantly dampens the maximum errors in the data and improves the performance of network RTK in short periods (minutes) of observations, which is the typical method of use for network RTK.

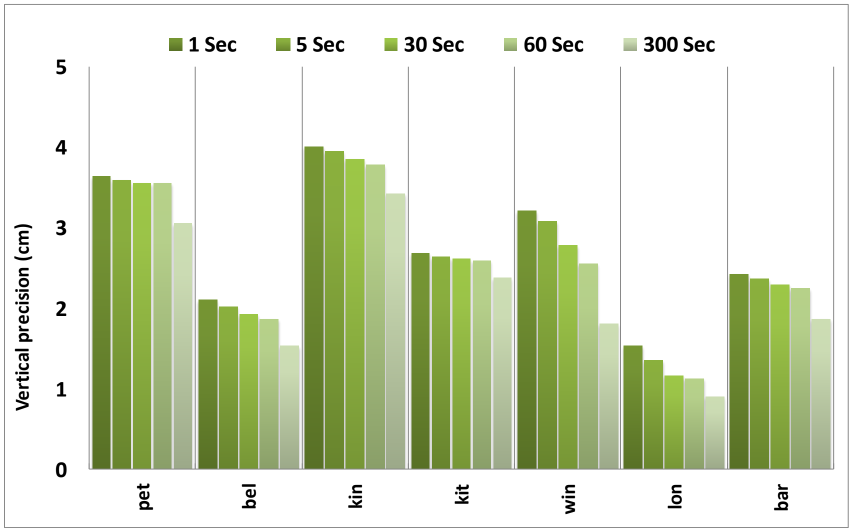

Figure 4.70: Moving average filtering vs. vertical precision for Company ‘C’

Table 4.10: Statistics for improvement of vertical precision with various time bin sizes

Time bins	Company ‘A’ (cm)	Company ‘B’	Company ‘C’	Overall
5 sec	0.1	0.1	0.1	0.1
30 sec	0.3	0.3	0.2	0.3
60 sec	0.4	0.3	0.3	0.3
300 sec	0.8	0.6	0.7	0.7

4.11.2 Maximum Error

The reduction of maximum error can explain the improvement of vertical precision using moving average filtering. Typically, the maximum errors are outliers within the network RTK data sets and last for very short periods of time (few epochs up to a few minutes). This characteristic deems moving average filtering as a successful method of mitigating against short period outliers. Figure 4.71 shows the improvement of maximum error with moving average filtering for Company 'A'. It can be seen that even the 5 second time bin reduces the vertical maximum error significantly. Test site 'win', shows a ~3 cm improvement for the 5 second time bin.

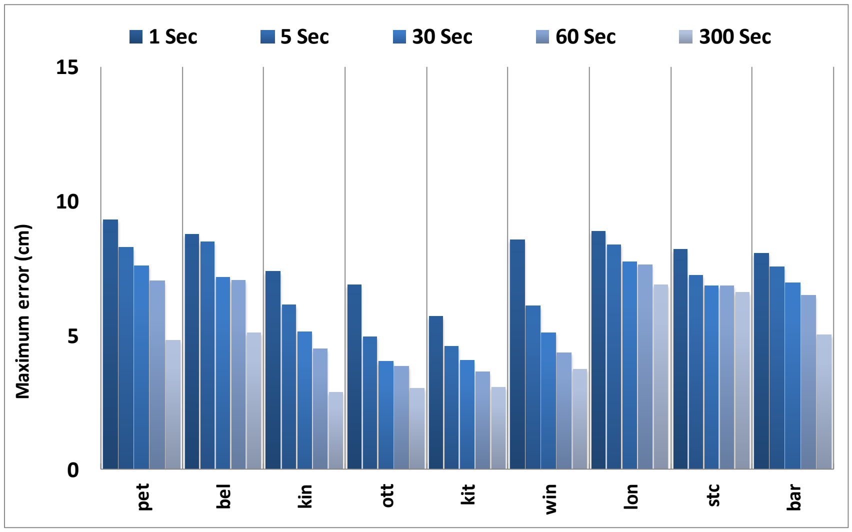

Figure 4.71: Moving average filtering vs. maximum error for Company 'A'

Figure 4.72 shows more extreme cases of maximum error dampening. In site 'kit' the maximum error is reduced by over 50% (~16 cm reduced to ~8 cm) and in site 'stc' a maximum error of ~90 cm is reduced to ~10 cm. This is significant considering how just a few minutes of observation can make a hefty difference. Similar effects were shown on the maximum error for the horizontal results for Company 'B'.

Figure 4.73 shows the improvement of maximum error on the Company 'C' data. The affects similar to that of Company 'A'. The most significant improvement is in site 'lon' with a reduction of over 80% in the maximum error is seen (~6 cm reduced to ~1 cm).

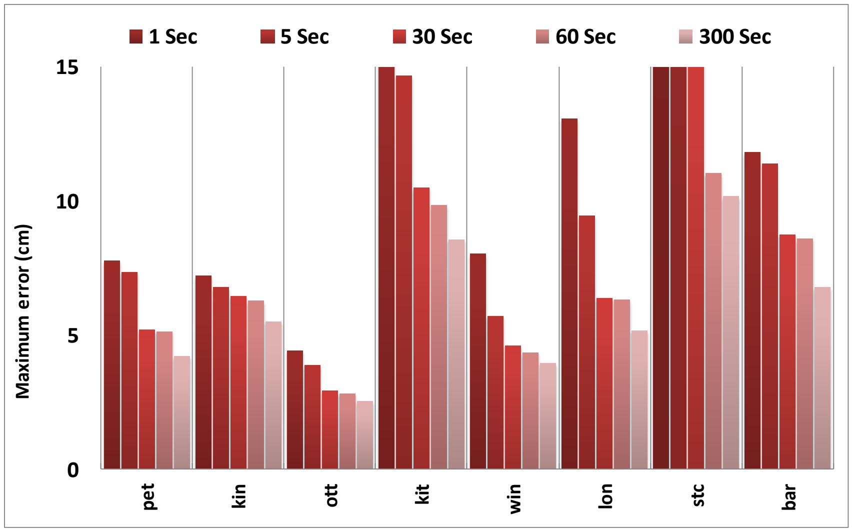

Figure 4.72: Moving average filtering vs. maximum error for Company ‘B’

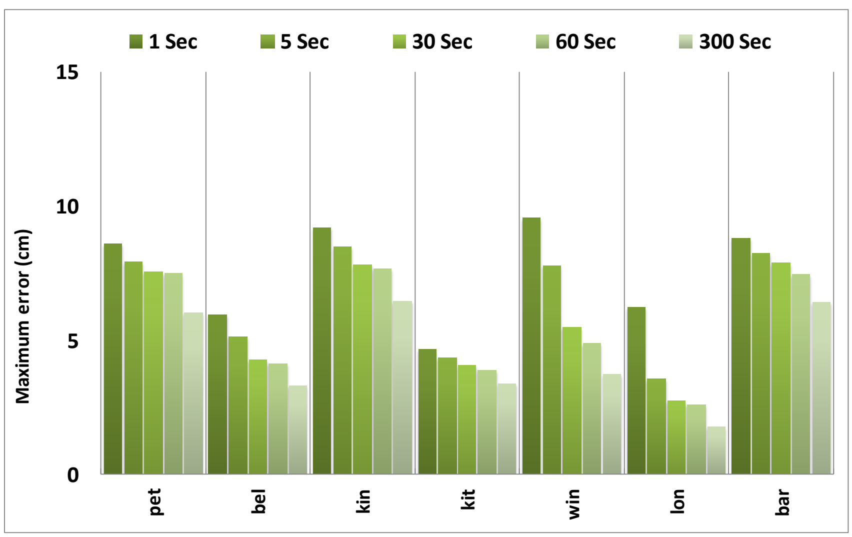

Figure 4.73: Moving average filtering vs. maximum error for Company ‘C’

Similar to the horizontal results, Table 4.11 shows significant improvement over the original 1 Hz results in terms of reducing the magnitude of maximum error in the solutions. The 30 and 60 time bins, on average for all three service providers, are showing similar improvements (up to 30%); however, the 5 minute time bins provide over 40% improvement, and in the case of Company 'B' 50%, which can significantly affect the precision and accuracy of network RTK solution, especially in short observation periods.

Table 4.11: Statistics for improvement of maximum error with various time bin sizes

Time bins	Company 'A' (% improvement)	Company 'B' (% improvement)	Company 'C' (% improvement)	Overall (% improvement)
5 sec	14.5	12.0	15.0	14.5
30 sec	24.6	39.5	25.3	24.6
60 sec	29.1	42.0	28.4	29.1
300 sec	43.3	50.3	41.6	43.3

4.12 Summary

The main goal of this chapter was to evaluate the quality of static positioning using network RTK services in southern Ontario using the predefined performance metrics. Hundreds of hours of data were collected while visiting nine test sites in southern Ontario. Fieldwork was completed in two campaigns in December 2010 and July 2011. Equipment and networks from the three service providers in southern Ontario were used at each test site, close to 8 hours of data per site per receiver were collected in the winter and 6 hours of data per site per receiver in the summer, which included network RTK and raw GPS observations. The data collected were used to analyze the quality of network RTK services in terms of six performance metrics: availability, time-to-first-fix (TTFF), precision, accuracy, integrity and long-term repeatability. The availability results show that service performance can vary significantly, but solution availability of 82% to 97% can be expected. This large range is attributed to differing equipment and field locations.

TTFF of 30 seconds, on average, can be expected with extreme cases of 100 seconds or more before obtaining an ambiguity-fixed, network RTK solution. Generally, TTFF performance is affected by the latency of the cellular connection at the user's location. The results indicate precision of ~2.5 cm (95%) or lower in the horizontal. The results also show biases that can be up to 4 cm in the horizontal. In terms of accuracy, each service provider's solution had these biases, to varying amounts, at sites across southern Ontario. These biases result in rms ranging from 2 to 5 cm. The biases also showed systematic behaviours and the cases of company 'A' and 'B' showed translational and rotational biases. In terms of long-term repeatability, biases in the solutions are mostly repeatable in terms of direction; however, statistical testing of the mean errors and the standard deviations revealed that the accuracy and precision seen are not statistically repeatable. The precision levels vary by up to centimetre in the 95% over period of seven months, although still within typical network RTK levels (1-3 cm). Moving average filtering for 5 minutes time bins showed a precision improvement of 25% and maximum error reduction of 40% of over the original 1 Hz data sets. Note that short-term averaging does not reduce long-term biases. Overall, the results of the analyses have not been uniform and each network possesses individual characteristics, which could be address by regulatory guidelines for performance and quality of the services provided.

5. KINEMATIC NETWORK RTK EVALUATION

The kinematic data collection and analysis was a secondary objective of this thesis, as the main objective was set by the MTO project. The kinematic tests for network RTK solutions in southern Ontario were performed in parallel to the static tests. In each kinematic run, the three different equipment packages were mounted on the roof of the transport vehicle and run simultaneously. The aim of this chapter is to evaluate and discuss the results obtained from these kinematic data sets. The evaluation metrics used to demonstrate the level of performance from network RTK in kinematic mode include: solution availability, precision, baseline accuracy and solution integrity. Examples of solution quality and solution integrity plots are shows in this chapter, though all plots related to the kinematic analysis can be found in Appendix D.

5.1 Analysis Methodology

Typically, for the testing of any precise positioning technique, the solutions obtained need to be compared to a reference ("truth") solution. For kinematic applications, short baseline RTK can provide centimetre-level accuracy positioning. However in this study, due to the long distance trajectories and the unique experimental set-up, the use of short baseline RTK as the reference was not possible. The use of kinematic PPP data processing is an option, though due to convergence issues inherent with PPP and continuous interruptions of the observations, it was not possible to obtain centimetre-level positioning. Due to the lack of consistently reliable reference solutions, and in order to characterize the kinematic quality of network RTK, each solution set was compared against the other, which provides the major portion of the analysis. It is important to note that the comparisons between network RTK solutions do not represent a kinematic performance evaluation between companies, but rather an evaluation of network RTK kinematic performance in southern Ontario.

When comparing two sets of simultaneous network RTK solutions, the time-tags become one of the most important pieces of information that organize the positions in the correct order for comparison. However, one of the major issues seen in most of the collected kinematic data sets is the association of a positioning solution with an incorrect time-tag. For most commonly used network RTK receivers, the solution coordinates along with additional information such as the solution rms are recorded using accompanying the data collectors. Some receivers have the option to directly record points in the receiver; however, most network RTK equipment set-ups involve the use of a handheld data collector. The issue of time-tags become apparent when the solutions are recorded with the data collector's estimated time as opposed to the actual GPS observation time. This phenomena is not of importance when analyzing a static solution set, but it becomes vital when comparing two different kinematic data sets. The issue of synchronization can create large biases when comparing two solution sets based on using time-tags. Figure 5.1 shows the described time-tag discrepancy between two different solution sets. For the outliers shown in the top plot, the recorded time different between both solution sets is exactly 1 second. As it can be seen from Figure 5.1, the baseline between both receivers follows closely the shape of the vehicle speed plot, indicating direct correlation between the biases. Also, it should be noted that while the vehicle was stationary, no outliers of this nature can be seen. This result is due to the fact that since the vehicle was not moving, a 1 second bias cannot cause outliers in the comparison; however, as soon as the vehicle begins to move, the difference can be readily seen.

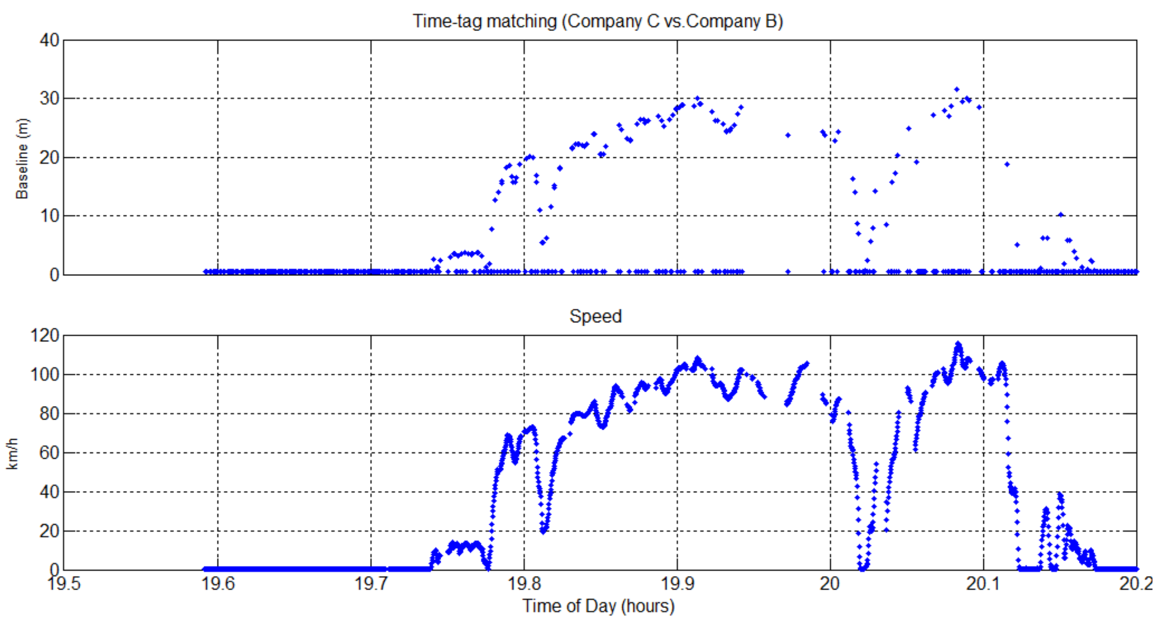

Figure 5.1: Linear time-tag discrepancy for Company 'C' vs. Company 'B'

To further examine the issue of the time-tags, the correlation plot can be shown of speed and baseline error. With a constant whole-seconds time bias between the two solution sets a linear relationship is expected. Figure 5.2 shows such a linear correlation between speed and baseline error in the comparison of network RTK solutions between Company ‘A’ and Company ‘C’ for one kinematic run. The baseline error is the deviation of the baseline between two antennas with respect to the calibrated baselines determined from the static portion of the data sets. Two discreet lines can be seen in Figure 5.2. The lower line centred about zero is the baseline error obtained using successful time-tag matching. The points along this line, although vary in centimetres, represent common solutions with correct time-tags between the two sets of equipment. The second line represents the linear relationship that exists between the speed and baseline error between the two solutions. However, the biases tends to behave unpredictably from one epoch to the next, making them extremely difficult to remove. As discussed, this unpredictability is mainly due to the lack of synchronization of data collector clocks with GPS time.

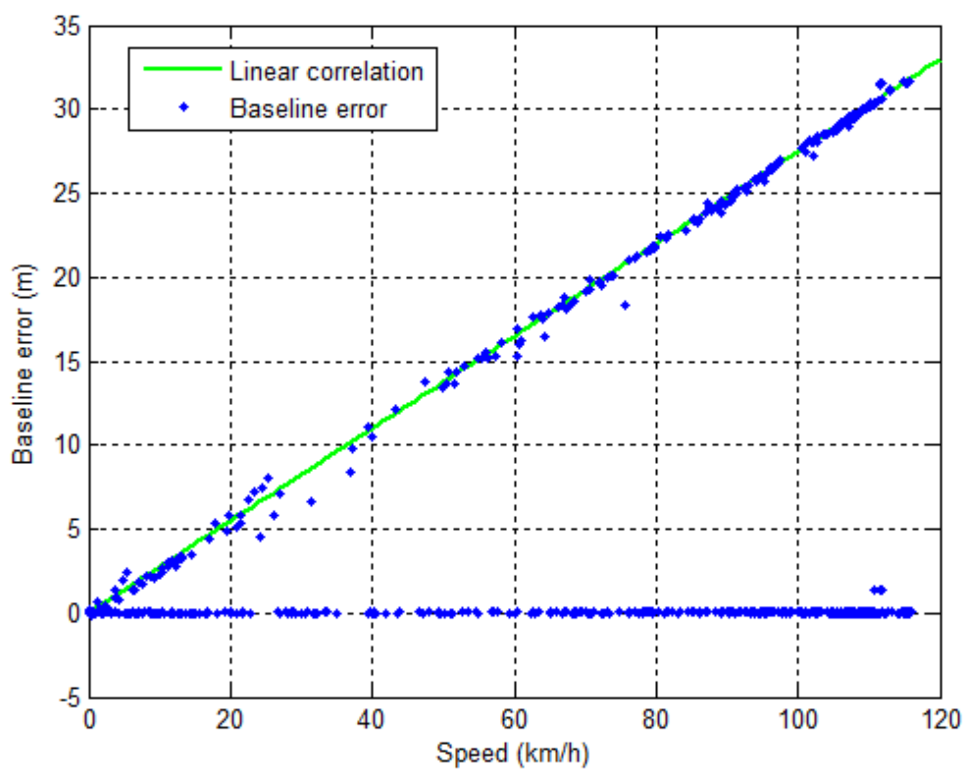

Figure 5.2: Correlation between baseline error and vehicle speed for Company 'A' vs. Company 'B'

Another issue that appears in the data are sub-second solution differences. All of the equipments were operating in 1 Hz mode; however, some of the solutions exhibit this characteristic. In particular, solution comparisons involving Company 'A' show this particular eccentricity. This effect causes the consecutive data points to be a fraction of a second ahead or behind the actual GPS observation time. Figure 5.3 shows discreet points that are equally spaced due to the vehicle travelling at a constant speed (~110 km/h). In this case the solution time-tags are ahead by multiples of 0.2 of a second (0.2, 0.4, 0.6, 0.8 and 1). Each set of discreet data points represents a network RTK position computed a fraction of a second faster and slower than the correct time of observation.

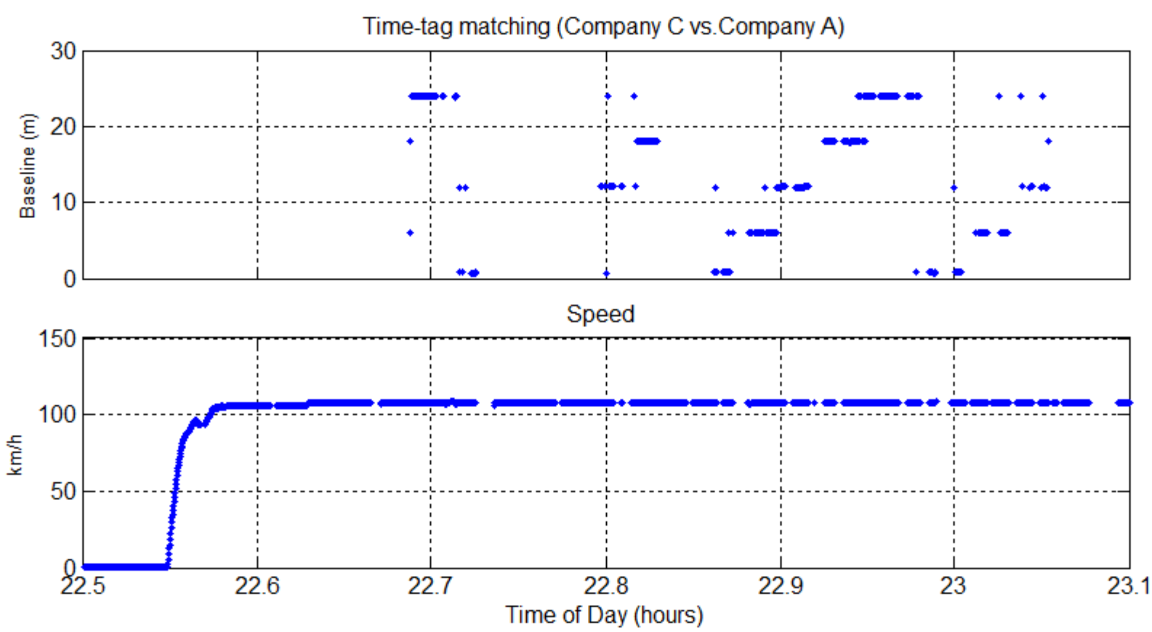

Figure 5.3: Solution discrepancy due to time-tags being fraction of a second ahead or behind actual GPS observation time for Company 'A'

In light of all the issues that exist in the solution time-tags, the best way to match and compare two different solutions is to sort and compare by position. The recorded network

RTK solutions are all ambiguity fixed positions, so centimetre-level accuracy can be expected; this make positioning matching a fairly simple process. Taking into consideration the speed of the vehicle, positions can be matched based on a baseline threshold. Each data set has at least a few minutes of static solutions, which are used to calibrate the baselines between each set of receivers. The thresholds are then set based on this estimated "fixed" relative baseline. Any two sets of position that are not within the threshold defined can be ignored. Another important aspect of position matching is that since the positions are matched, the time differences can be computed to analyze the time-tag differences.

5.2 Availability

In terms of availability, total existing epochs from each solution set are compared to the total number of epochs that should be available, which is obtained from the time span of each kinematic run. Table 5.1 shows the percentages of data available for each kinematic test run. Company 'C' solutions indicate consistently low availability percentages throughout all of the tests, with the exception of the ~80% for the Kitchener to Windsor run, which is possibly due to coverage issues as similar coverage problems were seen in the static data set. It is important to note that there are significant amounts of float solutions (decimetre-level accuracy) available for Company 'C' data sets; however, they are not included in this analysis for across company consistency.

Table 5.1: Kinematic run total solution availabilities for each kinematic run

Kinematic run	Company 'A' (availability %)	Company 'B' (availability %)	Company 'C' (availability %)
St. Catharines to Kitchener	64	35	5
Kitchener to Windsor	42	27	79
Windsor to London	83	38	6
Jarvis to Toronto	60	37	4
Barrie to Toronto	63	32	<1 %

In the kinematic data sets, the solution availability becomes heavily affected by the number of obstacles encountered. At certain times, the fixed solution is lost when approaching and passing an overpass and the equipment is unable to obtain another fixed solution for a few minutes. Figure 5.4 shows an example of the fixed solution being lost due to travelling under an overpass. In this particular case it takes over 5 minutes for the to recover its ambiguity fixed network RTK solution. Situations such as this happen due to travelling through consecutive obstructions, which effect visibility and in turn keep the receiver from re-obtaining an ambiguity fixed solution.

Figure 5.4: Fixed solution lost due to bridge

In particular, the test run from Kitchener to Windsor for Company 'C' is examined in more detail using Google Earth to determine the number of obstructions interrupting the availability of continuous 1 Hz data. The total number of obstructions met by the vehicle according to Company 'C' data is 117. Figure 5.5 shows the recovery times of each obstruction met during the kinematic test run. The 117 obstructions include any interruptions due to lack of GPS satellite observations while travelling through densely developed areas (buildings), dense vegetation and under overpasses. It is expected for a kinematic data set to have discontinuities; however, the recovery time of the ambiguity fixed position is of great concern. The average recovery time for the receiver during this kinematic run was approximately 21 seconds, which is very close to the results produced by the time-to-first-fix analysis in the previous chapter. As it can be seen from Figure

5.5, predominantly the solution recovery times are below 30 seconds; however, there exist a few instances where the recovery of the ambiguity fixed solution has taken more than a minute in duration which are due to travelling through consecutive obstructions. These are interesting results which indicate that the time-to-first-fix from a "warm" start (receiver was operating prior to losing ambiguity fixed solution) only improves by a few seconds, in comparison to a "cold" start, and the availability of the last ambiguity fixed epoch cannot help the solution recover any quicker.

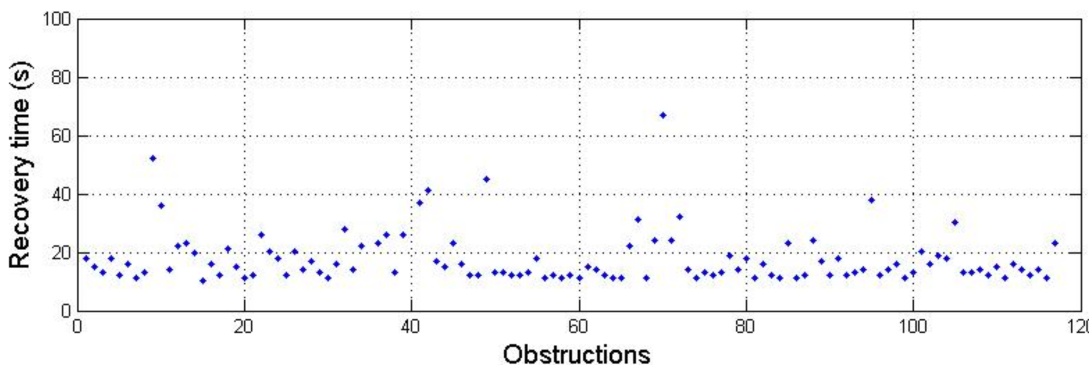

Figure 5.5: Solution recovery time after encountering obstacles

5.3 Solution Quality

The solution quality section aims to define the quality of the baseline error between different set of receivers. Two different kinematic data sets are shown for the Kitchener to Windsor and Jarvis to Toronto runs. These two data sets represent some of the best and worst data collected in terms of availability. The calibrated baseline lengths are removed from each set of comparison and the end results are shown as errors in the baselines between each pair of antennas. In the following sections, the standard deviations and means of the baseline errors are used to characterize the accuracy and precision of the solutions.

Figure 5.6 shows the quality of the solution for the test run between Kitchener and Windsor. Matching common data points between two sets of data causes the further reduction in data availability. A comparison can only be performed when both data sets have an available solution at a particular position. In Figure 5.6, the reported baseline errors are on average at the millimetre-level, which presents a very accurate kinematic solution. The standard deviations, ranging from 1.7 cm to 2.3 cm (1σ), also show typical network RTK precision, which was seen from the static tests. However, it is important to note that each of these solutions is accompanied by an inherent uncertainty, which should be at the centimetre-level, based on the static results of this study and other similar studies (Rubinov et al., 2011; Aponte et al., 2009). By comparing one solution against the other, the solution uncertainties are accumulated, causing the compared solution error to appear larger than the error in each individual data set.

Figure 5.7 shows another data set from the test run between Jarvis and Toronto. Here, the lack of availability from Company 'C' reduces the size of the comparison that can be made between solutions. Large, mean baseline errors ranging at 2-9 cm can be seen, but the precision of the baseline is at 1.5-2.5 cm range as shown in the previous results. The comparison between Companies 'A' and 'B' has a slow drift of ~5 cm in the baseline error. However, the difference reduces and is close to zero towards the end of the comparison period. The third plot shows the comparison between companies 'C' and 'B', and even though there are a few large outliers, in comparison to the rest of the points, the standard deviation of 1.2 cm and the mean of 4.1 cm are not severely affected, which shows that a large number of solution are available for comparison for the 10 minute period.

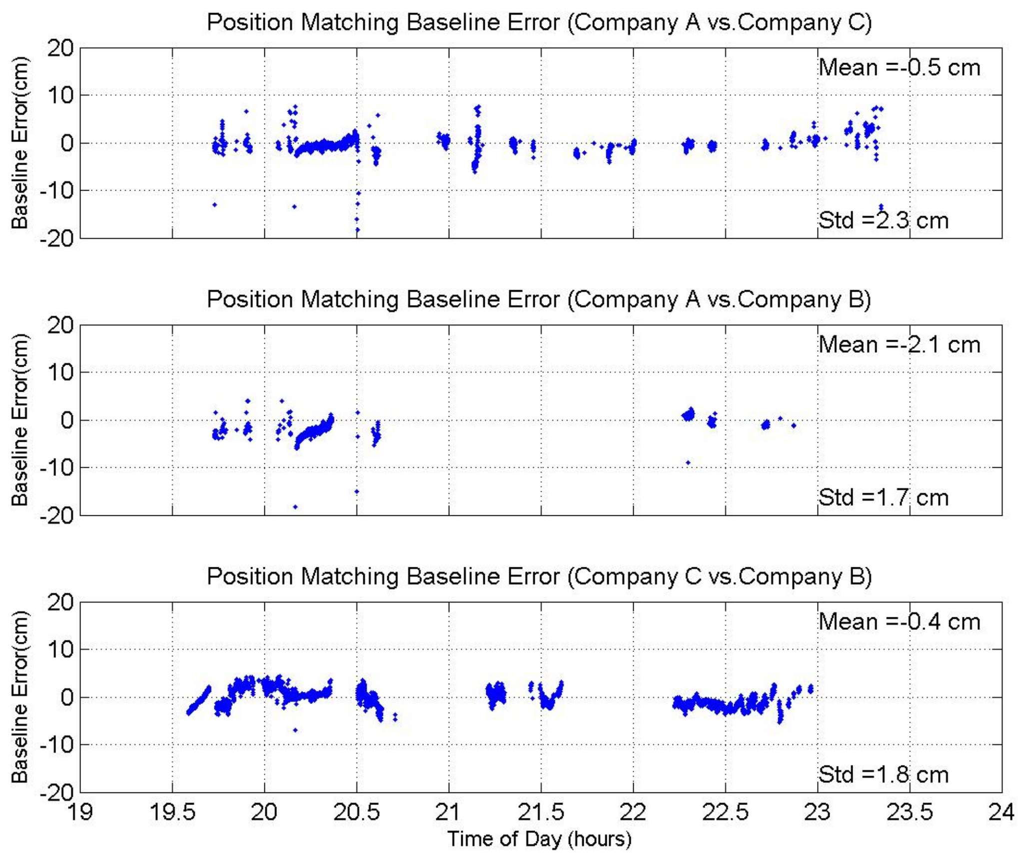

Figure 5.6: Kinematic baseline error between three pairs of antennas (Kitchener → Windsor)

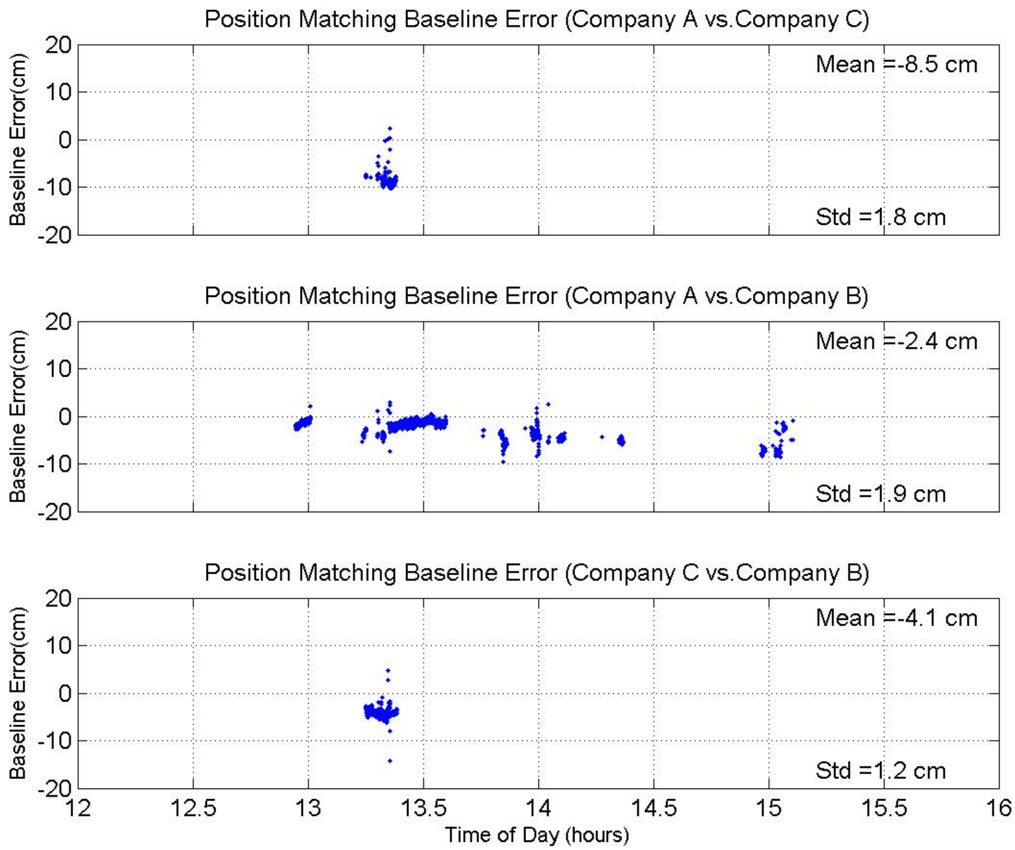

Figure 5.7: Kinematic baseline error between three pairs of antennas (Jarvis → Toronto)

5.4 Precision

In order to examine the precision of the compared solutions, the 3D standard deviation of the baseline error is computed. Here the average baseline length between the receivers is removed from each set of solution comparisons and the standard deviation of each solution is computed. In terms of typically expected precision, as shown earlier in Aponte et al. (2008), a standard deviation (3D) of ~2 cm (1σ) is reasonable. Figure 5.8 shows the 1σ precision levels for each set of solution comparison. As it can be seen, for the majority of the results, the precision values are ranging from 1-3 cm which is within the expected range. However, the large standard deviation shown for the comparison of Company 'A' and 'C' solutions in the Windsor to London test run is more than twice the expected value of ~2 cm. This unusually large standard deviation is primarily due to the lack of solution availability for Company 'C' for that particular run. Only 225 epochs of common solutions are available between Company 'A' and 'C' data sets, which means less than 4 minutes of common solutions were available for comparison. The effect of the lack of availability can also be seen for the Company 'C' and 'B' comparison in the same test run.

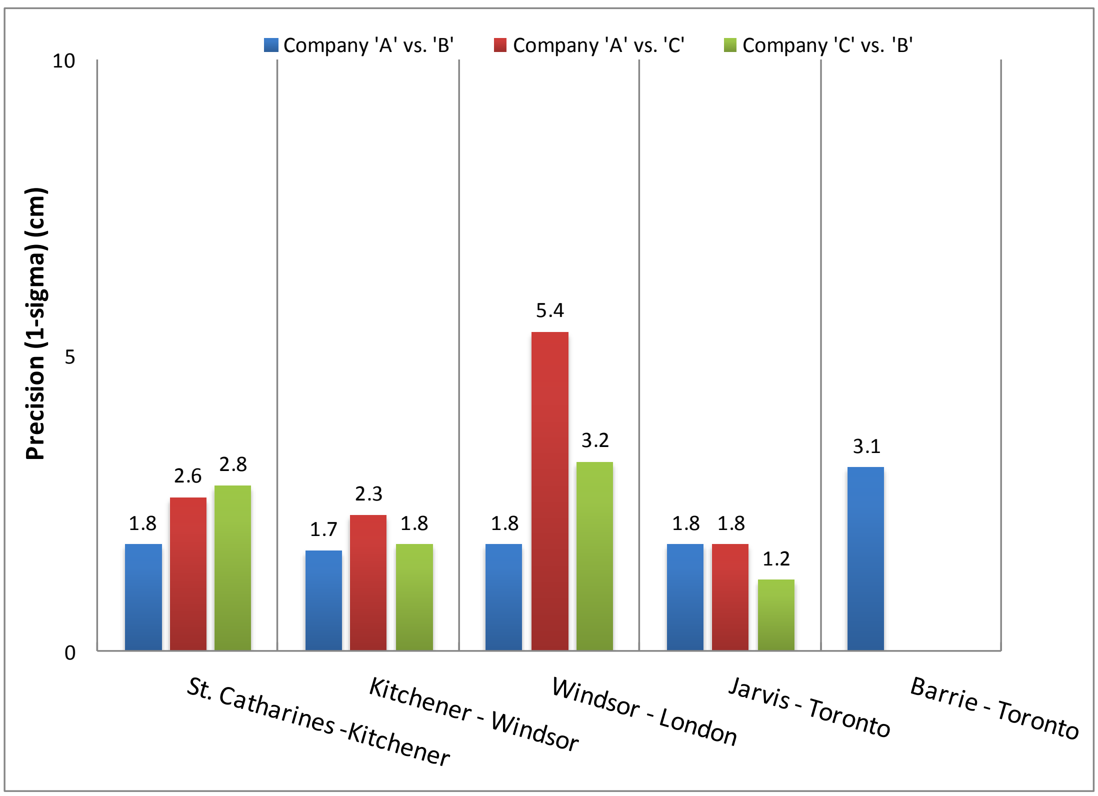

Figure 5.8: Kinematic 3D 1σ precision for each set of comparison in each kinematic run

Emphasizing the importance of data availability when performing this type of comparison, all test data sets which have over 30% data availability have very good results in terms of precision. On average the precision of solutions compared are ~2 cm 3D (1σ), which illustrates typical kinematic network RTK performance.

5.5 Baseline Accuracy

The baseline accuracy is a difficult comparison to make. Since there is no independently determined reference position computed, one solution needs to be compared directly to another. The mean baseline error is computed by comparing two data sets (using position matching), determining the average baseline between the antennas and then removing that average from the comparison. This procedure provides the mean error or the mean deviation of the solution from the calibrated baseline between the antennas. Figure 5.9 shows the mean baseline error for each pair of available data sets. The large errors seen for the Company 'A' versus 'C' in Windsor to London and Jarvis to Toronto test runs are primarily due to the low availability of fixed solutions from Company 'C'. In contrast, for the Kitchener to Windsor test runs, where Company 'C' has the most availability (refer to Table 5.1) the mean errors involving Company 'C' are sub-centimetre. Ideally, to determine the error considering all three solutions, the zero-sum differential vector comparison between the antennas would be a better comparison than strictly using the baseline magnitudes. Though, this is not possible because it is very difficult to find a period of at least a few minutes when all three solutions are available. This lack of data is the primary reason that the magnitudes of the mean biases do not complement each other. It is expected for the magnitudes of the mean errors of two solution comparisons to sum to approximately the third comparison. Each comparison is performed within a different time frame and can be verified by examining some of the results. In test run Windsor to London, the mean baseline error between Company 'A' and 'B' is 7 mm. Also, in the same test the mean baseline error between Company 'C' and 'B' is 8 mm. Since both comparisons involving Company 'B' show such good results, it is expected that the comparison between Company 'A' and 'C' to not exceed a baseline error of 2 cm, however this result is not the case, which is because the comparisons are not made at the same time intervals.

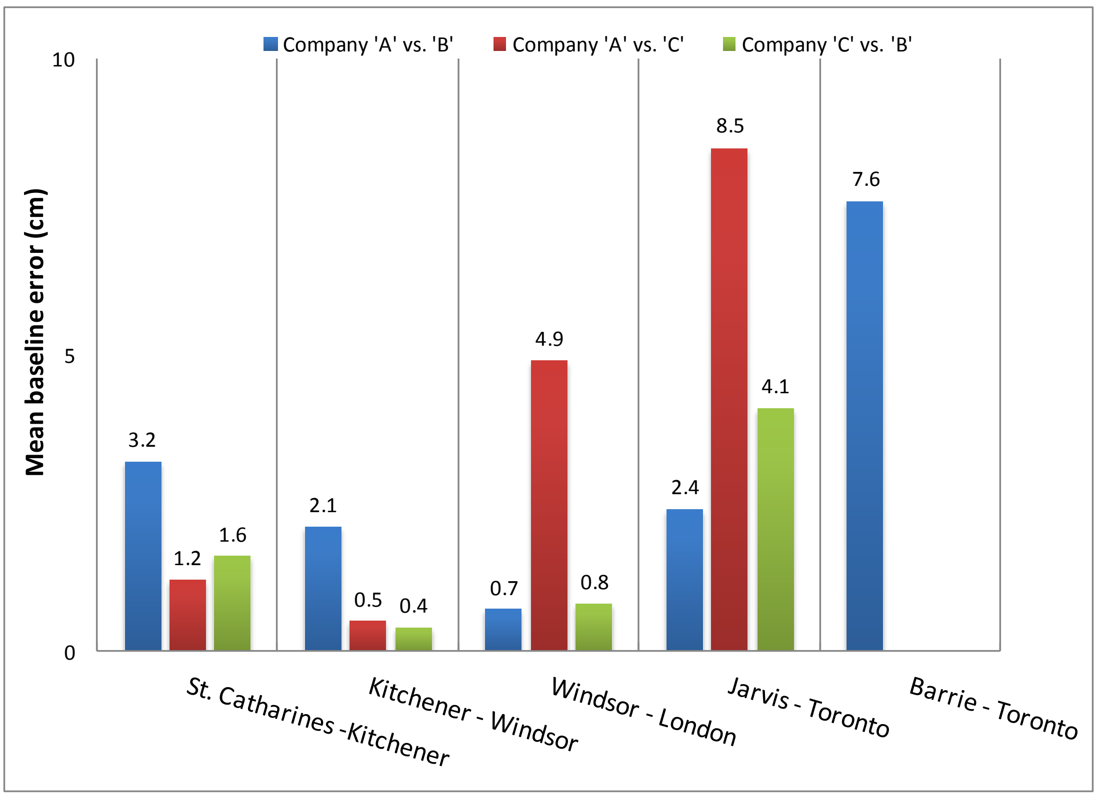

Figure 5.9: Mean baseline errors for each set of comparison in each kinematic run

To examine the accuracy comparison between the different data sets, the rms of the baselines can be computed. Figure 5.10 shows the rms values for each set of solutions compared. Primarily, large mean errors account for the rms values. In the Jarvis to Toronto data set, the rms for the Company 'A' and 'C' comparison is 8.7 cm; however, this outlier is mostly affected by the mean error of 8.5 cm. Ignoring the isolated large outliers, the rms values range from approximately2 - 4 cm in 3D. Considering that these values include the height component, which tends to be the least accurate, the rms results are at a reasonable level and comparable to static horizontal results and within the 1.5-4 cm range.

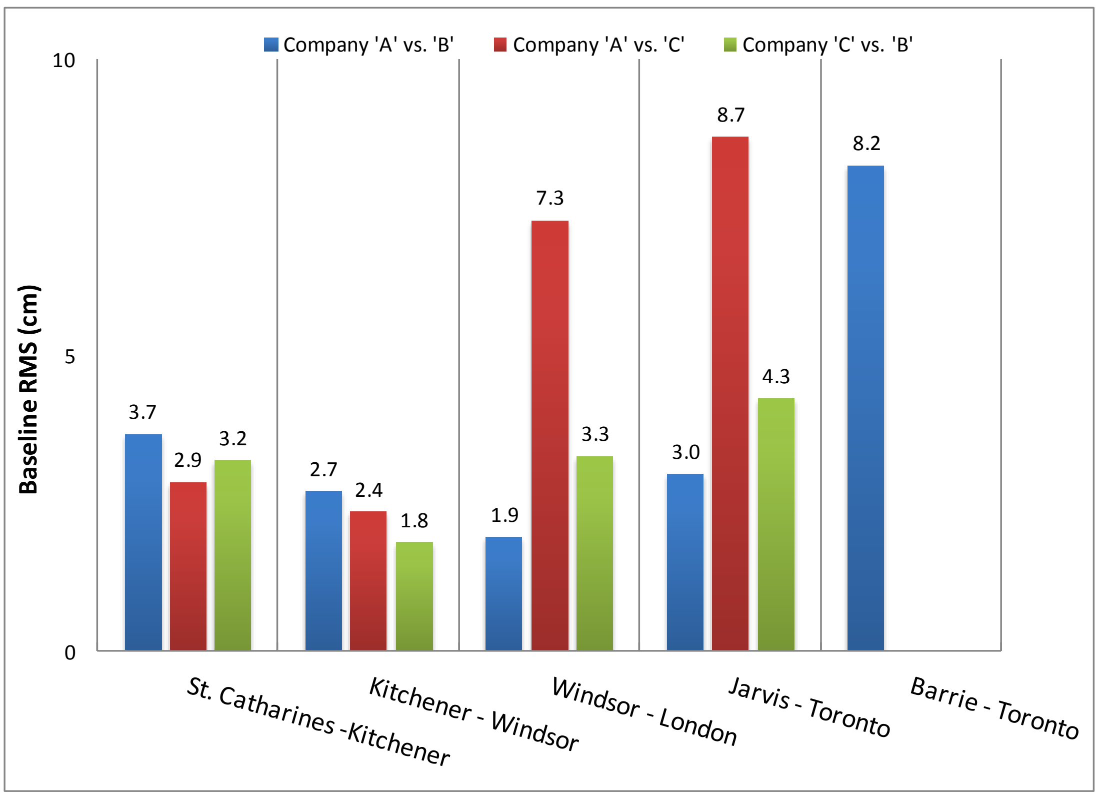

Figure 5.10: Baseline rms for each set of comparison in each kinematic run

It is difficult to determine the reasons for the large rms shown in the results. The issue is most likely due to the unavailability of fixed solutions. For both the Windsor to London and Jarvis to Toronto test runs, Company 'C' has less than 10% availability and a total of under 5 minutes of common data with Company 'A'. Hence, there is not enough data to report accurate and realistic results.

5.6 Solution Integrity

This main aim of this section is to study the integrity of the network RTK solution error in kinematic mode with respect to the equipment provided uncertainties. A comparison of the network RTK baseline error, which was computed to examine the accuracy of the solutions, is plotted against the reported uncertainties. The 3D uncertainties for the baseline error are computed using the general law of error propagation to combine two sets of equipment rms values into one comparable uncertainty (Wang, 2009). Two sets of plots are generated for this analysis, which have the same basic format as the solution integrity plots in the static analysis sections. The first set of plots display the magnitude of the baseline error and the computed uncertainties from the equipment. Figure 5.11 shows an example of the computed baseline error compared to the propagated equipment uncertainty values for each common epoch where a solution comparison is possible. This particular example is between Company 'B' and Company 'A' solution sets. The red, magenta and green lines represent the scaled 1σ, 2σ and 3σ uncertainties. The uncertainties used are the 1σ horizontal and vertical uncertainties provided by the equipment and scaled to appropriate confidence intervals. In this particular example the baseline error is completely contained by the 2σ (~95%) confidence interval and it is only outside of the 1σ (~68%) confidence interval briefly. Ignoring occasional large outliers, this is typical behaviour seen for the baseline error for other solution set comparisons as well.

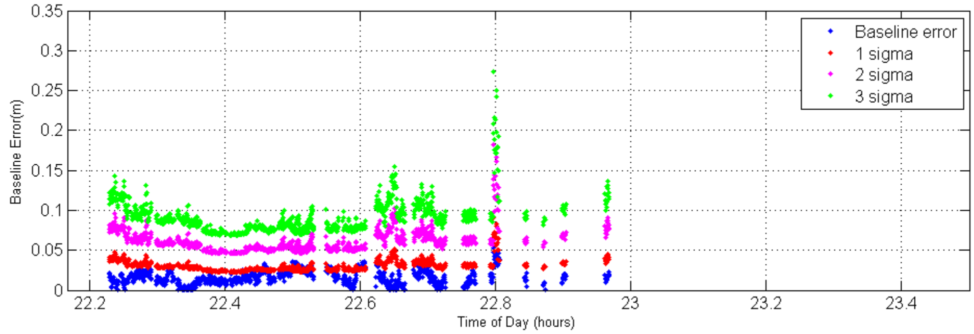

Figure 5.11: Baseline error vs. scaled 1σ, 2σ and 3σ internal equipment uncertainties

The second sets of plots show the correlation between the computed uncertainties versus the baseline error. This plot is designed to examine the integrity of the equipment provided uncertainties by comparing the results to a perfectly correlated solution line, which represents ideal case uncertainties that display the actual error in the solutions. Here, the number of "optimistic" epochs is reported to show the total percentage of computed solutions, which had higher actual errors than the reported uncertainty by the equipment. Predominantly, as shown in the static analysis sections, the network RTK solution uncertainties tend to be higher than the actual errors; however, large biases in the solutions can significantly affect the number of optimistic uncertainties. An example of the correlation plot can be seen in Figure 5.12. In this example, which contains the comparison between Company 'A' and Company 'C' data sets, the total number of epochs that were eligible for comparison is reported to be 2127 and optimistic epochs are shown at 2% of the total epochs. Most of the combined uncertainties are located within the 4-6 cm range. Also, since most of the points are located to the left and situated very close to the Y-axis, the actual errors in the baselines tend to be significantly smaller than the reported 95% confidence interval equipment uncertainties. The plotted points form a line along the ~2 cm baseline error and move along the Y-axis. This result suggests that the uncertainties are reported to be increasing in size, however the solutions are quite accurate. This phenomenon is expected with kinematic data sets, as the equipment reported uncertainties are based on the observations made during the test run. Frequent obstructions tend to cause the equipment to overestimate the uncertainty due to lack of measurements, which in most cases may not have a direct impact on the quality of the solutions.

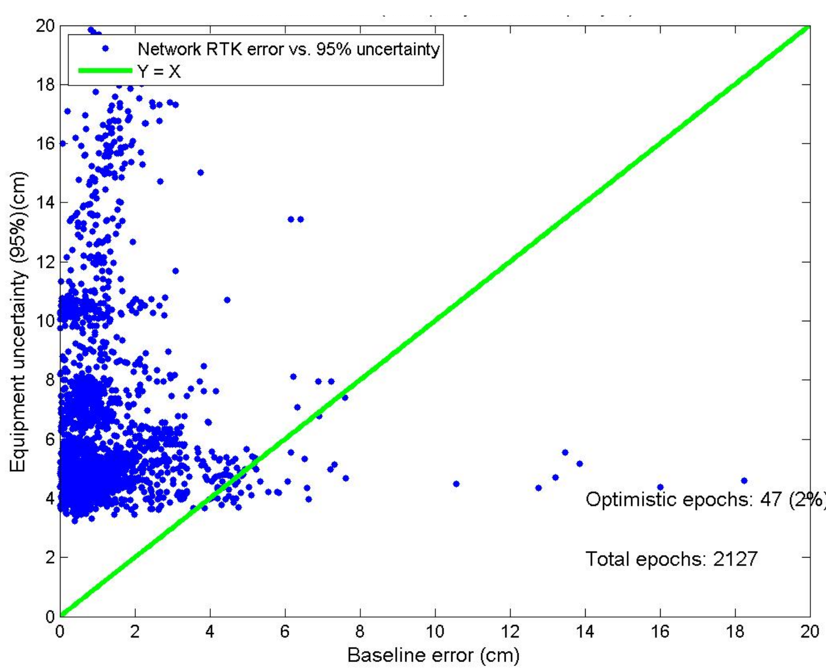

Figure 5.12: Correlation between 95% equipment uncertainty and the actual baseline error

5.7 Summary

The main objective of this chapter has been to characterize the performance of network RTK in kinematic mode. Five test runs were performed and the test run durations range from 1 to 4 hours. A unique test set-up was used. Baselines between the antennas were used as metrics for measuring precision and accuracy of the solutions. The major issue encountered in the analysis of the data collected was the time-tag issues. Each set of equipment recorded solutions with a data recorder time-tag and not necessarily based on the GPS-observation time. This issue makes the comparisons of the solutions more difficult and hence a position matching algorithm was used to produce the results. Further analysis was done on the solution reacquisition time for one the kinematic data sets with the highest data availability which revealed that, on average, 20 seconds are needed for the equipment to reacquire ambiguity fixed network RTK solution. The results show typical ambiguity fixed solution availability according to similar studies on kinematic performance of network RTK (Aponte et al., 2008; Rubinov et al., 2011). However, Company 'C' shows less than 10% availability on a number of test runs. The analysis on the data reveals ~2 cm (1σ) precision that is within acceptable levels for typical network RTK performance in kinematic mode. Isolated, large outliers were seen in the precision results, however they can be explained by the lack of data availability for a comprehensive solution comparison. In terms of accuracy, rms values ranging from 2 to 4 cm in 3D were shown as well as, three large outliers of ~8 cm in magnitude. As with precision, the large outliers were the results for tests runs where the equipment was unable to obtain a certain level of availability.

6. CONCLUSIONS, RECOMMENDATIONS AND FUTURE STUDIES

The main objective of this study was to collect network RTK data from presently operating service providers in southern Ontario and analyze the results to determine the performance of network RTK in the region. A lack of previous independent studies completed for a province-wide study aroused interest, particularly at MTO, to examine the quality of network RTK solutions for use in low-order control surveys. Traditional methods of static GPS surveying are costly and time consuming; however, they are required for the high level of accuracy and precision needed for control surveys. A major portion of this study involved the testing of network RTK solutions to analyze, whether or not, they could replace the traditional method of static GPS surveying. The advantages to using network RTK rather than the traditional methods are:

- Cost, as only one receiver is needed and less labor is required; however, the cost of network RTK service subscription should be considered.
- Absolute solutions as opposed relative baselines. The equipment provides one set of coordinates and any required adjustments are implicitly performed by the network RTK software.
- Ease of use, as currently network RTK services are provided as a turn-key product.

In an effort to collect as much data as possible, 9 test sites in southern Ontario were visited and close to 300 hours of network RTK data were collected for three difference service providers. To ensure a thorough analysis, a comprehensive set of metrics were chosen to examine performance and to form guidelines for MTO use. The MTO concern was the evaluation of the accuracy of the horizontal component. The recommendations that were presented in the MTO report are briefly outlined in the next section here. Upon completion of the requirements of the MTO project, the analysis of the results was expanded to the vertical and kinematic solution.

6.1 Conclusions

The results of this study show that the solution availability and cold-start TTFF can vary in different locations as it is affected by a variety of different issues such as cellular coverage and visibility. Overall static solution availability of 82% to 97% can be expected, but the kinematic solution availability, on average was below 50% and unpredictable. Static TTFF of 30 seconds on average can be expected with extreme cases of 100 seconds or longer. Interestingly, the kinematic analysis of solution recovery time after encountering an obstacle showed an average of 21 seconds, which is very similar to the static TTFF results. The precision of the static results show unified levels of short-term repeatability. In both vertical and horizontal components of the solution precision, results indicate an overall precision of ~2.5 cm (95%) or better. However, one of the main issues of network RTK in southern Ontario is solution biases in the horizontal components, which can be up to 4 cm in isolated cases, which can severely undermine the accuracy of user solutions. The rms values from results showed accuracies ranging from ~2-4 cm in the horizontal and the vertical. The vertical accuracy results showed lower values than the horizontal; however, the horizontal showed higher repeatability in the long-term. The horizontal mean errors were mapped and produced patterns of rotations and translations for two of the service providers' networks. The vertical mean errors showed surprisingly good results; though, unlike the horizontal mean errors, no definitive network bias patterns could be deduced. Solution integrity analysis revealed that in most cases the horizontal and vertical errors were lower than the 3σ solution uncertainties, unless large biases exist. In terms of long-term repeatability, the revisited sites showed biases and precision levels in similar ranges. Repeatable directions and in some cases magnitudes of mean errors suggested that the solution is potentially the same. However, after further statistical testing on the means and standard deviations of the data sets, it was shown that they were not, in most cases, statistically repeatable. Moving average filtering was employed to determine the observation period that is needed to improve the 1 Hz results significantly, and the results show that a 5 minute observation window increases the precision of the solution by up to ~25% and maximum error is reduced by up to ~40%, for both horizontal and vertical components.

The kinematic accuracy and precision results, in some isolated cases, show mixed results, however rms values ranging from 2-4 cm were seen in 3D, which is excellent for kinematic results. The kinematic results also revealed issues with non-matching time-tags. A position matching algorithm was employed to analyze the kinematic data. Solutions from one service provider shows signs of non-uniform kinematic solutions as the collected 1 Hz coordinates seen from this service provider, are randomly behind or ahead of the others by fractions of a second, which is not due to whole-second biases.

The dominant issue that was encountered during the course of this study was the lack of a unified set of guidelines or procedures for the private networks to be integrated into Ontario's official datum, NAD83 CSRS epoch 2007.0, which may account for the noticeable centimetre-level biases that are present in many of the solutions. Large network biases in some of the solutions undermine the capability of network RTK as a whole. Another issue is the fact that not all locations within these networks were assessed. With sufficient testing, "blind spots" can be found (as a few were found in this study), where the rover is well within the network RTK and yet no solution could be provided to the user. Comparing network RTK in southern Ontario with similar places such as Great Britain and urban regions of Australia, in terms of both accuracy and availability, the services provided in Ontario tend to underperform. In most places, network RTK installations have been an extension of the state (or province) owned and operated reference stations, contracted to private companies and regulated by the government. This is not the case in Ontario, as there are only a few CACS in place and they are owned and operated by the federal government and are hundreds of kilometres apart in some case. Generally, the results have shown that network RTK can be used for MTO third order control surveying or lower; however, there are improvements that can be made to the existing systems to make them comparable to the high-performance network RTK services.

6.2 Recommendations

This section will primarily focus on the main recommendations made based on the final results of the MTO project. A set of recommendations and procedures were discussed in the final report submitted to MTO, in order to help users of network RTK meet MTO's specifications in horizontal control surveying.

6.2.1 Network Geometry

In order to use network RTK technology, it is important for the user to closely examine the network geometry around the work area, to ensure that the work area is enclosed by the reference stations, as network geometry is one of the most important factors affecting network RTK solution quality. Good planning aids solution quality, and also increases productivity when using network RTK. Long distances from the main reference station to the user location could affect the quality of solutions, even leading to loss of fixed solutions or not being able to obtain fixed solutions at all. A few occurrences of this nature were encountered during the campaigns. In general, the issue of distance from the primary reference station was not a principal concern of the study, and no quantitative value can be given as the maximum distance from the primary reference station. However, another study has shown that for centimetre accuracy solutions, the length of baselines needed to be shorter than 30 - 40 km (Grejner-Brzezinska et al., 2005). This is not a critical issue in southern Ontario with the existing network RTK services. But there are locations within each network where the user needs to take extra care such as Kingston and south of St. Catharines closer to the U.S. border.

6.2.2 Datum

The commonly-used official datum in Ontario is NAD83 CSRS epoch 1997.0. The differences between epochs (i.e., 1997 and 2002) within the same datum can be more than 2 cm horizontally in southern Ontario. This difference can account for a significant amount of the error budget for third order accuracy for control surveying. It is imperative that the officially-specified datum and epoch be used when using network RTK. A user should ensure that the datum used by the service provider conforms to that of the project. If this is not the case, transformations may be needed to be performed. The Geodetic Survey Division of Natural Resources Canada can provide a variety of tools to aid with transformation of coordinates from widely used datum to NAD83 CSRS. Among them, TRNOBS (GSD, 2011) is the utility that converts various epochs of International Terrestrial Reference Frame (ITRF) into NAD83 (CSRS) and vice versa. A good practice would be for commercial services to the current official standard, and not leave the responsibility to the user community.

6.2.3 Quality Control

Network RTK equipment typically includes visual aids for the quality of the solution. The user is recommended to pay attention to these aids to determine whether a solution is ambiguity fixed. Also, it is recommended to wait for a period of at least 30 seconds after a cellular modem connection has been made before collecting observations. This can ensure that the equipment is able to receive all possible corrections and does not report “false quick fixes”. It is recommended to turn on all internal quality controls. Horizontal quality control should be set to a value no larger than 5 cm. The threshold for the internal coordinate quality can be set to a value lower than 5 cm. Otherwise, this may cause a significant number of observations to be rejected and extend observation time undermining the efficiency of the survey depending on the location. In other words, the coordinate quality threshold should not be significantly lower than the accuracy of the survey (5 cm in horizontal for third order accuracy). Also, most receivers give the user the option of a Geometric Dilution of Precision (GDOP) quality control indicator, with the maximum tolerable GDOP value of 3 in this case (Edwards et al., 2008).

6.2.4 Window of Observation

The benefit of having a large observation window on precision and maximum error is significant. It is recommended that at least 5 minutes of network RTK observation should be made for each occupation. Based on the results from the moving averages analysis, the best solutions in terms of precision and maximum error were delivered from the large windows, which provided significant improvement over short observation windows. For the sake of time efficiency in a survey when using network RTK, the 5 minute observation time is preferable. Furthermore, it is recommended that points be re-occupied at least once (preferably twice) after a time delay of at least a few hours to take advantage of changing satellite geometry. This procedure will reduce the effects of network RTK solution drift (as seen from the campaign position error time series), and issues caused by human error, such as: incorrect set up, incorrect antenna heights, wrong point occupied and other such errors that could possibly jeopardize the quality of the survey.

6.2.5 Visibility

For areas where there are visibility issues with GPS constellations, the other GNSS satellite constellations (assuming GNSS enabled receiver) will suffer from the same problem. Therefore terrestrial measurement techniques may have to be applied. For areas with little visibility, such as over hangs or close to bridges, it is recommended to utilize traditional terrestrial observations instead of using network RTK.

6.2.6 Raw GPS Observations

A network RTK service provider should ensure that their users are provided with the ability to record raw GPS observations concurrently with network RTK observations. This option empowers a user to be able to post-process the data and identify potential issue that may have adversely affected the real-time solution. This recommendation will not only improve traceability, but also aid in addressing any legal inquiries made of the survey.

6.2.7 Sectioning

Sectioning of the network can be performed as recommended by MTO for the single baseline RTK observation. MTO recommends the maximum distance for the site calibration sections to be 5 km, to minimize the error in the calibration of the coordinates and also to reduce communication problems between base and rover. The communication issue does not exist with network RTK in areas where there is sufficient cellular coverage. Although the official datum in Ontario is NAD83 CSRS epoch 1997.0, some companies use variations of this datum, i.e., a different epoch of the same datum. Hence, this difference must be taken into consideration for precise applications such as control survey. Surely, a site calibration as for traditional RTK may be required while applying the network RTK technology in case of a discrepancy between the project datum and the provided official coordinates of the existing control points.

6.2.8 Solution Calibration

The purpose of a calibration is to estimate the transformation parameters, normally a seven parameter Helmert conformal transformation between datum ***A*** and datum ***B***. For an arbitrary common point, the transformation is expressed as in (Anderson and Mikhail, 1998) (42):

$$\begin{bmatrix} X_B \\ Y_B \\ Z_B \end{bmatrix} = \begin{bmatrix} D_X \\ D_Y \\ D_Z \end{bmatrix} + (1 + ds) \begin{bmatrix} 1 & -r_z & r_y \\ r_z & 1 & -r_X \\ -r_y & r_X & 1 \end{bmatrix} \begin{bmatrix} X_A \\ Y_A \\ Z_A \end{bmatrix} \tag{42}$$

wherein D_X, D_Y and D_Z are three translations, $\boldsymbol{s}$ is the scaling factor, and r_x, r_y and r_z are the three rotational parameters. Three small angular rotations are expected as no significant rotations exist between two geodetic datum in practice. At least three common points are required to solve this seven parameters system. The estimated parameters from a calibration are used to transform the network RTK solutions into the official datum used by the primary control monuments, so that a consistent datum is maintained in the entire network. This approach is more preferable locally than the transformation based the official datum transformation parameters, as there may contain certain biases in the existing local control points. Note that for more straightforward transformations, the scale and even the rotations can be removed from (42).

6.2.9 Network RTK Solution Quality

Each primary control monument should be occupied for a minimum of 5 minutes, which allows continuously collecting at least 300 epochs of network RTK solution at a 1 Hz data rate. A double run observation should be introduced in two different time frames (hours apart) in order to take advantage of the geometry change of the satellite constellation for two independent solution sets.

6.2.10 Fieldwork: Traversing

The observation of a traverse starts from a primary control monument and all the traverse sections should be visited one by one at both of the end points. After each observation period the receiver should be at least disconnected from the Internet and left to lose ambiguity fixed network RTK solution, which should simulate a cold start for any successive observation either at the same traverse point or at a different traverse point until all points in the traverse sections are occupied. As shown in Figure 6.1, one starts at the beginning of the traverse with the existing monument and visiting each new monument to perform the individual observations at least 5 minutes for each observation period. Once the end point (or the adjacent existing monument) is reached, a whole run is completed. A second run is required for the entire traverse in a different time frame. A double run observation makes two sets of results for each traverse section available and provides users with good opportunity to minimize issues of equipment set up such as centering mistakes or antenna height blunders together with good opportunity to monitor the solution consistency. Maintaining a fixed rover rod antenna height, if possible, is also similarly helpful.

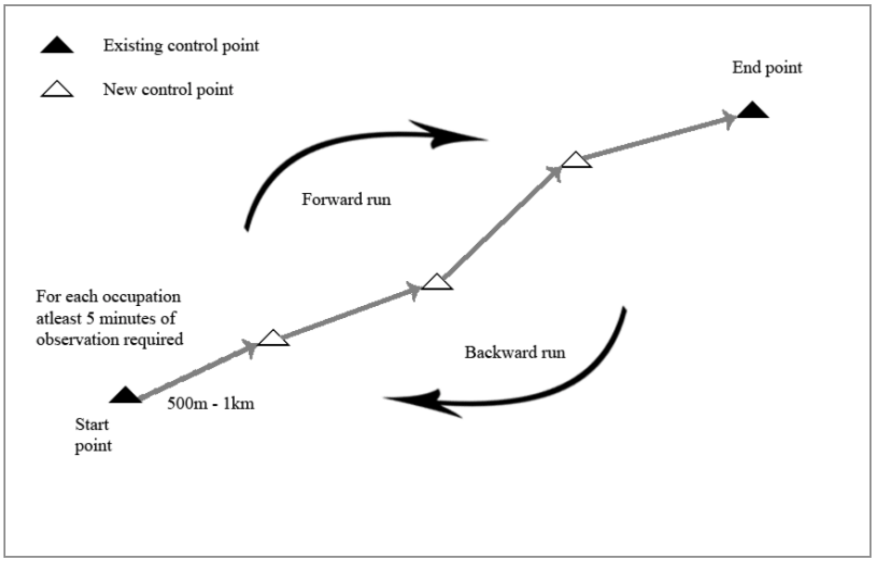

Figure 6.1: Forward and backward traversing for control survey set-up using network RTK

6.3 Future Studies

One major topic as an extension to this study can be the examining the rigours of the methods each service provider is using to tie their network into the Ontario official datum. This study can use the currently collected data, as well as a few specifics on the operating networks' structures to determine the issues of each network's integration methodology. A comprehensive study could also include a tested set of procedures for integrating networks operating in Ontario into the NAD83 CSRS datum and to reduce the magnitude of solution biases that currently reside in the network RTK services in Ontario. These procedures could potentially become industry standards, which could be used by a governing body to provide certificates for networks operating in Ontario and help to ensure that all the networks are within an accepted standard of performance. This study could also be expanded include the integration and coordination of new reference station added to an existing network.

One of the most important topics to study for network RTK is to discover ways of monitoring network RTK performance. Common performance studies on whole networks can be a costly and time consuming task. Newer and more efficient methods of continuously monitoring performance need to be introduced to increase the quality of network RTK solutions overall. Also, studies on developing new methods of detecting outliers for kinematic applications would be beneficial.

Further studies could be done on expanding network RTK services to locations at the extents, which can also help provide coverage to blind spots. PPP-RTK is an example of this service that uses the errors estimated by a network of reference stations and extrapolates the results to aid and improve out-of-network solutions using real-time PPP.

7. REFERENCES

Abidin, H.Z. (1993), "Computational and Geometrical Aspects of on-the-Fly Ambiguity Resolution," PhD thesis, Dept. of Surveying Engineering, Technical Report No. 164, University of New Brunswick, Fredericton, Canada, 314 pp.

AIUB (2005), Bernese (Version 5), Astronomical Institute, University of Bern, Switzerland.

Al Marzooqi, Y., H. Fashir, T. Babiker (2006), "Establishment of Dubai Virtual Reference System (DVSR) National GPS-RTK Network," FIG Working Week 2005, April 16-21, Cairo Egypt, 17 p.

Anderson, J.M., and E.M. Mikhail (1998), "Surveying, theory and practice," McGraw-Hill, 7th edition, Boston, 1200 p.

Aponte, J., X. Meng, C. Hill, T. Moore, M. Burbidge, and A Dodson (2009), "Quality Assessment of A Network Based RTK GPS Service in the UK," *Journal of Applied Geodesy*, Vol. 3, pp. 25-34.

Bisnath, S. (2011), "Satellite Positioning Systems", Lecture notes, York University, Toronto, Canada.

Bisnath, S., J. Wang, A. Saeidi, and G. Seepersad (2012), "Utilization of Network RTK GPS in MTO Highway Surveys," Highway Infrastructure Innovation Funding Program (HIIFP) 2010, Ministry of Transportation of Ontario, St. Catharines, Canada.

Brown, N., I. Geisler, and L. Troyer (2006), " RTK Rover Performance Using the Master-Auxiliary Concept," *Journal of Global Positioning Systems 2006*, Vol. 5, No. 1-2, pp. 135-144.

Cannon, M.E., G. Lachapelle, B. FalkenBerg, and P. Fenton (1992), "Precise Real-time Kinematic Differential GPS Using a Cellular Radio Modem," NovAtel Communications Ltd., Calgary, Alberta, 8 p.

Chen, D., and G. Lachapelle (1995), "A Comparison of the FASF and Least Squares Search Algorithms for on-the-Fly Ambiguity Resolution," *Navigation: Journal of The Institute of Navigation*, Vol. 42, No. 2, pp. 371-390.

Dai, L., S. Han, J. Wang, and C. Rizos (2004), "Comparison of Interpolation Algorithms in Network-Based GPS Techniques," *Navigation: Journal of The Institute of Navigation*, Vol. 50, No. 4, Winter 2003-2004, pp. 277-293.

Delcev, S., V. Ogrizovic, V. Vasilic, and J. Gucevic (2009), "Accuracy Testing of RTK Service of the Permanent Station Network in the Republic of Serbia," Surveyors Key Role in Accelerated Development, FIG Working Week 2009, Eilat, Israel, 3-8 May 2009, 15 p.

Edwards, S., P. Clarke, S. Goebell, and N. Penna (2008), “An Examination of Commercial Network RTK GPS Services in Great Britain,” Newcastle University, UK, 114 p.

Euler, H.J., C.R. Keenan, B.E. Zebhauser, and G. Wubbena (2001), "Study of a Simplified Approach in Utilizing Information from Permanent Reference Station Arrays," Proceedings of ION GPS 2001, Salt Lake City, September 2001, pp. 379-391.

Euler, H.J., O. Zelzer, F. Takac, and B.E. Zebhauser (2003), "Applicability of Standardized Network RTK Message for Surveying Rovers," Proceedings of ION GNSS 2003, Portland, Oregon, September 9-12, pp. 1361-1369.

Fotopoulos, G., and M.E. Cannon (2001), "An Overview of Multi-Reference Station Methods for Cm-Level Positioning," *GPS Solutions*, Vol. 4, No. 3, pp 1-10.

Frei, E., and G. Beutler, "Rapid Static Positioning Based on the Fast Ambiguity Resolution Approach FARA: Theory and First Results," *Manuscripts Geo-daetia*, 1990, pp. 325-356.

GLONASS ICD Version 5 (2002), Moscow, Russia.

Grejner-Brzezinska, D.A., I. Kashani and P. Wielgosz (2005), “On Accuracy and Reliability of Instantaneous Network RTK as a Function of Network Geometry, Station Separation, and Data Processing Strategy,” *GPS Solutions*, Vol. 9, No. 3, pp. 212-225.

GSD, Natural Resources Canada (1996), “Accuracy Standards for Positioning,” Version 1.0, Ottawa, Ontario, 31 p.

GSD (2011), “TRNOBS - 3-D Coordinate Transformation Program,” http://webapp .csrs.nrcan.gc.ca/index_e/online_apps_e/trnobs_e/termtrnobs_e.html, accessed July 2011.

Harre, I. (2001) “A Standardized Algorithm for the Determination of Position Errors by the Example of GPS with and without 'Selective Availability’,” 9 p.

Hatch, R. (1989), "Ambiguity Resolution in the Fast Lane," Proceedings of ION GPS 1989, Second International Technical Meeting of the Satellite Division of the Institute of Navigation, September 27-29, Colorado Springs, pp. 45-50.

Hatch, R. (1990), "Instantaneous Ambiguity Resolution," Springer Verlag, Proceedings of International Association of Geodesy Symposia No. 107 Kinematic Systems in Geodesy, 10-13 September, Banff, Canada, pp. 299-308.

Hoffman-Wellenhof, B., H. Litchenegger, and J. Collins (2001), "*GPS: Theory and Practice*," Springer-Verlag Wein New York, 5th edition, 382 p.

IGS (2012), http://igscb.jpl.nasa.gov/network/guide_igs.html#allsites, accessed March 2012.

Janssen, V. (2009), "A Comparison of the VRS and MAC Principles for Network RTK," IGNSS Symposium 2009, Australia, December 1 - 3, 13 p.

Jonsson, B., G. Hedling, and P. Wiklund (2002), "Some experiences of network-RTK in the SWEPOS™ network," Proceedings of the 14th General Meeting of the Nordic Geodetic Commission, NKG, 14th General Meeting, pp. 284-290.

Lachapelle, G., and P. Alves (2002), "Multiple Reference Station Approach. Overview and Current Research," *Journal of Global Positioning Systems*, Vol. 1, No 2, pp. 133-136.

Leica (2005), "Networked Reference Stations," white technical paper, June 2005, 10 p.

Leica Geosystems (2010), “Leica SmartNet Commercial RTK Network Solution for North America,” http://smartnet.leica-geosystems.us/, accessed September 2010.

Leick, A. (2004),"*GPS Satellite Surveying*", Jon Wiley and Sons, Inc., 5th edition, 435 p.

Lin, M. (2006), "RTCM 3.0 Implementation in Network RTK and Performance Analysis," MASc Thesis, UCGE Report Number 20236, University of Calgary, January 2006, 151 p.

Mader, G.L (1990), "Ambiguity Function Techniques for GPS Phase Initialization and Kinematic Solutions," Proceedings of Second International Symposium on Precise Positioning with the Global Positioning System, 3-7 September, Ottawa, Canada, pp. 1233-1247.

Mader, G.L. (1992), "Rapid Static and Kinematic Global Positioning System Solutions Using the Ambiguity Function Technique," *Journal of Geophysical Research*, Vol. 97, No. B3, pp. 3271-3283.

MNR (2011), http://www.cosine.mnr.gov.on.ca/cosine/cgi-bin/COSN_RetrFuncts.asp?task=gen_homepage, accessed January 2011.

NRCan (2011), http://www.geod.nrcan.gc.ca/index_e.php, accessed January 2011.

NRCan (2012), http://www.nrcan.gc.ca/earth-sciences/node/5240, accessed February 2012.

Rubinov, E., G. Hausler, and P. Collier (2011), “Evaluation of NRTK Heighting in Victoria: Impact of a Temporary Reference Station,” IGNSS Symposium 2011, 16 p.

Remondi, B.W. (1985), "Performing Centimetre-level Surveys in Seconds with GPS Carrier Phase: Initial Results," *Navigation: Journal of The Institute of Navigation*, Vol. 32, No 4, pp. 386-400.

Saeidi, A., S. Bisnath, J. Wang, and G. Seepersad (2011), "On the use of network RTK to replace static relative positioning for geodetic GPS surveys, ION GNSS 2011 Conference, 20-24 Sept. 2011, Portland Oregon, pp. 2310 - 2317.

Seeber, G., and G. Wubbena (1989), "Kinematic Positioning with Carrier Phases and "On the Way" Ambiguity Solution," Proceedings of the Fifth International Geodetic Symposium of Satellite Positioning, Las Cruces, New Mexico, March 1989.

Stone, A.W. (2002), http://www.ngs.noaa.gov/PUBS_LIB/GPS_CORS.html, National Geodetic Survey, Albuquerque, New Mexico.

Sun, H., M.E. Cannon, and T. E. Melgard (1999), "Real Time GPS Reference Network Carrier Phase Ambiguity Resolution, " Proceedings of ION National Technical Meeting, San Diego California, January 1999, pp. 193-199.

Tekmon (2012), http://tekmon.gr/2011/03/master-auxiliary-concept/, accessed February 2012.

Teunissen, P.J.G. (1993), "Least Squares Estimation of Integer GPS Ambiguities," Invited Lecture, Section IV Theory and Methodology. IAG General Meeting, Beijing, China, August 1993. 16 p.

Vollath, U., H. Ladau, X. Chen, K. Doucet and C. Pagels (2002), "Network RTK Versus Single Base RTK - Understanding the Error Characteristics," Proceedings of ION GNSS 2002, September 24-27, Portland, OR., 8 p.

Wang, J. (2009), "Adjustment Calculus", Lecture notes, York University, Toronto, Canada.

Wang, J., M. P. Stewart, and M. Tsakiri (2000), "A Comparative Study of the Integer Ambiguity Validation Procedures," *Earth, Planets Space*, Vol. 52, pp. 813-817.

Weber G., D. Dettmering, and H. Hebhard (2006), "Network Transport of RTCM via Internet Protocol (NTRIP)," International Association of Geodesy Symposia, Vol. 128, 11 p.

Wei, E., H. Chai, and Z. An (2006)," VRS Virtual Observations Generation Algorithm," *Journal of Global Positioning Systems*, Vol. 5, No. 1-2, pp. 76-81.

Wubbena, G., A. Bagge, G. Seeber, B. Volker, and P. Hankemeier (1996), "Reducing Distance Dependent Errors for Real Time DGPS Applications by Establishing Reference Station Networks," Proceedings of ION GPS 1996, September 17-20, Vol. 2., pp. 1845-1852.

Wubbena, G., M. Schmitz,and A. Bagge (2005), "PPP-RTK: Precise Point Positioning Using State-Space Representation in RTK Networks," Proceedings of ION GPS 2005, September 13-16, Long Beach, California, pp. 2584-2594.

Wubbena, G., and A. Baggge (2006), "RTCM Message Type 59 - FKP for Transmission of FKP," Geo++ White paper, 8 p.